Structure, Dynamics and Control of Complex Networks

A thesis
Submitted in partial fulfillment of the requirements
of the degree of
Doctor of Philosophy

By

Snehal M. Shekatkar
20103073

INDIAN INSTITUTE OF SCIENCE EDUCATION AND RESEARCH PUNE

January 2016

I dedicate the present thesis to the loving memory of my father - the first person who taught me the scientific method.

Certificate

I certify that the thesis entitled "Structure, dynamics and control of complex networks" presented by Mr. Snehal M. Shekatkar represents his original work which was carried out by him at IISER, Pune under my guidance and supervision. The work presented here or any part of it has not been included in any other thesis submitted previously for the award of any degree or diploma from any other University or institution.

Prof. G. Ambika
(Supervisor)

Date:

Declaration

I declare that this written submission represents my idea in my own words and where others' ideas have been included; I have adequately cited and referenced the original sources. I also declare that I have adhered to all principles of academic honesty and integrity and have not misrepresented or fabricated or falsified any idea/data/fact/source in my submission. I understand that violation of the above will be cause for disciplinary action by the Institute and can also evoke penal action from the sources which have thus not been properly cited or from whom proper permission has not been taken when needed.

Snehal M. Shekatkar
(20103073)

Date:

Acknowledgements

The present thesis would not have come into existence without the help of many people whom I owe my greatest thanks.

I find myself very lucky to have Prof. G. Ambika as my thesis supervisor and mentor. She is the first person who introduced me to complex networks and has been a great advisor to me since last five years. I hope that I would be able to learn her extremely organized way of working at some point of my life. I owe my deepest gratitude to you my teacher for your advice, support, guidance and the inspiration that I got from you to work in this field.

I am extremely grateful to Dr. Chandrasheel Bhagwat with whom I collaborated. He has also been a very good friend of mine for several years. Many sincere thanks to him for his contribution to the present thesis, to my understanding of many ideas from mathematics and a great help that he provided me from time to time.

It was an honor for me to work with Prof. Jürgen Kurths, Dr. Bedartha Goswami and Dr. Aljoscha Rheinwalt (Potsdam Institute of Climate Impact Research, Potsdam, Germany). I enjoyed my stay in Potsdam and had a great research experience with the group of Prof. Jürgen Kurths. It is my pleasure to thank them all. Special thanks to my friend Abhijit Bendre for being extremely helpful during my stay in Potsdam and making it a nice experience.

I would like to extend my gratitude to my research advisory committee members Prof. Anil Gangal, Prof. Avinash Khare and Dr. M.S. Santhanam. All of them have been extremely nice and helpful to me throughout my research and I got to learn many things from them.

I would like to thank Prof. K.N. Ganesh, Director, IISER Pune for providing the excellent research facilities and nice academic environment here in IISER.

I acknowledge the financial support from University Grants Commission, New Delhi in the form of a research fellowship as well as the financial support from The Department of Science and Technology, Govt. of India and The German Academic Exchange Service, Germany for my two trips to PIK, Potsdam, Germany.

Many thanks to Prabhakar, Kalpesh and Tushar; they have been extremely nice and helpful to me. I also extend my sincere thanks to IISER administration, transport, library and house-keeping.

I enjoyed being a part of the research group of Prof. Ambika with Resmi, Kajari, Sandip, Kashyap and Chiranjit. I learned a lot from all of them and also enjoyed the regular research discussions as well as debates about many social and political topics. Many thanks to you all.

Life in IISER would have been extremely dull without a company of many of my friends here in IISER with whom I spent a great time. I thank Resmi, Mayur, Vimal, Rashmi, Chandrasheel, Avdhoot, Shishir, Sunil, Arindam, Koushik, Swathi, Nitin, Abhijit, Sasi, Abhishek, Kanika, Uday, Kajari, Sandip, Kashyap and many others for making my stay in IISER a great fun. Those birthday celebrations, frequent luncheons, chess and cricket matches and the gossips and fun which accompanied these are unforgettable. Nitin's unique mocking style has always spiced up many of these occasions. Special thanks to Resmi and Mayur for teaching me many technical things. Scientific and philosophical discussions with Vimal, Resmi, Mayur, Chandrasheel, Abhijit, Sandip and Kajari have had big positive impact on my understanding of the world. Shishir and Mayur were always available for every help, even at midnight. I owe my biggest gratitudes to both of you. Bhakti, Abhijit and Sandip were very kind to help me with the writing of my thesis. Thanks to you all.

I am eternally grateful to Aai and Bhakti for everything that I am unable to delineate. I think I cannot thank you enough and would better choose not to thank. Kailas and Shishir stayed with me during my illness and I would remember their support forever. My old friends Abhijit, Anil, Bhakti, Indrajeet, Kailas, Mahendra, Mangesh, Mayur, Mukul, Pankaj, Pradeep, Pritesh, Sachin, Sandesh, Shashikant, Shishir, Vikram, Yogesh and many others have contributed a lot to my life and I am extremely grateful to all of them for making the journey so far a real fun!

Snehal

Abstract

Complex networks have emerged as a powerful tool for studying the real world complex systems, comprising of many similar interacting units. The behavior of such a complex system is decided by the properties of these individual units and the pattern of interactions between them. The examples of such systems include human society, World Wide Web, chemical reactions happening inside a living cell, human languages, economics and human brain. When such systems are represented as networks, the individual units which make up the bigger system are represented as nodes while interactions between them are represented as links between them. The two important aspects of the study of complex networks are their structure and their dynamics. The structural aspect tries to quantify the interaction patterns of the individual nodes while the dynamical aspect is concerned with the effect of interactions on the dynamics of individual nodes.

For many natural and engineered complex systems, control of their dynamical behavior is often very relevant and required. For example, the interaction between the neurons in human brain can give rise to unwanted patterns of excitations in the brain which may lead to pathological situations. Similarly, chaotic behavior in extended engineering systems might lead to degradation in their performance. In this thesis, we investigate a relatively less explored issue of control in extended systems like lattices and networks of dynamical systems and propose a new scheme to achieve such control. We also investigate the mechanisms which possibly shape the structure of real networks and propose a 'mediated attachment' model to explain the empirically observed structure of real networks. Finally, we use the theory of complex networks to probe the structure of divisibility patterns of natural numbers and show that this approach leads to interesting insights about natural numbers.

The thesis is organized as follows. In *Chapter 1*, we briefly review the important literature related to the structural aspects of complex networks. Here we talk about different types of networks, various measures to quantify their structure and important generative models of complex networks. In *Chapter 2*, we provide a short overview of the isolated and coupled nonlinear systems. We start by the formal definition of a dynamical system, continuous and discrete systems and attractors of the dynamical system. We then briefly talk about the stability theory for few of these attractors. We discuss few standard continuous and discrete chaotic systems and then introduce the concept of Lyapunov exponents to quantify the behavior of chaotic systems. In the same chapter,

we then move on to nonlinear systems coupled in the form of a complex network and discuss several emergent behaviors like synchronization, amplitude death and chimera states that can occur in them. At the end, we review various methods that have been developed over the years to control the dynamics of isolated and interacting dynamical systems.

In *Chapter 3*, we talk about a novel coupling scheme that we introduced to control the dynamics of extended systems like lattices and complex networks. This scheme involves coupling an external network to the system network with a feedback type of coupling. We start with the control mechanism for coupled discrete dynamical systems. The nodal dynamics in this case is taken to be a chaotic logistic map and Henon map. We analyze the stability of the controlled states for a single unit analytically and isolate the regions of effective control in various parameter planes. These analytical results are then verified using extensive numerical computation. We then move on to 1d lattices of such discrete systems and perform stability analysis using properties of circulant matrices. In this context, the randomized connections between the system network and the external network are then shown to work effectively. As an application of the scheme, we then show how an experimentally realizable chimera state in a non-locally coupled 1d coupled map lattice can be controlled to various periodic and steady states. We then move on to a control scheme for 2d lattices and using Rulkov map as a system dynamics, we show how the unwanted excitations on such lattice can be suppressed using the proposed scheme. We extend the control scheme to random networks. In this case, we analyze the stability of controlled steady state using a master stability formalism and relate the largest eigenvalue of the Laplacian of the network to its stability. We also show the validity of the control scheme when the controller network is not topologically identical to the system network. We also study the scheme for the case of continuous time dynamical systems. Taking Rössler system and Hindmarsh-Rose neuron model as typical examples, we show how the rings of these systems can be controlled to various periodic or steady states.

In *Chapter 4*, we introduce a generative model of network formation called a 'mediated attachment model'. The model considers a growing network without a direct preferential attachment in which links are also created internally by the process of triadic closure. We argue that this process is less likely for hubs in the network as compared to low degree nodes. This principle, which we phrase as "hubs are weak mediators" is then shown to give rise to a network that is scale-free and also has a hierarchical community structure. We show that the local clustering coefficient of a node in the network decreases with increase in its degree. This is a necessary condition for the existence of hierarchical community structure in the network. We then use a community detection algorithm and show that a "mediated network" is modular on multiple scales confirming the existence of hierarchical community structure. We also calculate other important structural characteristics like clustering coefficients, path lengths and assortativity coefficients of the networks so generated and compare these characteristics with the real world networks. This network is seen to have an average path length that varies logarithmically with size and it also has a high value of clustering coefficient. Thus, such network is also a small-world network in addition to being scale-free. We also show that as the size of the network increases, the assortativity coefficient of the network settles to a positive value. This is important since the social networks, where a triadic closure mechanism is dominant, are known to have positive degree correlations.

In *Chapter 5*, we study the divisibility relations between natural numbers using a paradigm of complex networks. For this, we construct an undirected network in which natural numbers are nodes and the connections between them are defined using a simple divisibility relation. We use rigorous methods from the field of statistical inference to show that the network exhibits a non-stationary power-law degree distribution and hence is scale-free. We also show that the local clustering coefficients for this networks are not randomly distributed and show a very interesting pattern that is stretched on a global scale if the size of the network is increased. Hence, we call this property exhibited by natural numbers a 'stretching similarity'. We find analytical expressions for the average degree of the network and the local clustering coefficients of nodes in the network and also discuss the relation between average and global clustering coefficients with the help of analytical and numerical arguments.

In the concluding chapter, we present the important conclusions that have come out from all the different aspects of research presented in this thesis. We also indicate the future directions of research that have opened up from our work and their relevance in understanding the intricacies in the dynamics of complex systems.

Publications

The work presented in this thesis has appeared in the following publications:

1. Snehal M. Shekatkar and G. Ambika, “Novel coupling scheme to control dynamics of coupled discrete systems", *Commun. Nonlinear Sci. Numer. Simulat.*,**25**,(2015).

2. Snehal M. Shekatkar and G. Ambika, “Complex networks with scale-free nature and hierarchical modularity", *Eur. Phys. J. B.*, **88**,(2015).

3. Snehal M. Shekatkar, Chandrasheel Bhagwat and G. Ambika, “Divisibility patterns of natural numbers on a complex network", *Scientific Reports*, **5:14280**,(2015).

Contents

Chapter 1

Complex Networks

1.1 Introduction

The paradigm of complex networks has become one of the most important and powerful approaches to the study of complex systems [1,2]. Systems belonging to diverse fields like social sciences [3,4], biology [5–9], ecology [10], neuroscience [11], technology [12,13], economy [14], climate [15,16] and transport [17–19] can be modelled as complex networks. They have also been applied to several problems from pure mathematics [20, 21]. In essence, complex networks are mathematical abstractions of complex systems comprising of many identical units interacting with each other. The individual systems in the bigger system are represented as nodes of the complex networks and the interactions or connections between them are represented by links connecting these nodes (Fig. 1.1(a)). The real world complex systems are then modelled using random networks where only the statistical pattern of connections between various nodes is important. Over the last fifteen years, this field has become one of the most active fields of study in interdisciplinary sciences and there has been a flurry of research addressing various aspects.

Networks can be classified in various ways. They can either be regular or random , undirected or directed and weighted or unweighted . The number of links a node has in the network is called its degree . The networks in which every node has the same degree (like lattices) are called regular networks whereas networks in which connections between nodes are made randomly (like Erdös-Rényi network) are called random networks. The links in the directed networks have directions that represent the direction of the interaction between the two nodes in the network. In weighted networks, links also have weights representing the strength of the interaction between a given pair of nodes. A small weighted and directed network is shown in Fig.1.1(b). We will look at this classification scheme in more detail in the following section.

The empirical observations about the networked systems in real world have made it clear that they are neither completely regular nor completely random and lie somewhere in the middle of these two extremes. These observations also show that connection topologies of networked systems belonging to diverse fields like biology, social sciences

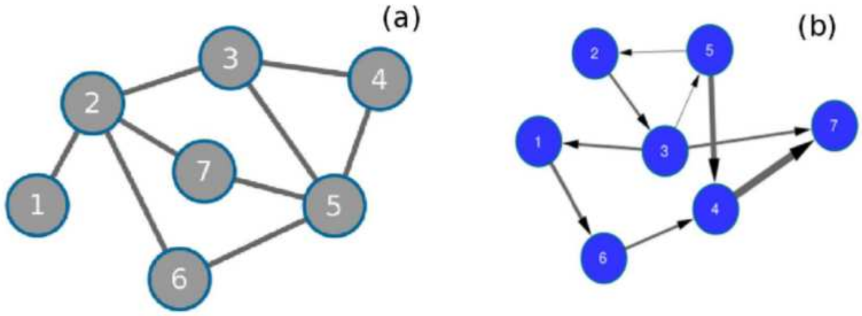

Figure 1.1: (a) Graphical representation of a small network with 7 nodes and 9 links. The circles in the figure are nodes and are representative of individual systems which constitute the bigger complex system. The lines connecting the nodes are called links and represent the interactions or connections between the individual systems. (b) A small weighted and directed network with 7 nodes and 9 links. The arrows are used to show the directions of links and thickness of links corresponds to their weights.

and technology share many striking similarities and universal features. These findings imply that the evolution of the structure of these networks is governed by robust organizing principles which are largely system independent. To distinguish such networks from completely regular and completely random networks, they are termed as "Complex Networks".

The whole study of complex networks can in general be divided into two distinct parts. The first part deals with the characterization of their structure and finding the mathematical models to explain the structure of real world networks while the second part deals with the study of processes and dynamics taking place on them. From the point of view of both these aspects of study, it is important to first characterize the structure of networks. Over the years, many quantifiers or measures have been developed to characterize the structure of networks, important ones of which will be presented in later sections.

Another very important problem in the study of networks is to find out the physical mechanisms which lead to empirically observed structure of real world networks. Mathematical models based on such mechanisms are expected to produce networks with structures similar to the real networks. This is important since it allows us to understand the temporal growth of networks and hence leads to better insights into many universalities observed in real networks. In the following sections, we review a few such models. These models are termed as generative models since they try to generate the networks similar to real networks by incorporating the underlying physical mechanisms.

The functions of complex physical systems, when they are represented as networks, are best understood by considering various processes on networks. For example, when a city is viewed as a network of sub-regions connected by roads, the transportation in the city can be viewed as a random walk on the corresponding network. This in turn allows one to study problems like traffic jams in the city. When human society is viewed as a network of human connected by acquaintance or other interactions , the propagation of epidemics in the society can be seen as a diffusion process taking place on this social network and so on. The topic of processes on networks is thus extremely important from a practical point of view and many important results have been reported in this context.

Finally, a very important area of study in the theory of networks is the study of deterministic dynamical systems coupled on networks. Such a representation finds applications in modeling a large number of complex physical systems like human brain , power grid network , human heart , coupled LASERs and so on. The coupling between the dynamical units on networks gives rise to many interesting emergent phenomena like synchronization , amplitude/oscillation death and chimera states. We will describe these phenomena in detail in the next chapter.

1.2 Classification of networks

In this section we describe the various ways in which networks are classified based on their structure. As mentioned above, the complex networks can be classified in a very broad sense, in the following three ways.

1.2.1 Regular and random networks

The networks in which all the nodes have the same degree are called regular networks. Infinite lattices in 1-d and 2-d are examples of regular networks. The networks in which connections between the nodes are made at random are known as random networks . Fig. 1.2 shows typical regular and random networks.

1.2.2 Directed networks

In many physical systems, the interactions between the nodes are unidirectional. For example, when the World Wide Web is represented as a network of websites, the hyperlinks represent the links between the individual nodes. Generally it is possible to navigate from one web-page to other but not the other way round since hyperlink to the previous page may not be present in the second page. Such information about directions in the connections or interactions can be represented by directed links and networks in which such directed links are present are known as directed networks. On the other hand, if the interactions between the nodes are bidirectional, the links are undirected and networks with undirected links, are called undirected networks.

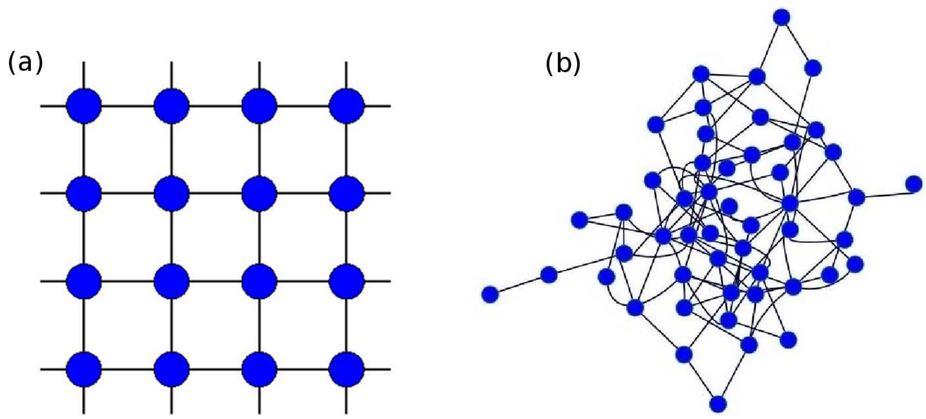

Figure 1.2: **Graphical representation of regular and random networks.** (a) An infinite 2-d lattice is an example of a regular network since every node in the lattice has same degree of 4. (b) In random networks, since the connections are made randomly, the degree values of different nodes are usually different.

1.2.3 Weighted networks

When real world systems are represented as networks, the links represent the interactions between the subsystems which form the bigger system. In most cases, the strength of the interaction varies from one pair of nodes to others. For example, in social networks, some relations like family membership or close friendship are much stronger than relation of mere acquaintance. It is possible to encode this information of the strength of the interactions between individual nodes by assigning different weights to different links in the network. Usually this is done by representing the stronger interactions by links with higher weights. Networks in which links are weighted, are then called weighted networks. If all the links in the network have the same value of the weight, the network is called unweighted.

In many real world networks, these three aspects overlap so that many networks like social networks are in fact random, directed and weighted simultaneously though many times one or more of these features may be ignored while studying a particular aspect.

1.3 Characterization of networks

In this section, we describe the main quantifiers used to characterize the structure of complex networks. The characterization is restricted mainly to undirected networks since such networks are most important from the point of view of the present thesis.

Mathematically, a network is usually represented by a matrix called adjacency matrix A. For an undirected and unweighted network, an adjacency matrix is a binary square matrix with $A_{ij} = 1$ if i and j are neighbors of each other and $A_{ij} = 0$ otherwise. The adjacency matrix for the network represented in Fig. 1.1(a), is as follows:

$$A = \begin{bmatrix} 0 & 1 & 0 & 0 & 0 & 0 & 0 \\ 1 & 0 & 1 & 0 & 0 & 1 & 1 \\ 0 & 1 & 0 & 1 & 1 & 0 & 0 \\ 0 & 0 & 1 & 0 & 1 & 0 & 0 \\ 0 & 0 & 1 & 1 & 0 & 1 & 1 \\ 0 & 1 & 0 & 0 & 1 & 0 & 0 \\ 0 & 1 & 0 & 0 & 1 & 0 & 0 \end{bmatrix} \tag{1.1}$$

Also, since the number of links a node has in the network is called its degree, the degree of node i is equal to the sum of the elements in i^{th} row (or column) of the adjacency matrix.

Another important matrix for a network apart from adjacency matrix is its Laplacian matrix . It is defined as follows. Consider a simple, unweighted and undirected network with adjacency matrix A and let $k_1, k_2, \cdots k_N$ be the degree values of nodes in this network. The degree matrix D of this network is defined as a diagonal matrix with these degree values on its diagonal. The Laplacian of the network is then defined as the matrix:

$$L = D - A \tag{1.2}$$

This matrix arises while studying the problem of diffusion on a network but turns out to have a much wider scope in the study of networks in general. One of the important things which make this matrix special is related to its spectrum i.e. the set of its eigenvalues. It turns out that all the eigenvalues of this matrix are non-negative and the smallest eigenvalue is always equal to zero. Because of this, the spectrum of a Laplacian matrix is written as:

$$\lambda_0 = 0 \leq \lambda_1 \leq \cdots \lambda_N \tag{1.3}$$

It can be easily shown that the multiplicity of zero eigenvalue of the Laplacian is equal to the number of connected components that a network contains.

The important measures and concepts used for the characterization of complex networks are given below.

1.3.1 Degree distribution

When two nodes in the network are connected by a link, they are said to be neighbors of each other. Thus, the number of neighbors of a given node will be the **degree** of that node. A very important network measure related to degree is its degree distribution. The degree distribution $p(k)$ of the network is defined as the fraction of nodes of the network which have degree k or equivalently, the probability that a randomly chosen node from the network has degree k.

1.3.2 Paths and path lengths

A path in a network is a sequence of nodes such that every consecutive pair of nodes in the sequence is connected by an edge in the network [1]. The length of a path is the number of edges traversed along the path. In general, there can be more than one path connecting the given two nodes in the network. The distance between two nodes in the network is defined as the length of the shortest path connecting them. The average of these distances over all pairs of nodes is called the average path length or characteristic path length of the network. The diameter of the network is defined as the maximum of the distances over all pairs of the nodes.

In directed networks, it may not be possible to traverse the same path in a reverse way since the links are directed. This also has to be considered while defining paths in directed networks. [1]

1.3.3 Clustering coefficients

Clustering coefficients quantify the density of triangles in the network and are defined in three different ways: Local clustering coefficient (defined for individual nodes in the network), average (Watts-Strogatz) clustering coefficient (defined for the whole network) and global clustering coefficient (defined for the whole network).

1. **Local clustering coefficient:** A node i with degree k in the network can have at most ${}^kC_2$ links among its neighbors. In reality, all of these links are not usually present. If E_i is the actual number of links present among the neighbors of i, then its clustering coefficient (also known as local clustering coefficient) is defined as the ratio:

$$c_i = E_i / {}^kC_2 \tag{1.4}$$

   It is clear that the value of c_i always lies between 0 and 1.

2. **Average clustering coefficient:** The average clustering coefficient of the network (also known as Watts-Strogatz clustering coefficient) is defined as the average of all c_i over all the nodes of the networks:

$$C_{ave} = \frac{1}{N} \sum_{i=1}^{N} c_i \tag{1.5}$$

3. **Global clustering coefficient:** The global clustering coefficient of a network is defined to be the ratio of the number of closed triplets to the number of connected triplets in the network:

$$C = \frac{\text{Number of closed triplets}}{\text{Number of connected triplets}} \tag{1.6}$$

The path of length 2 is called a connected triplet in the network since this path contains three vertices connected to each other by a continuous path. A path $i \to j \to k$ can be closed i.e. the nodes i and k could also be connected by a link in the network. Such path is called a closed triplet. In fact, every triangle in the network counts as three closed triplets, one centered at each of the vertices of the triangle. Hence the above formula can also be written as:

$$C = \frac{3 \times \text{Number of triangles}}{\text{Number of connected triplets}} \tag{1.7}$$

The values of the two quantities C_{ave} and C are in general different with $C < C_{ave}$.

1.3.4 Community structure

In the context of networks, a community is defined as a set of nodes which are densely connected to each other than to the rest of the network. Many real networks are found to be divided into communities of various sizes [22,23]. Existence of community structure in the network provides important information about the function of the underlying system represented as the network. For example, in case of protein interaction network, such communities represent the various functional groups of proteins which act together [9]. Similarly, in social networks, such communities may represent the group of people working in the same field or having similar interests [24]. Many methods for the detection of communities are being developed over the years [1,23].

1.3.5 Degree correlations

A well studied topic in network theory is about the correlation between the degree values of the two nodes connected by a link in the network. In general, the correlation of the values of a quantity or property on nodes other than degree can also be considered. The networks in which similar nodes tend to connect each other are called assortative networks while those in which dissimilar nodes tend to connect each other are called dissortative networks. The strength of assortativity is usually calculated using the assortativity coefficient when the quantity in question takes continuous values on nodes. Examples of such quantities are age of people or their wealth in social networks. On the other hand, when the quantity is allowed to take only finitely many discrete values, the strength of assortativity is calculated using a quantity called modularity [1]. The assortativity coefficient is derived from Pearson's correlation coefficient. In particular, degree is considered as a continuous variable in networks and the degree-assortativity for a given network is defined as follows [1]:

$$r = \frac{\sum_{ij}(A_{ij} - k_i k_j/2m)k_i k_j}{\sum_{ij}(k_i \delta_{ij} - k_i k_j/2m)k_i k_j} \tag{1.8}$$

Here, A_{ij} is $(i,j)^{th}$ element of an adjacency matrix of the network, m is the number of links in the network, k_i is the degree of node i and δ_{ij} is the Kronecker delta whose value is 1 when $i = j$ and is 0 otherwise. Empirically, it has been observed that except social networks, all other real networks exhibit negative degree correlations [4, 25].

1.4 Processes on networks

The various examples of the processes happening on networks include the dynamics of action potentials in the neurons [26–28] of the human brain, spreading of rumors in the city [29], a computer virus spreading over the World Wide Web [30–32], epidemics spreading through a population [33, 34], traffic jams on high-ways [35, 36], synchronization of dynamical systems [37, 38], network resilience [39] and so on.

This regime of the study is centered about understanding the effect of structure of underlying network on the processes that happen on it. This is important since it allows one to control these processes simply by changing the structure of the network. The spreading processes like rumor spreading, epidemics and computer viruses are usually modelled using simple random walk models on the networks [40, 41]. On the other hand, processes in which every node is always active, for example neuron activity or power grids, are modelled by putting a deterministic dynamical system (continuous or discrete) on each of the nodes of the network and making them interact along the edges of the network. Also, when dynamical systems are coupled in the form of a network using diffusive type of coupling, the eigenvalues of the corresponding Laplacian determine the stability of the synchronized state of these systems.

1.5 Generative network models

The generative network models in general try to explain the empirically observed structure of real networks based on a set of small number of underlying hypotheses. The most important empirically observed features of real networks include scale-free nature, small average path length, high clustering, finite degree correlations and simple or hierarchical community structure. We present below three most important network models, Erdös-Renyi model, Watts-Strogatz model and Barabási-Albert model.

1.5.1 Erdös-Renyi model

In this model, we start with a set of fixed N number of nodes and then every pair of nodes is connected with a fixed probability p. The degree distribution of the Erdös-Renyi model in the limit $N \to \infty$ with a fixed average degree λ is given by the Poisson distribution:

$$p(k) = e^{-\lambda} \frac{\lambda^k}{k!} \tag{1.9}$$

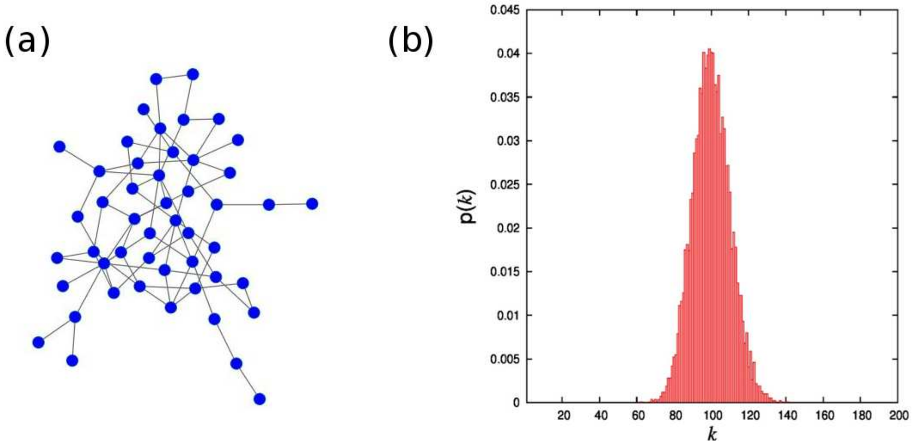

Figure 1.3: (a) Graphical representation of a typical Erdös-Rényi network. (b) Degree distribution of a big Erdös-Rényi network. The distribution can be seen to be close to a binomial distribution.

This model, however, turns out to be a poor representation for real networks. Many real networks have a degree distribution that follows an approximate power-law asymptotically instead of a Poissonian distribution. Also, the global and average clustering coefficients of Erdös-Renyi network decay to zero in the limit of an infinite size and it has zero value for the assortativity coefficient. Despite these drawbacks, this model has an important place in the theory of networks since it is the first random network model that was proposed and also because it provides insight into the small average path length of real networks. Moreover, because of its simplicity, it is possible to solve this model exactly for many of its properties like connectivity. This provides insight into the connectivity properties of other network models which are more accurate at representing real networked systems.

1.5.2 Watts-Strogatz model

The Erdös-Renyi model provides insight into the small average path length of real networks but fails to explain another important property of real networks, the high value of the clustering coefficient. The Watts-Strogatz model tries to overcome this drawback by changing the conceptual paradigm of Erdös-Renyi model. The main observation that motivates the construction of Watts-Strogatz model is that the completely regular networks like lattice and completely random networks like Erdös-Renyi network stand at opposite extremes. Regular lattices with very high clustering coefficients can be easily constructed but their average path length is usually very large. On the other hand, completely random networks like Erdös-Rényi network have low average path length but also have low values for their clustering coefficients. The Watts-Strogatz model lies somewhere between these two extremes and exhibits low average path length with high clustering.

The construction of the Watts-Strogatz network starts with a ring of n vertices and k links at each vertex which are connected to k nearest neighbors. Then each link is rewired at random with a probability p. This construction tunes the parameter p between regularity ($p = 0$) and disorder ($p = 1$). The network thus constructed shows both high clustering and small average path length. However this model fails to explain the fat tailed degree distribution seen in many real networks and hence cannot be used as a model for many real world networks. The graphical representation of constructing a Watts-Strogatz model is depicted in Fig. 1.4

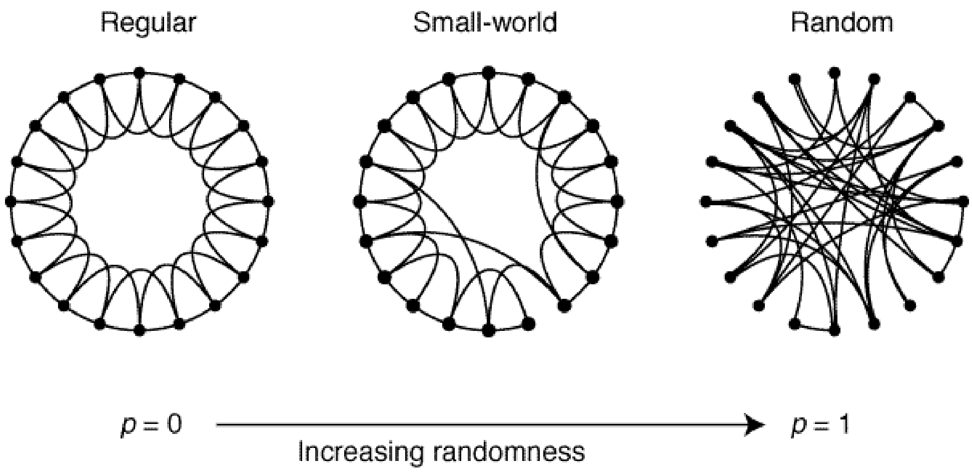

Figure 1.4: Construction procedure of Watts-Strogatz network. Starting with a regular network, in which each node is connected to few nearest neighbors, each link in the network is rewired with a given probability p. Intermediate values of p give rise to Watts-Strogatz network while increasing p to 1, we get completely random network. (Taken from Watts and Strogatz [42])

1.5.3 Barabási-Albert model

In many real networks, the distribution of degrees of nodes exhibits a fat tail. This means that the probability of very high degree nodes being present in the network is not practically zero. In fact, in many cases the degree distribution is an approximate power law, at least asymptotically. The existence of very high degree values in the network as compared to the average degree has profound consequences for the structural and dynamical features of the network. For example, very high degree nodes (also called hubs) can act as drivers for many nodes simultaneously and influence the other nodes easily. Similarly, removal of such high degree nodes can break the network into disjoint parts and hence stop its functioning. Spreading processes like epidemics, rumors or information also get affected because of the presence or absence of such high degree nodes. Thus, it is of utmost importance to find out the hypotheses that lead to the existence of such high degree nodes in real networks. Such hypotheses should also explain the observed universality in the degree distribution of real networks pertaining to diverse physical systems.

The Barabási-Albert model explains the observed power-law degree distributions in real networks using two generic mechanisms: growth and preferential attachment. Almost all real networks are not static in size and keep increasing their sizes by the addition of nodes. The typical time span over which such growth happens can vary drastically from system to system. For example, social networking sites like Facebook increase their size by thousands of users every day whereas the protein interaction network present inside living cells might take several generations for the addition of a single node. However, increase in size seems to be the universal feature of real networks. Secondly, when new node enters the network, it joins to some of the previously present nodes. These nodes, to which a new node gets attached are selected by the new node randomly but the nodes with higher degree have higher probability to get selected. This is called 'preferential attachment'. At least for some real networks, existence of preferential attachment is obvious. For example, in World Wide Web , a newly created page would usually connect to famous pages like Google, Yahoo or Amazon which already have quite high degree values. Similarly, a highly cited scientific paper is more visible to researchers and hence gets cited even more resulting in the rapid increase in its degree.

In concrete terms, the Barabási-Albert model starts with a small number (m_0) nodes and at every time step a new node is added to the network. The new node connects to m ($< m_0$) different vertices present previously such that the probability $\Pi(k)$ of connecting to a node with degree k is proportional to k. This model gives rise to a network that has a power-law degree distribution asymptotically. Almost all of the more accurate generative models of real networks use the basic features of this model directly or indirectly. A small Barabási-Albert network is shown in Fig. 1.5(a) and the degree distribution of such networks is shown in Fig. 1.5(b).

1.6 Summary

In this chapter we describe various aspects in the study of complex networks. The two themes that arise in this study are structure of complex networks and processes on networks. We describe the classification of networks based on the structure and introduce various quantifiers that have been developed to quantify the structure of complex networks. In the next chapter we describe the nonlinear dynamical systems and their collective behavior when they are coupled on complex networks. In the same chapter we also describe the importance and various methods that are used to control the dynamics on networks. In chapter 3, we present a novel coupling scheme proposed by us for controlling the dynamics on lattices and networks. In chapter 4, we discuss the generative model that we developed to explain the structure of real world networks and finally in chapter 5, we talk about the application of the framework of complex networks to the

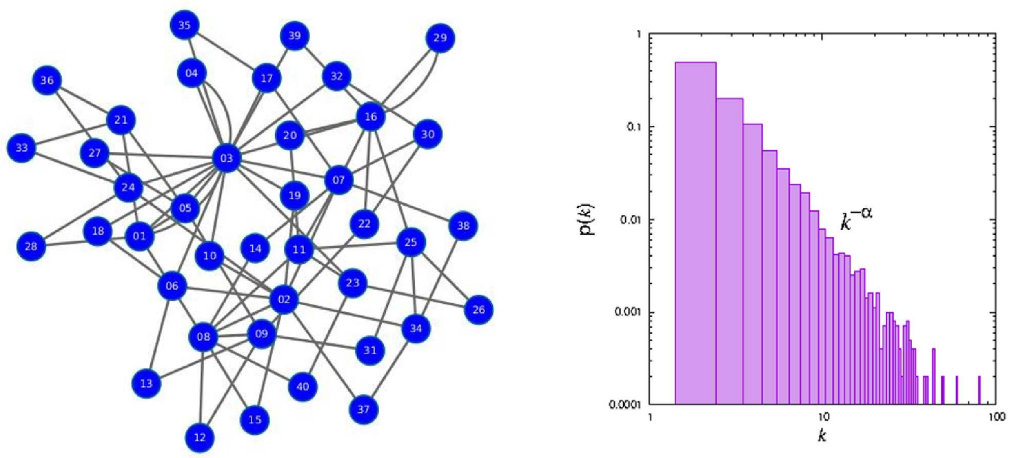

Figure 1.5: (a) Graphical representation of a small Barabási-Albert network with $N = 40$. Node 3 can be seen to be the biggest hub in this network. (b) Degree distribution of a large Barabási-Albert network ($N = 10000$). The distribution can be seen to be following a power-law with index α.

problem of divisibility patterns of natural numbers. The thesis ends with a summary of the important results of our work and scope for further study in the concluding chapter.

Chapter 2

Dynamical Systems on Networks

2.1 Introduction

A very important subfield of the theory of complex networks is the study of nonlinear dynamical systems coupled in the form of a complex network. Many interesting behaviors emerge in such coupled systems which are otherwise absent in isolated nonlinear systems. Before looking at these emergent behaviors in detail, let us first describe the framework of dynamical systems briefly.

A dynamical system is an abstract mathematical construct that is used to model a deterministic physical situation involving time evolution of one or more physical quantities like population, atmospheric temperature or a phase of an oscillator. In particular, the nonlinear dynamical systems are of great relevance since many physical processes are inherently nonlinear. Many nonlinear dynamical systems show a rich variety of dynamical behavior including the very interesting dynamics called chaos. In the chaotic state, the system's variables evolve in an apparently irregular fashion even though their evolution equations themselves are completely deterministic.

The discovery of chaos in nonlinear systems has led to the complete and correct understanding of the systems which were otherwise thought of as having an element of randomness in them and has enabled us to develop many new theoretical and conceptual tools which can be used to understand the complicated behaviors occurring in these systems. Despite the complex behaviors shown by these systems, the dimensionality of these systems is usually found to be surprisingly small. Also, the chaotic behavior in nonlinear systems is seen to be quite universal and appears in many different systems like planetary motion, mechanical pendulums, optical systems, electrical circuits, chemical reactions, human heart, earth's atmosphere, nerve cells, ecology, lasers and so on. More importantly, the qualitative and quantitative features shown by these systems are remarkably similar and this makes the study of nonlinear dynamical systems very important as well as interesting. Because there exist such universal features which are independent of the details of the particular system, often the study of a particular nonlinear system provides insights into the behavior of other similar nonlinear systems.

Almost all nonlinear systems show a sudden qualitative change in their behavior as one or more parameters controlling them are varied. This phenomenon, called bifurcation, has many features that show a quantitative similarity across a diverse range of dynamical systems. Thus, it is important to quantify the types of bifurcations that can occur in nonlinear dynamical systems and hence a very big part of the theory of dynamical systems is devoted to the study of such bifurcations.

As mentioned above, nonlinear dynamical systems occur in many biological and technological contexts and many times their chaotic behavior is undesirable. In such situations, it becomes important to control them and make them behave in accordance with a desired dynamics. Several methods of control have been addressed over the years and now well suited techniques exist to bring chaotic systems to periodic or steady state behavior.

2.2 Nonlinear Dynamical Systems

A dynamical system represents time evolution and interdependence of several variables in a deterministic fashion. The variables in the dynamical systems can represent any physical quantity like population of a given species, temperature at a particular location, level of a particular enzyme in the human body or phase of an oscillator. Given the initial values of variables in the dynamical system, their values in the future are then deterministically determined by the relationships included in the dynamical system's equations. Dynamical systems can either be continuous or discrete.

A continuous dynamical system represents the relationships among its variables in the form of a set of coupled ordinary differential equations each one of which is of first order. Mathematically such continuous dynamical system is represented as follows.

$$\dot{\mathbf{x}} = \mathbf{f}(\mathbf{x}) \tag{2.1}$$

where the vector $\mathbf{x} \in \mathbb{R}^m$ and $\mathbf{f} : \mathbb{R}^m \Rightarrow \mathbb{R}^m$ and $\dot{\mathbf{x}}$ represents the derivative of $\mathbf{x}$ with respect to time t. The function $\mathbf{f}$ is assumed to be at least C^1 which means that it is differentiable and its first derivative is continuous.

A discrete dynamical system is represented by an iterated map as follows.

$$\mathbf{x}_{n+1} = \mathbf{f}(\mathbf{x}_n) \tag{2.2}$$

where n represents the discrete time and $\mathbf{x}_n$ is the vector at time n.

2.2.1 Phase space, attractors and basins

A mathematical space with a separate independent direction for each of the variables of the given dynamical system is called its phase space or state space. At any given moment, the state of the dynamical system can be represented by a single point in the system's phase space and as the state of the system evolves in time, this point traces a trajectory in the phase space. A very large number of nonlinear systems are dissipative, meaning that the volume of the set of initial conditions decreases under the system's time evolution and asymptotically the set of all those initial conditions settles to a region of phase space with a dimension smaller than the original dimension. This is guaranteed by Liouville's theorem [43]. The set of points in the phase space to which initial conditions of the dissipative system settle to is called an attractor of the system corresponding to those initial conditions. A system can have multiple coexisting attractors in the phase space.

The types of attractors occurring in dissipative systems are fixed points, limit cycles, quasiperiodic attractors, strange chaotic attractors, strange non-chaotic attractors and hyperchaotic attractors. Let us briefly have a look at all these attractors.

1. **Fixed point:** A fixed point of a dynamical system is defined as the point in phase space such that if the system starts with that point as its initial condition, it would remain there forever. In other words, the fixed point maps to itself under the time evolution of the system.

   For continuous systems, fixed point satisfies:

   $$\dot{\mathbf{x}}^* = \mathbf{0} \Longrightarrow \mathbf{f}(\mathbf{x}^*) = \mathbf{0} \tag{2.3}$$

   For discrete systems, it satisfies:

   $$\mathbf{x}^*_{n+1} = \mathbf{x}^*_n \Longrightarrow \mathbf{x}^*_n = \mathbf{f}(\mathbf{x}^*_n) \tag{2.4}$$

   Thus, the fixed points of a given dynamical system can be found out by solving these equations. In cases where it may not be possible to solve them analytically, numerical methods can be used.

   Also, it is perfectly plausible for a dynamical system to have no fixed point at all. For example, a one dimensional system $\dot{x} = x^2 + 1$ does not have any fixed point since the equation $x^2 + 1 = 0$ does not have any real solution.

2. **Limit cycle:** A limit cycle in the phase space of a dynamical system is the set of points which form a closed loop in the phase space such that if the system starts with one of the points in the set as its initial condition, it would keep traversing the same loop with a periodicity.

3. **Quasiperiodic attractor:** In certain cases, the oscillations of a nonlinear system can be a combination of two or more frequencies which can be inherent to the system itself or some of which might come from the external periodic forcing of the system. In such systems, if the ratios of all these frequencies is a rational number, asymptotically the system locks itself to the periodic behavior or limit cycle. On the other hand, if the ratio of two frequencies is irrational numbers, the motion of the system never exactly repeats itself but comes arbitrarily close to the previously traced trajectory in the phase space. Thus, the motion in this case seems like a

periodic case even though in the strict sense it is not periodic. Hence the attractor corresponding to such behavior is called quasiperiodic attractor. [44, 45]

4. **Strange chaotic attractor:** This attractor corresponds to the most complicated motion a dynamical system can exhibit. This type of attractor is bounded, usually has fractional dimensionality and any two infinitesimally close points on the attractor diverge exponentially from each other under system's time evolution. This is also known as sensitivity to initial conditions since any two slightly different initial conditions in this case lead to very different future states of the system. We will look at the chaotic behavior more closely as we go along.

In addition, higher dimensional systems can exhibit **strange nonchaotic states** where the attractor exhibits fractal nature without sensitivity to initial conditions. [46] So also, attractors can be **hyperchaotic** if there exist two or more independent directions in phase-space in which trajectories of the system diverge from each other. [47]

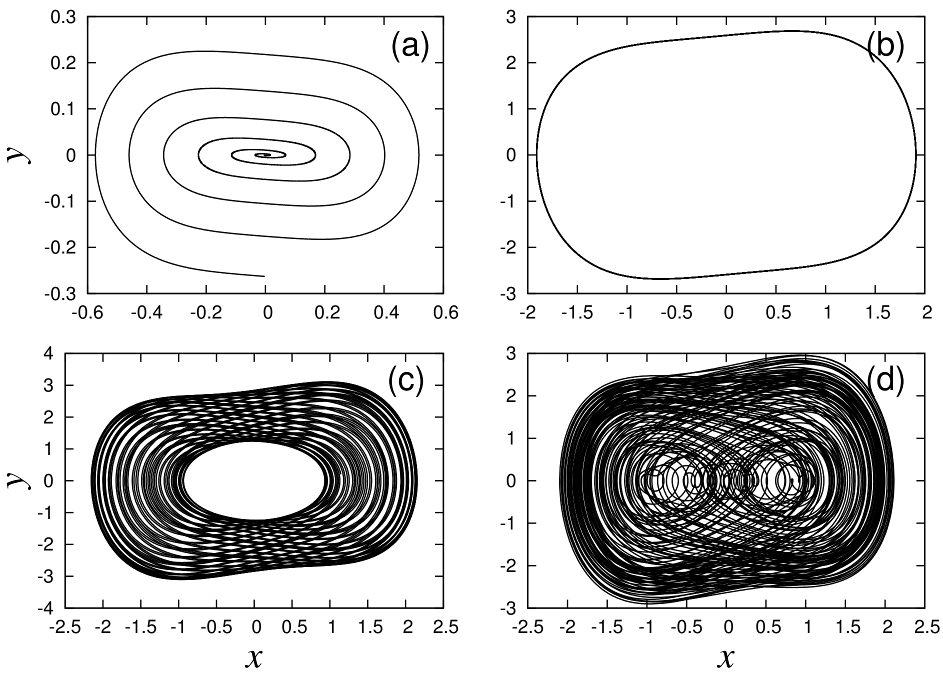

Figure 2.1: Plot showing different attractors for a typical nonlinear system. (a) Fixed point (including transients), (b) Limit cycle, (c) Quasi-periodic attractor, (d) Chaotic attractor

2.2.2 Basin of attraction

For certain dynamical systems, two or more attractors can coexist in the phase space. When multiple attractors coexist, which attractor the system would settle to depends on the initial condition of the system. The set of initial conditions in the phase space which eventually settle to a given attractor is called the basin of that particular attractor. The structure of a basin ranges from very simple to extremely complicated one depending upon the system. The complicated structure of the basin is not correlated with the complicated structure of the corresponding attractor and even fixed points can have very complicated basin structures like basins with fractal boundaries [48, 49].

2.2.3 Stability of the attractors

Stability refers to the robustness of the motion of the system on attractors against any perturbation. While the system is on the attractor, if the system is displaced slightly, its trajectory may or may not return to the attractor. If it doesn't and either reaches to another attractor or flies off to infinity, the attractor is said to be unstable. If the trajectory remains in the vicinity of the attractor or asymptotically settles back to attractor, the attractor is said to be stable. Below we discuss stability of fixed points and limit cycles.

- **Stability of a fixed point:** Consider a $m-$dimensional continuous time dynamical system $\dot{\mathbf{x}} = \mathbf{f}(\mathbf{x})$ with $\mathbf{x}^*$ as its fixed point. The stability of this fixed point can be checked by considering the evolution of a perturbed state $\mathbf{x}^* + \delta\mathbf{x}$ where $\delta\mathbf{x}$ is an initial perturbation vector. Thus, we have:

$$\dot{\mathbf{x}}^* + \delta\dot{\mathbf{x}} = \mathbf{f}(\mathbf{x}^* + \delta\mathbf{x}) \tag{2.5}$$

Expanding the L.H.S. into Taylor series, we get:

$$\dot{\mathbf{x}}^* + \delta\dot{\mathbf{x}} = \mathbf{f}(\mathbf{x}^*) + \left.\frac{d\mathbf{f}}{d\mathbf{x}}\right|_{\mathbf{x}^*} \delta\mathbf{x} + O(\delta\mathbf{x}^2) \tag{2.6}$$

where, the derivative in the second term represents the Jacobian $\left.\frac{d\mathbf{f}}{d\mathbf{x}}\right|_{\mathbf{x}^*}$ evaluated at x^*:

$$\mathbf{J} = \begin{bmatrix} \frac{df_1}{dx_1^*} & \frac{df_1}{dx_2^*} & \frac{df_1}{dx_3^*} & \cdots & \frac{df_1}{dx_m^*} \\ \frac{df_2}{dx_1^*} & \frac{df_2}{dx_2^*} & \frac{df_2}{dx_3^*} & \cdots & \frac{df_2}{dx_m^*} \\ \cdots & \cdots & \cdots & \cdots & \cdots \\ \frac{df_m}{dx_1^*} & \frac{df_m}{dx_2^*} & \frac{df_m}{dx_3^*} & \cdots & \frac{df_m}{dx_m^*} \end{bmatrix} \tag{2.7}$$

where f_i and x_i are i^{th} components of vectors $\mathbf{f}$ and $\mathbf{x}$ and $\frac{df_i}{dx_j^*}$ represents the derivative of f_i with respect to x_j evaluated at the fixed point $\mathbf{x}^* = [x_1^* \quad x_2^* \quad \ldots \quad x_m^*]^T$.

Neglecting the higher order terms in Eq.(2.6) and noting that $\dot{\mathbf{x}}^* = \mathbf{f}(\mathbf{x}^*)$, we get a linear system:

$$\delta\dot{\mathbf{x}} = \mathbf{J}\delta\mathbf{x} \tag{2.8}$$

The perturbation $\delta\mathbf{x}$ would go to 0 if real parts of all the eigenvalues λ_i of Jacobian matrix J are negative. If any one of them is positive, the perturbation would grow in time and hence the fixed point would not be stable. Thus, the stability of a fixed point, can be analyzed by calculating all the eigenvalues of the Jacobian matrix of the corresponding dynamical system evaluated at the that fixed point and fixed point is stable only if:

$$\mathrm{Re}(\lambda_i) < 0 \quad \text{for} \quad i = 1, 2, \ldots m \tag{2.9}$$

The fixed point for which all the eigenvalues of the corresponding Jacobian are non-zero is called an **hyperbolic fixed point**. If the fixed point $\mathbf{x}^*$ is not hyperbolic, the stability cannot be analyzed only by looking at the spectrum of the Jacobian and one must consider the contribution of the higher order terms.

In a similar way, the stability of the fixed point of a discrete dynamical system can be analyzed in terms of the eigenvalues of the Jacobian. Again, consider a discrete dynamical system $\mathbf{x}_{n+1} = \mathbf{f}(\mathbf{x}_n)$ with $\mathbf{x}^*$ as its fixed point. Thus, $\mathbf{f}(\mathbf{x}^*) = \mathbf{x}^*$. To check the stability, let us consider the time evolution of a perturbed state $\mathbf{x}^* + \delta\mathbf{x}$. If $\delta\mathbf{x}_n$ is the perturbation vector at time n, then we have:

$$\begin{aligned} \mathbf{x}^* + \delta\mathbf{x}_{n+1} &= \mathbf{f}(\mathbf{x}^* + \delta\mathbf{x}_n) \\ \mathbf{x}^* + \delta\mathbf{x}_{n+1} &= \mathbf{f}(\mathbf{x}^*) + \left.\frac{d\mathbf{f}}{d\mathbf{x}}\right|_{\mathbf{x}^*} \delta\mathbf{x}_n + O(\delta\mathbf{x}_n^2) \end{aligned} \tag{2.10}$$

Here, similar to the continuous system case, the derivative in the second term on R.H.S. represents the Jacobian of the system evaluated at the fixed point. Again, noting that $\mathbf{f}(\mathbf{x}^*) = \mathbf{x}^*$ and neglecting the higher order terms, we get a linear system:

$$\delta\mathbf{x}_{n+1} = \mathbf{J}\delta\mathbf{x}_n \tag{2.11}$$

However, unlike the case of continuous systems, the perturbation vector $\delta\mathbf{x}$ would vanish with time only if the absolute values of all the eigenvalues λ_i of the Jacobian J evaluated at fixed point are less than 1. Thus, the stability conditions for the fixed point for discrete systems can be represented as:

$$|\lambda_i| < 1 \quad \text{for} \quad i = 1, 2, \ldots m \tag{2.12}$$

- **Stability of a limit cycle:** Similar to the case of a fixed point, the stability of the limit cycle of the continuous time system can be analyzed by perturbing it slightly and then observing the behavior of the perturbation. If the perturbation dies off in the course of time, the limit cycle is stable; otherwise it is unstable. The stability analysis for the limit cycle is more complicated and is done by calculating the Floquet multipliers of the system [43]. Or in a simpler way, one constructs a discrete system called a **Poincare map** corresponding to the limit cycle motion. The stability of the fixed point of the Poincare map then implies the stability of the limit cycle [43].

2.2.4 Chaotic systems

Many nonlinear systems show chaotic behavior at least for some ranges of values of their parameters. As mentioned above, such behavior is characterized by a sensitive dependence on the initial conditions and apparently random trajectories in the system's phase space though the equations of motion themselves are completely deterministic. These systems are found in nature ubiquitously. Some typical examples of such systems are Belousov-Zhabotinsky reaction (chemistry) [50], lasers (nonlinear optics) [51], MLC circuit (electronics) [52], Rayleigh-Bénard convection (fluid dynamics) [53], neurons in brain (biology) [54], chaotically pulsating stars (astrophysics) [55] and so on. Two of the most famous and well studied mathematical models of continuous time dynamical systems that exhibit chaotic behavior are Lorenz system and Rössler system. Similarly, the prototypical discrete dynamical systems that exhibit chaos include logistic map and Hénon map [43]. We present their characteristics briefly below.

- **Lorenz system:** The Lorenz system is an oversimplified model for the atmospheric convection [56]. The model equations are developed from the Navier-Stokes equations for fluid flow and the equation describing thermal energy diffusion [43]. It consists of a set of three coupled first order nonlinear differential equations as given below:

$$\begin{aligned} \dot{x} &= \sigma(y-x) \\ \dot{y} &= x(\rho-z)-y \\ \dot{z} &= xy-\beta z \end{aligned} \tag{2.13}$$

  In this set of equations, σ, ρ and β are the parameters whose values depend on the physical situation. Depending on their values, the Lorenz system exhibits fixed point, limit cycle or chaotic behavior. The same set of equations also arise in the simplified models of lasers [57], chemical reactions [58] and chaotic water wheel [59]. A typical limit cycle and chaotic attractor of the Lorenz system are shown in Fig. 2.2.

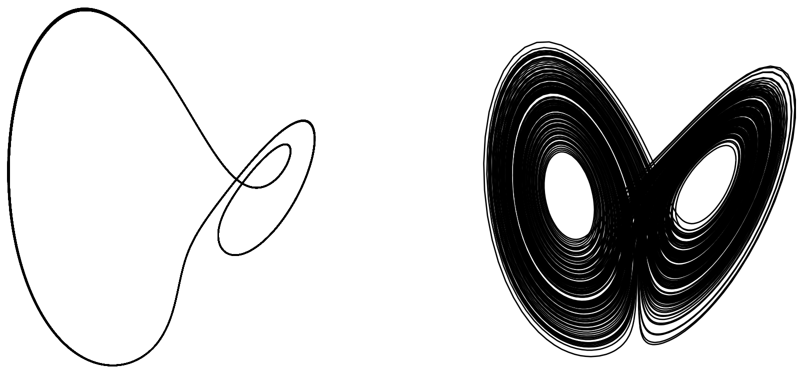

Figure 2.2: Limit cycle and chaotic attractor for Lorenz model (Eq.(2.13)). The parameter values are: $\sigma = 10, \beta = 8/3, \rho = 100.5$ (periodic attractor) and $\sigma = 10, \beta = 8/3, \rho = 28$ (chaotic attractor).

Rössler system: Rössler system is another prototype system exhibiting chaos and is represented by the following equations [43].

$$\begin{aligned} \dot{x} &= -y - z \\ \dot{y} &= x + ay \\ \dot{z} &= b + z(x - c) \end{aligned} \tag{2.14}$$

Similar to Lorenz system, depending upon the values of parameters a, b, c the Rössler system exhibits periodic or chaotic motion. These attractors for Rössler system are shown in Fig. 2.3.

- **Logistic map:** The logistic map is a one-dimensional discrete system represented by the following equation:

$$x_{n+1} = rx_n(1 - x_n) \tag{2.15}$$

where $r \in [0, 4]$ is a parameter that controls the nonlinearity and x is restricted to the interval $[0, 1]$. This map shows a diverse range of behaviors depending upon the value of r. These behaviors include fixed points, cycles and chaotic behavior. This map arises in population dynamics and can model several other physical situations

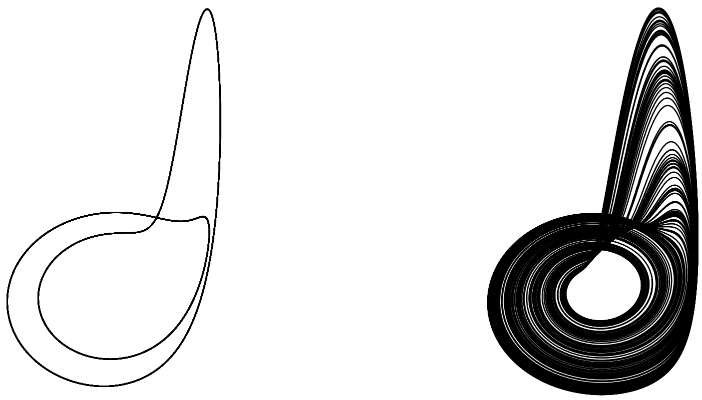

Figure 2.3: Limit cycle and chaotic attractor for Rössler model (Eq.(2.14)). The parameter values are: $a = 0.2, b = 1, c = 5.7$ (periodic attractor) and $a = 0.2, b = 0.2, \rho = 5.7$ (chaotic attractor).

[43, 59]. The time series of the logistic map is represented in Fig. 2.4 for $r = 4$ which corresponds to chaotic regime.

The whole range of behaviors of this map can be visualized succinctly using a bifurcation diagram. The bifurcation diagram shows the asymptotic values of a given variable of a dynamical system as a function of a parameter of the system. The bifurcation diagram of the logistic map as the parameter r is varied, is shown in Fig. 2.5. It can be seen that as the parameter r is varied, the map becomes chaotic at $\simeq 3.56$ via a period doubling sequence. It can also be seen that there exists windows of periodic behavior inside chaotic regime.

Hénon map: This map is a two dimensional discrete dynamical system and is represented by the following equations:

$$\begin{aligned} x_{n+1} &= 1 - a x_n^2 + y_n \\ y_{n+1} &= b x_n \end{aligned} \tag{2.16}$$

It exhibits chaotic behavior for the parameter values $a = 1.4$ and $b = 0.3$. The attractor in phase space for Hénon map for these parameter values is shown in Fig. 2.6(a) and a corresponding bifurcation diagram in Fig. 2.6(b).

Rulkov map: This is a two-dimensional discrete system that is used to model a biological neuron. In its simplest form, the model can be written in the following

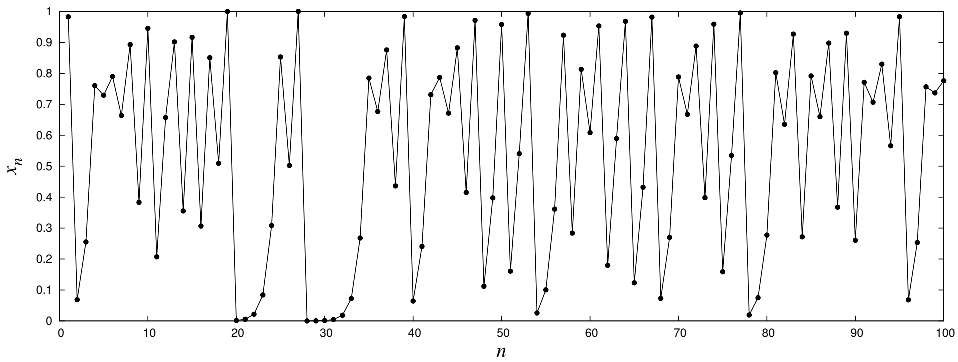

Figure 2.4: Time series of a logistic map for $r = 4$ exhibiting chaotic behavior.

form [60–62]:

$$\begin{aligned} x_{n+1} &= \frac{\alpha}{1+x_n^2} + y_n \\ y_{n+1} &= y_n - \beta x_n - \gamma \end{aligned} \tag{2.17}$$

In this set of equations, the time evolution of the variable x is fast as compared to that of the variable y. This is because the variables β and γ have much smaller values as compared to parameter α. The map exhibits different types of dynamical behaviors for different values of the parameter α as shown in Fig. 2.7.

2.2.5 Lyapunov exponents

The signature of chaotic behavior is the exponential divergence of trajectories which start from initial conditions that are very close to each other. However, since the trajectories on the attractor always remain bounded, the divergence is only local and the rate of divergence varies from one region of the attractor to the other. Hence, one always talks in terms of average value of the divergence for a given attractor. A nice way to quantify the local divergence of the system is to define a set of quantities called Lyapunov exponents. In technical terms, if two trajectories start from two points on the attractor separated by an infinitesimal separation $|\delta\mathbf{X}(0)|$, the magnitude of the separation vector evolves in time as [43, 63]:

$$|\delta\mathbf{X}(t)| = e^{\lambda t}|\delta\mathbf{X}(0)| \tag{2.18}$$

The quantity λ in this equation is called a Lyapunov exponent which measures the rate of separation of nearby trajectories. The value of λ in general depends on the orientation of the initial separation vector and hence the dynamical system has as many Lyapunov exponents λ_i as the dimensionality of the system. The maximal Lyapunov exponent of

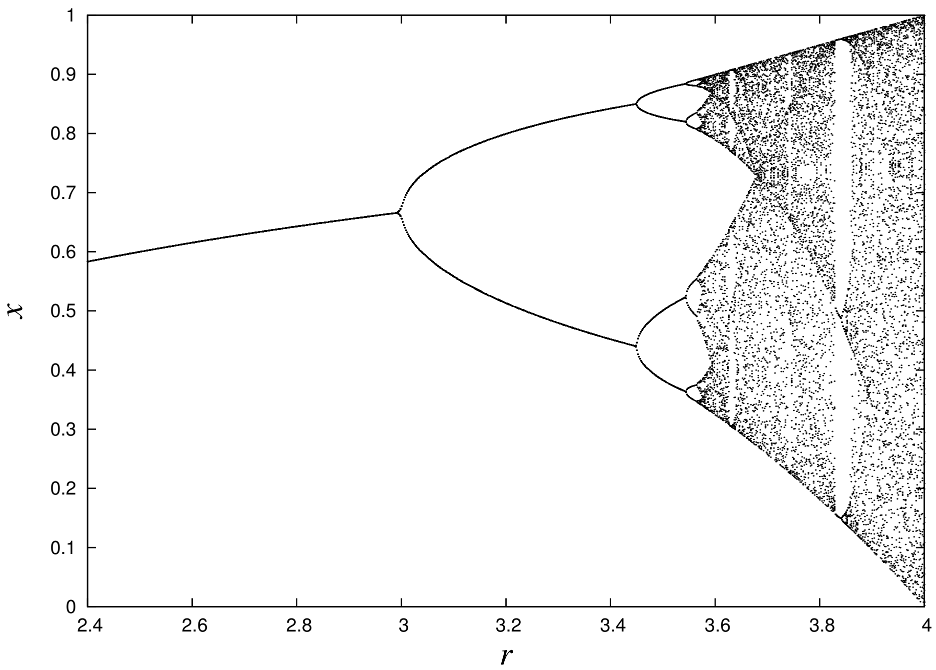

Figure 2.5: Bifurcation diagram of a logistic map as the parameter r is varied. The diagram is shown for values of r which are greater than 2.4 below which only the fixed point behavior exits. $Y-$axis shows the asymptotic values that variable x takes for a given value of r.

the system is defined as follows:

$$\lambda_m = \lim_{t\to\infty} \lim_{\delta\mathbf{X}_0\to 0} \frac{1}{t} \ln \frac{|\delta\mathbf{X}(t)|}{|\delta\mathbf{X}(0)|} \tag{2.19}$$

The limit $\delta\mathbf{X}_0 \to 0$ ensures that the linear approximation is valid.

The nature of the attractor is linked to its Lyapunov exponents' spectrum. In particular, the necessary condition for the attractor to be chaotic is that at least one of the exponents should be positive since there should be divergence of trajectories at least in one direction. For systems that are chaotic, there would be maximum divergence in the direction of the maximal Lyapunov exponent λ_m. Thus, this exponent affects the predictability of the system most since the effect of the other exponents is obliterated in the course of time. Also, in case of continuous time dynamical systems, at least one Lyapunov exponent must be 0 since along the trajectory there is no divergence. Finally, since no trajectory can leave the attractor (fixed point, limit cycle or chaotic attractor) and the attractor is always bounded, at least one Lyapunov exponent must be negative.

The typical spectrum of Lyapunov exponents for various types of attractors is given below in Table 2.1 with the convection that $\lambda_1 \leq \lambda_2 \leq \cdots \leq \lambda_m$ where m is the dimensionality of the system.

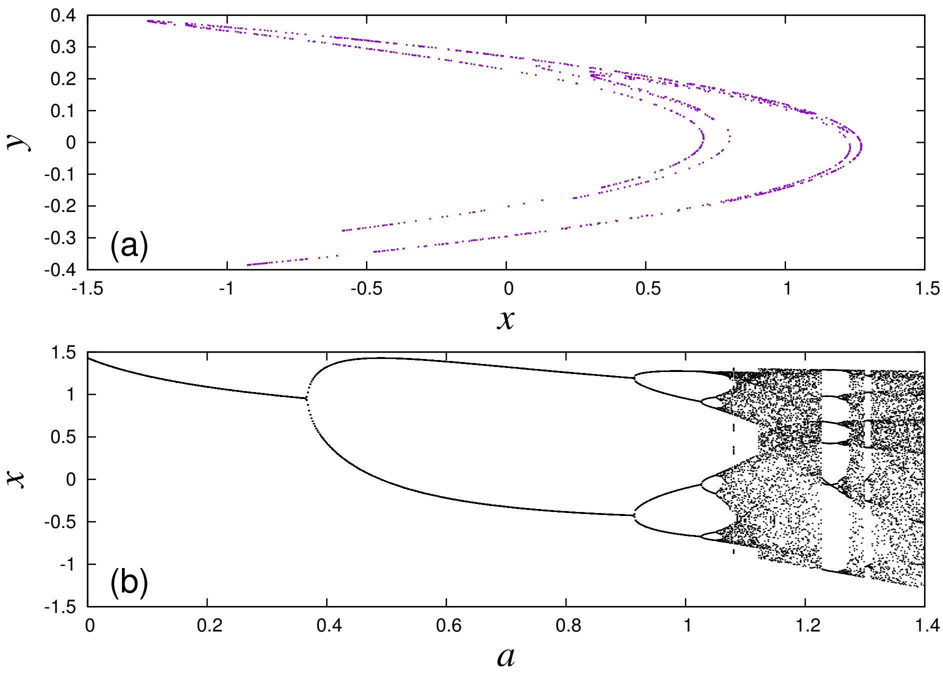

Figure 2.6: (a) Phase space plot for the Hénon map represented by Eq.(2.16) for $a = 1.4$ and $b = 0.3$ (chaotic regime) (b) bifurcation diagram for Hénon map with $b = 0.3$ and varying a.

There are specific algorithms for numerically calculating these exponents [43, 63]. In addition, the geometry of the attractor is characterized using fractal dimensions and multifractal spectrum. In general, even in cases where modelling equations are not known, these measures can be computed from an observed data of one of the variables of the system using the techniques developed in nonlinear time series analysis [64, 65].

2.3 Emergent dynamics on complex networks

When nonlinear systems are coupled to form a network, they affect each other's evolution. Such interactions between the nonlinear systems many times give rise to dynamics which are not present in isolated systems. Such emergent collective behaviors, apart from being very interesting in their own right, also provide explanation of complex behaviors observed in many natural systems. Such dynamical units coupled on networks can be represented by the following equation.

$$\dot{\mathbf{x}}_i = \mathbf{f}(\mathbf{x}_i) + D \sum_j A_{ij} \mathbf{g}(\mathbf{x}_i, \mathbf{x}_j) \tag{2.20}$$

Similarly, the discrete time dynamical units coupled in the form of a network can be

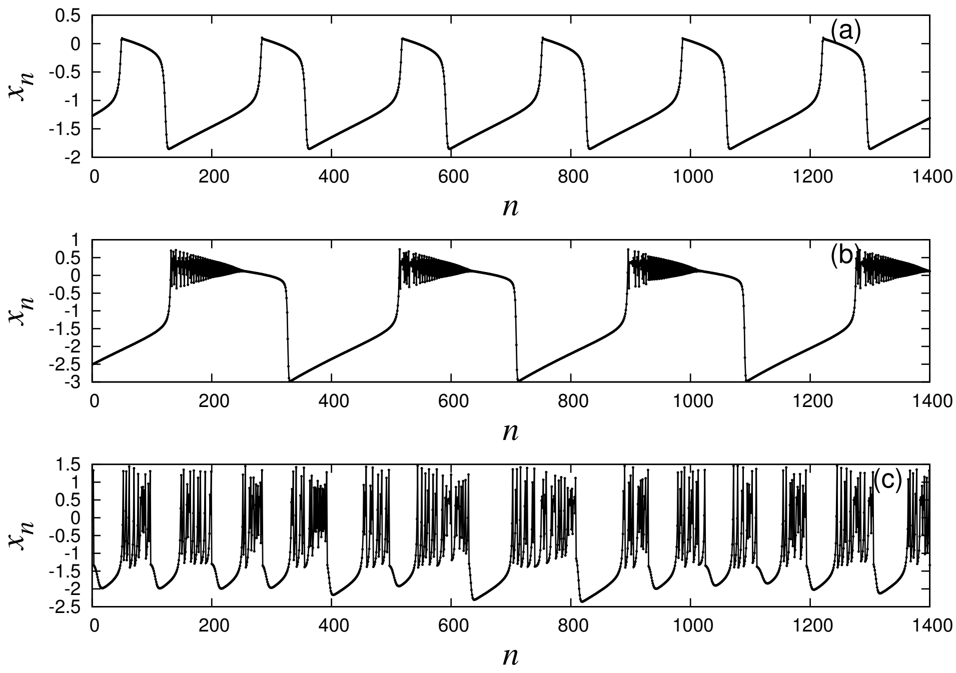

Figure 2.7: Time series of x variable of Rulkov map for three different values of the parameter α with $\beta = \gamma = 0.004$: (a) For $\alpha = 2.2$ the map exhibits a limit cycle behavior, (b) at $\alpha = 3.2$ map develops slight irregular bursts on top of spikes, (c) for $\alpha = 4.2$ map shows a fully chaotic burst behavior.

represented in the following way.

$$\mathbf{x}_i(n+1) = \mathbf{f}(\mathbf{x}_i(n)) + D \sum_j A_{ij} \mathbf{g}(\mathbf{x}(\mathbf{n})_i, \mathbf{x}(\mathbf{n})_j) \tag{2.21}$$

Here the function g is a coupling function, A_{ij} is an element of the adjacency matrix and D is a coupling strength. We describe some of the most important emergent behaviors exhibited by such coupled nonlinear systems.

2.3.1 Synchronization

Synchronization refers to the coordinated dynamics of the interacting units forming the network and is observed in a large number of natural and man made systems. Some of the typical systems which exhibit synchronization under suitable conditions are neurons in human brain connected by synapses, power grids connected by high voltage lines, coupled pendulums, cardiac cells in heart, fireflies flashing in synchrony and so on. This has found several engineering applications like secure communication [66]. Out of many different types of synchronizations that exist, two important ones are complete synchronization and phase synchronization [38].

Table 2.1

Sr.No.	Lyapunov exponents	Type of an attractor
1	$\lambda_i < 0 \quad \forall\ i$	Fixed point
2	$\lambda_1 = 0$, all other $\lambda_i < 0$	Limit cycle
3	$\lambda_{1,2} = 0$, all other $\lambda_i < 0$	Quasiperiodic attractor
4	$\lambda_1 > 0, \lambda_2 = 0$, all other $\lambda_i < 0$	Chaotic attractor
5	$\lambda_{1,2} > 0$ (at least), $\lambda_3 = 0$, all other $\lambda_i < 0$	Hyperchaotic attractor

Complete synchronization: In case of complete synchronization, all the systems in the network oscillate in unison even though they start with different initial conditions. In such a state, the values of corresponding variables of all the subsystems are exactly same. As an example of this, the time series of two x variables of two Rössler systems coupled on a network is shown in Fig. 2.8. It can be seen that even though the systems start with different initial conditions, they eventually completely synchronize and their trajectories fall on top of each other.

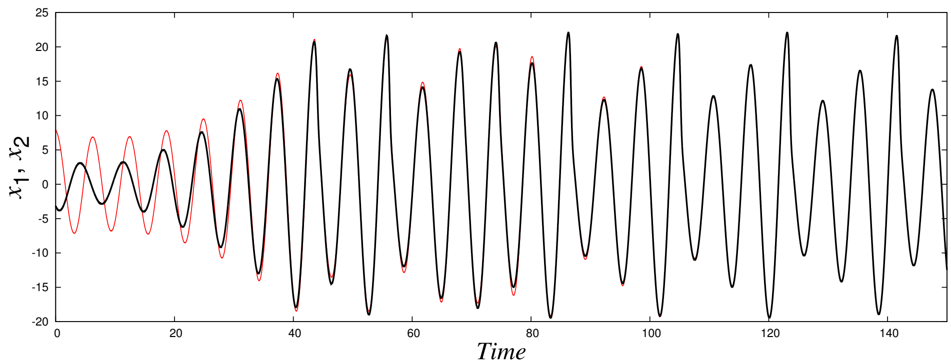

Figure 2.8: Complete synchronization: The time series of two interacting Rössler systems from a network of 10 systems. They start with different initial conditions, but because of coupling they become completely synchronized with time.

If there are N systems in the network, we can define a synchronization index as follows:

$$S(t) = \frac{1}{N}\sqrt{\sum_i (\langle x \rangle_t - x_i(t))^2} \tag{2.22}$$

where,

$$\langle x \rangle_t = \frac{1}{N}\sum_i x_i(t) \tag{2.23}$$

When asymptotically complete synchronization occurs for all the systems on the network, $S(t) \to 0$.

Apart from complete synchronization, many other types of synchronization occur in a network of coupled nonlinear systems like lag synchronization, phase synchronization, anti-phase synchronization, anticipatory synchronization, generalized synchronization and so on. Some of these are illustrated using time series in Fig. 2.9.

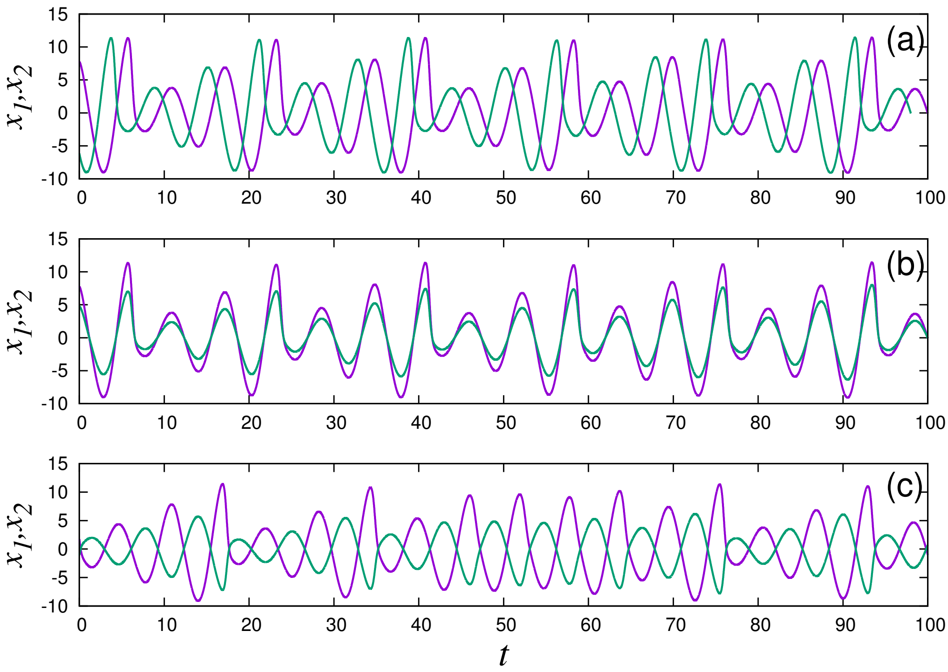

Figure 2.9: Time series of two coupled systems showing various types of synchronizations: (a) lag synchronization, (b) phase synchronization, (c) anti-phase synchronization.

2.3.2 Amplitude death and Oscillation death

When nonlinear dynamical systems are coupled together, under suitable conditions, all of them can go to a fixed point state of the coupled system. Various terms have been coined to describe this phenomenon depending upon the characteristics of the final fixed point state and the type of dynamical systems which are coupled [67, 68]. When the fixed point state of the coupled system is such that each of the subsystems reaches to the same value of the steady state, the phenomenon of cessation of oscillations is termed as **Amplitude death**. On the other hand, if in the asymptotic fixed point state each subsystem reaches to different values of the steady state (though some of them can be same), the phenomenon is called **Oscillation death** [68].

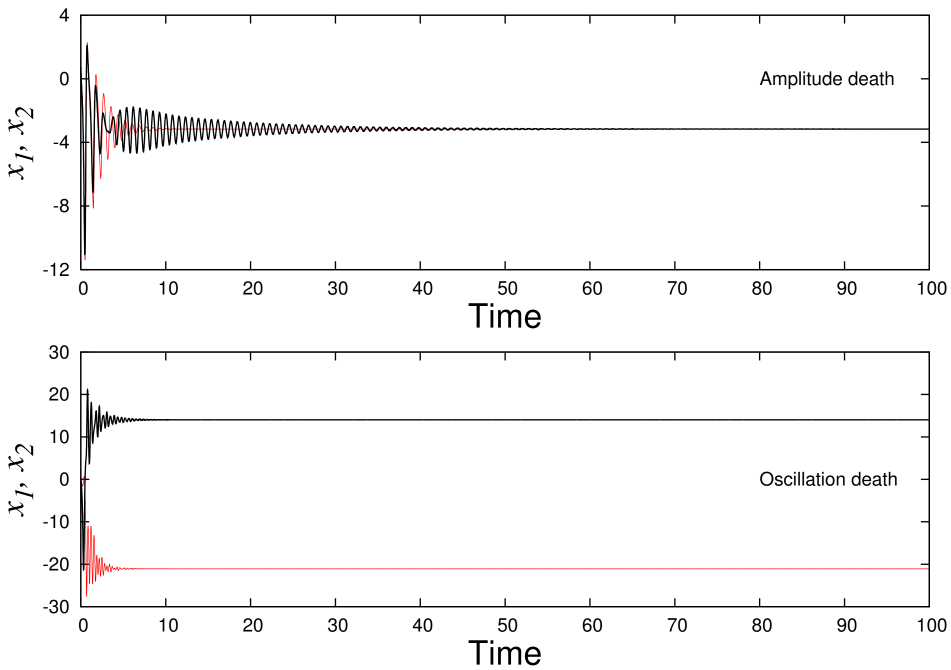

Figure 2.10: Amplitude death and Oscillation death: In case of amplitude death, the steady states of all the systems have the same value. In oscillation death, the systems generally go to the different steady states.

2.3.3 Chimera states

An extremely interesting behavior reported recently occurring in identical nonlinear systems coupled in an identical way, is the chimera states. This state characterized by spontaneous breakup of a population of identical oscillators into clusters of synchronized and desynchronized behavior [69, 70].

Existence of chimera states has been reported in many different types of systems including non-locally coupled identical nonlinear oscillators [71–73], globally coupled oscillators [70], discrete maps [74, 75], phase oscillators on complex networks [76] and so on. The unihemispherical sleep in many animals provides a natural example of chimera state where the awake side of the brain shows desynchronized electrical behavior whereas the sleeping side is synchronized [77, 78]. Recently, they have also been realized experimentally [79, 80] and have appeared in SQUID metamaterials [81]

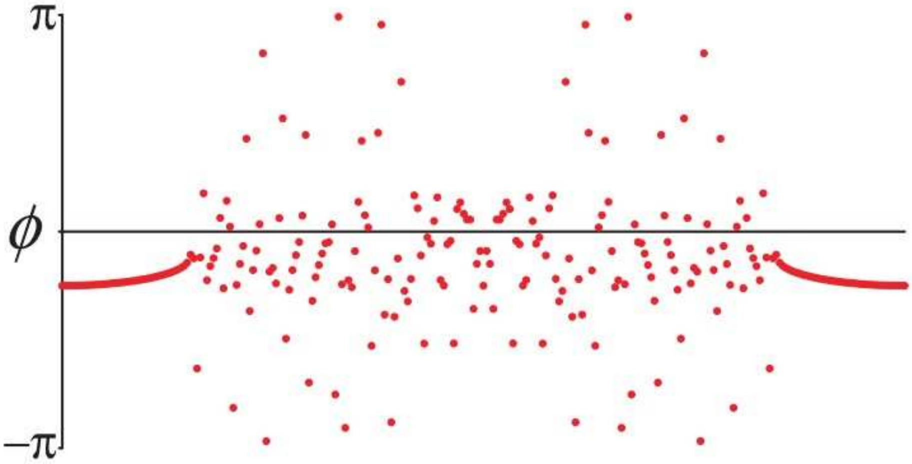

Figure 2.11: Graphical representation of the chimera state in a ring of nonlocally coupled limit cycle oscillators with oscillator indices on $X-$axis and phases ϕ of those oscillators on $Y-$axis.(from [69])

2.4 Control of dynamics in spatially extended systems and on networks

In many of the nonlinear systems, the chaotic behavior is undesirable and a periodic or a constant output from the system may be required. To achieve this, many strategies have been suggested which can suppress the chaos in the system.

There exists an infinite number of unstable periodic orbits (UPOs) inside a chaotic attractor [82]. Initial methods suggested to control chaos take advantage of the existence of these periodic orbits and stabilize one of them. Thus, these methods turn the chaotic motion in the system into an advantage since one can obtain an infinite number of periodic motions from the same system. The initial strategy suggested by Ott, Grebogi and Yorke uses a small time-dependent perturbations of an available system parameter [83]. It was shown by Ott et al that using such parametric perturbation, one can bring the initial chaotic trajectory of the system to a desired periodic trajectory. A different method of control to stabilize the UPOs was suggested by Pyragas which consists of a delayed feedback to the system [84].

Also, various other methods to eliminate chaos from the system were suggested around the same time. For example, it was shown that starting from a chaotic regime, a small parametric perturbation of suitable frequency can bring the system to a regular regime [85]. The another approach that was proposed was to use a small external periodic forcing to the system to suppress chaos [86].

The methods mentioned above have also been extended to control spatio-temporal chaos in spatially extended systems [87, 88] and networks [89]. This is relatively a more challenging task since the system to be controlled usually has many more degrees of freedom all of which need to be controlled. These methods are useful in many applications like controlling the dynamics in plasma devices and chemical reactions [90, 91] and to reduce intensity fluctuations in laser systems [92, 93].

The method of pinning control of spatio-temporal chaos has turned out to be a very powerful tool. In this method, only few nodes in the lattice of dynamical systems are pinned and the control of the spatio-temporal chaos on the whole lattice is achieved [87, 94]. Also, local tiny perturbations have been shown to be effective in controlling spatio-temporal chaos [95].

A method of controlling dynamics on networks that has become quite popular in recent years is that of environmental coupling [89]. This method uses a common environment like external system that is connected to all the systems in the network. The external system has a dynamics of over-damped oscillator and under a linear feedback to the network, this external system is able to quench the dynamics on the nodes of a complex network to a steady state. This model can be represented as follows [89]:

$$\begin{aligned} \dot{\mathbf{x}}_i &= \mathbf{f}(\mathbf{x}_i) + D\sum_j A_{ij}\mathbf{g}(\mathbf{x}_i, \mathbf{x}_j) + \varepsilon_e \gamma w \\ \dot{w} &= -kw - \frac{\varepsilon_e}{N}\gamma^T \sum_i \mathbf{x}_i \end{aligned} \tag{2.24}$$

where γ is a column matrix with elements 0 or 1 and decides which components of the system $\mathbf{x}_i$ get feedback from the external variable w. This method of controlling the dynamics on complex networks has been shown to be effective for diverse range of network topologies as well as for many different nonlinear systems. Also, it has been shown that there exists a universal relation between the largest eigenvalue of the coupling matrix and the critical value of the coupling at which the amplitude death happens in the network.

Another method of controlling the dynamics on networks is that of mean-field diffusion [96]. In this type of coupling scheme, each oscillator is coupled to a mean-field which is simply an average value of a dynamical variable on the nodes. Thus, the evolution of dynamics on i^{th} node is given by:

$$\dot{\mathbf{x}}_i = \mathbf{f}(\mathbf{x}_i) + D\beta(Q\langle\mathbf{x}\rangle - \mathbf{x}_i) \tag{2.25}$$

where as before,

$$\langle\mathbf{x}\rangle = \frac{1}{N}\sum_{j=1}^{N}\mathbf{x}_j \tag{2.26}$$

Also, β is $m \times m$ matrix and Q is an adjustable parameter describing the influx of the mean field in the individual systems. It has been shown that such coupling gives rise to amplitude death for all the systems in the network and the transition is via synchronization as the coupling strength is increased [96]. The same scheme has also been extended to cover the case of dynamical systems with intrinsic time-delay [97].

Another popular scheme which gives rise to amplitude death in a network of nonlinear systems is the coupling with various types of delays in the coupling [67]. For example, it has been demonstrated that when there is a mixing of instantaneous coupling and time-delayed coupling in the network of oscillators, amplitude death occurs for sufficiently large value of coupling [98]. Similarly, it has been shown that time-varying delay in the coupling can give rise to amplitude death in the network of dynamical systems [99]. So also, local repulsive links have been shown to give rise to oscillation death in a network of nonlinear oscillators [100]. Likewise, many other methods involving time delayed feedback to control dynamics have been invented [99, 101, 102]. Similar to the method of control in spatio-temporal chaos, pinning control, where only few nodes of the network are made to have a desired constant value has been shown to be effective in controlling the dynamics of all the nodes of the network [103].

2.5 Summary

In this chapter we describe various aspects of nonlinear dynamical systems and the emergent behavior which occur in them when they are coupled on a network. Dissipative nonlinear systems possess attractors, the set of points on which a system would eventually settle to and there exist several types of attractors like fixed points, limit cycles and chaotic attractors for nonlinear systems. We discuss the stability theory for fixed points and discuss the characterization of chaotic attractors in terms of Lyapunov exponents. Later in the chapter, we discuss the issue of control of dynamics in spatial extended systems and networks and various major schemes which have been developed over the years to achieve such a control. In the next chapter, we plan to describe a novel coupling scheme that we propose to achieve control of dynamics on random networks as well as in spatially extended systems.

Chapter 3

Novel coupling scheme to control dynamics of coupled systems

3.1 Introduction

As discussed in the previous chapter, dynamical systems can give rise to many different emergent behaviors like synchronization and amplitude death when they interact with each other on a complex network. In fact, many spatially extended systems can be modelled using simple two dimensional lattices where only the local interactions between the subsystems are enough to explain the behavior of the extended system. The examples of this include reaction-diffusion systems [104], crystal growth [105], excitable media [106, 107], heart [108], pancreas [109], boiling [110] and cloud dynamics [111]. As mentioned in the previous chapter, in many cases of interest, it is necessary to control the spatial as well as temporal dynamics of such extended systems which is much more difficult since the number of degrees of freedom is very large. The methods developed so far to achieve such control usually need to continuously monitor the system in question, take output from it and then change the amount of control depending upon the output.

In the present work, we introduce a novel control scheme which can be used to effectively control the dynamics of spatially extended systems like lattices as well as complex networks. The effectiveness of the scheme is evident from the fact that it does not need any prior information of the system's dynamics and hence can be applied to a wide variety of dynamics. This scheme can be thought of as a generalization of the scheme of environmental coupling introduced in [112] and [89] in two different directions. The environment or the external medium is now spatially extended which is a much more realistic view in case of spatially extended systems or an external medium. Secondly, the scheme can now control discrete dynamics also which is a non-trivial extension of the continuous time case.

We start by analyzing the scheme for controlling the dynamics in single units with logistic map and Hénon map and present the exact stability analysis of the steady states achieved by control. Then we apply the scheme to control the collective dynamics of a ring of such discrete time dynamical systems and using the theory of circulant matrices and the stability theory for discrete dynamical systems, analytically prove the existence of steady states in this case. In all these, we verify the analytical results by direct numerical simulations and show that the agreement is excellent in each of these cases. This allows us to isolate the regions of effective control in various parameter planes and we find that the scheme provides a sufficiently large range of parameter values for which the control can be achieved. We also present a generalization of this scheme with random interconnections between two rings. As an application, we demonstrate the effectiveness of the scheme for two physical situations: control of excitation patterns in neurons and control of experimentally realizable chimera states.

We also show that the proposed scheme works even for random networks and we find the stability of the steady state in this case using master stability method and verify the same with direct numerical simulations. The main result in this case is that the stability of the steady state as a function of the control parameter is directly related to the largest eigenvalue of the Laplacian of the network. We also generalize the scheme by considering the case of non-identical networks and demonstrate the validity of the scheme for such cases.

Further, we extend the scheme to coupled continuous dynamical systems and illustrate control using standard systems like Rössler system and Hindmarsh-Rose neuronal model.

The majority of the work presented in this chapter is published in *Commun. Nonlinear Sci. Numer. Simulat.* **25** (2015).

3.2 Control scheme for 1-d coupled map lattice

In this section we introduce our scheme for controlling a 1-d CML of size N by coupling with an equivalent lattice of damped systems. The dynamics at the i^{th} node of the system lattice constructed using the m-dimensional discrete dynamical system, $\mathbf{x}(n+1) = \mathbf{f}(\mathbf{x}(n))$, with time index n, is given by:

$$\mathbf{x}_i(n+1) \quad = \quad \mathbf{f}(\mathbf{x}_i(n)) + D\zeta(\mathbf{f}(\mathbf{x}_{i-1}(n)) + \mathbf{f}(\mathbf{x}_{i+1}(n)) - 2\mathbf{f}(\mathbf{x}_i(n))) \tag{3.1}$$

Here $\mathbf{x} \in \mathbb{R}^m$ is the state vector of the discrete system, $\mathbf{f} : \mathbb{R}^m \to \mathbb{R}^m$ is the nonlinear differentiable function. Also, D represents the strength of diffusive coupling and ζ is a $m \times m$ matrix, entries of which decide the variables of the system to be used in the coupling. The dynamics of a damped discrete map $z(n)$ in the external lattice is represented as:

$$z(n+1) = kz(n) \tag{3.2}$$

where k is a real number with $|k| < 1$. Thus for positive values of k, this map is analogous to over-damped oscillator while for negative values of k it is analogous to damped oscillator. The dynamics at the i^{th} node of the 1-d CML of size N of these maps with diffusive coupling can be represented by the following equation:

$$z_i(n+1) \quad = \quad g(z_i(n)) + D_e(g(z_{i-1}(n)) + g(z_{i+1}(n)) - 2g(z_i(n))) \tag{3.3}$$

We have, $g(z) = kz$ and D_e represents the strength of diffusive coupling among the nodes of the external lattice. We consider periodic boundary conditions for both the lattices. When the system lattice is coupled to the lattice of external systems, node to node, with feedback type of coupling, then the resulting system can be represented as:

$$\begin{aligned} \mathbf{x}_i(n+1) &= \mathbf{f}(\mathbf{x}_i(n)) + D\zeta(\mathbf{f}(\mathbf{x}_{i-1}(n)) + \mathbf{f}(\mathbf{x}_{i+1}(n)) - 2\mathbf{f}(\mathbf{x}_i(n))) + \varepsilon_1\xi z_i(n) \\ z_i(n+1) &= g(z_i(n)) + D_e(g(z_{i-1}(n)) + g(z_{i+1}(n)) - 2g(z_i(n))) + \varepsilon_2\xi^T\mathbf{x}_i(n) \end{aligned} \tag{3.4}$$

Here ξ is the $m \times 1$ matrix which determines the components of the state vector $\mathbf{x}$ which take part in the coupling with external system. Fig. 3.1 shows a schematic of the control system represented by these equations.

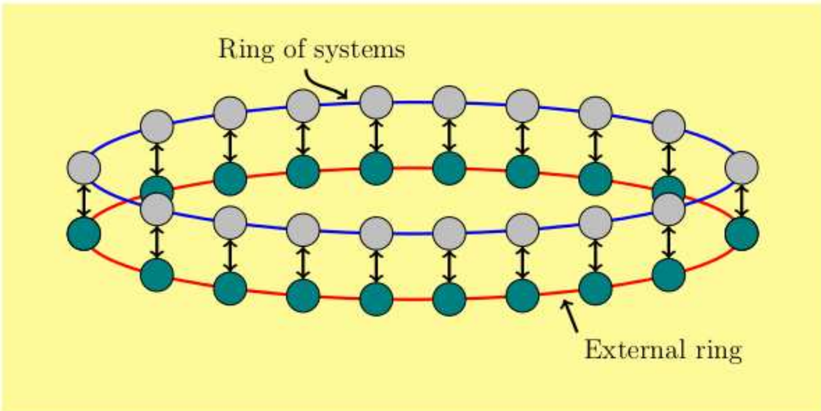

Figure 3.1: Schematic of a system ring coupled (upper) to an external ring (lower). The arrows between two rings represent the feedback coupling connections between the two rings.

In the next section we start with the analysis of control for one unit of this coupled system. Then we study the case of 1-d CML and 2-d CML and extend the scheme to random networks. In all these cases, for direct numerical simulations, the typical discrete systems considered are the logistic map and the Hénon map. As a typical application, we then show how the proposed scheme can be applied to control experimentally realizable chimera states as well as various types of patterns produced in the neuronal systems.

3.2.1 Analysis of control in a single unit of the model

The dynamics of a single unit of the model introduced in Eq.(3.4) is given by a discrete system coupled to an external system in a feedback loop as:

$$\begin{aligned}\mathbf{x}(n+1) &= \mathbf{f}(\mathbf{x}(n)) + \varepsilon_1 \xi z(n) \\ z(n+1) &= g(z(n)) + \varepsilon_2 \xi^{\mathbf{T}} \mathbf{x}(n)\end{aligned} \tag{3.5}$$

To proceed further we consider logistic map as system dynamics to get:

$$\begin{aligned}x(n+1) &= rx(n)(1-x(n)) + \varepsilon_1 z(n) \\ z(n+1) &= kz(n) + \varepsilon_2 x(n)\end{aligned} \tag{3.6}$$

The parameter r whose value determines the intrinsic nature of dynamics of logistic map is chosen as $r = 3.6$, so that the map is in the chaotic regime. Time series $x(n)$ obtained from Eq.(3.6) numerically is plotted in Fig. 3.2 for two different values of coupling strength with $\varepsilon_1 = -\varepsilon_2$. The control is switched on at $n = 50$ and we find that depending on the coupling strength, the chaotic dynamics can be controlled to periodic or steady state.

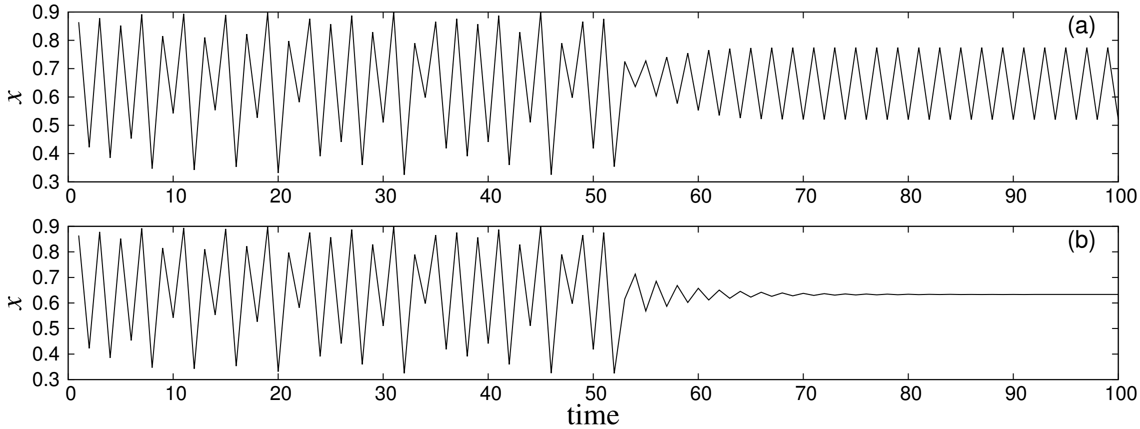

Figure 3.2: Time series, $x(n)$ of the system in Eq.(3.6) for 2 different values of feedback coupling strength with $k = 0.5$ and $\varepsilon_1 = -\varepsilon_2$. Initially the logistic map is in the chaotic regime with $r = 3.6$ and the coupling with external system is switched on at time $n = 50$.(a) For $\varepsilon_1 = 0.3$, chaotic dynamics is controlled to periodic dynamics. (b) For $\varepsilon_1 = 0.4$, the controlled state is a fixed point.

We find that there are 2 fixed points for the system in Eq.(3.6) given by the following equations:

$$x^* = 0, z^* = 0 \tag{3.7}$$

and

$$x^* = \left(\frac{1}{r}\right)\left(-1 + r + \frac{\varepsilon_1\varepsilon_2}{1-k}\right);$$
$$z^* = \frac{\varepsilon_2}{1-k}\left(\frac{1}{r}\right)\left(-1 + r + \frac{\varepsilon_1\varepsilon_2}{1-k}\right) \tag{3.8}$$

To analyze the stability of these fixed points, we consider Jacobian of the system in (3.6) evaluated at the fixed point.

$$J = \begin{pmatrix} r - 2rx^* & \varepsilon_1 \\ \varepsilon_2 & k \end{pmatrix} \tag{3.9}$$

The characteristic equation for this matrix is given by:

$$\lambda^2 + c_1\lambda + c_2 = 0 \tag{3.10}$$

where

$$c_1 = -(r - 2rx^* + k)$$
$$c_2 = (r - 2rx^*)k - \varepsilon_1\varepsilon_2 \tag{3.11}$$

The corresponding fixed point will be stable if the absolute values of all the eigenvalues given by Eq.(3.10) are less than 1. Using Routh-Hurwitz's conditions for discrete systems, this would happen when the following conditions are satisfied [113]:

$$b_0 = 1 + c_1 + c_2 > 0$$
$$b_1 = 1 - c_1 + c_2 > 0 \tag{3.12}$$
$$\triangle = 1 - c_2 > 0$$

Using these conditions, we find that the fixed point $(x^*, z^*) = (0, 0)$ is unstable. The other fixed point given by Eq.(3.8) is stable for a range of parameter values and these ranges can be obtained using the analysis described above. The numerical and analytical results thus obtained are shown in Fig. 3.3. From Fig. 3.3(a) it is clear that the steady state region (black) is symmetric about the line $\varepsilon_1 = \varepsilon_2$ and the line $\varepsilon_1 = -\varepsilon_2$. Fig. 3.3(b) shows the region of steady state behavior in ε-k plane where $\varepsilon_1 = -\varepsilon_2 = \varepsilon$. These plots also show regions of different dynamical behavior including 2-cycle, 4-cycle, other higher cycles, chaotic regime as well as regions of unstable behavior. It is clear that the boundaries of the regions that correspond to steady state, obtained analytically using Eq.(3.12), agree well with the results of numerical analysis.

We observe that the transition to steady state behavior for this system, for a given value of k as ε is varied, happens through reverse doubling bifurcations as shown in Fig. 3.4. This would mean that by tuning ε, it is possible to control the system to any periodic cycle or fixed point.

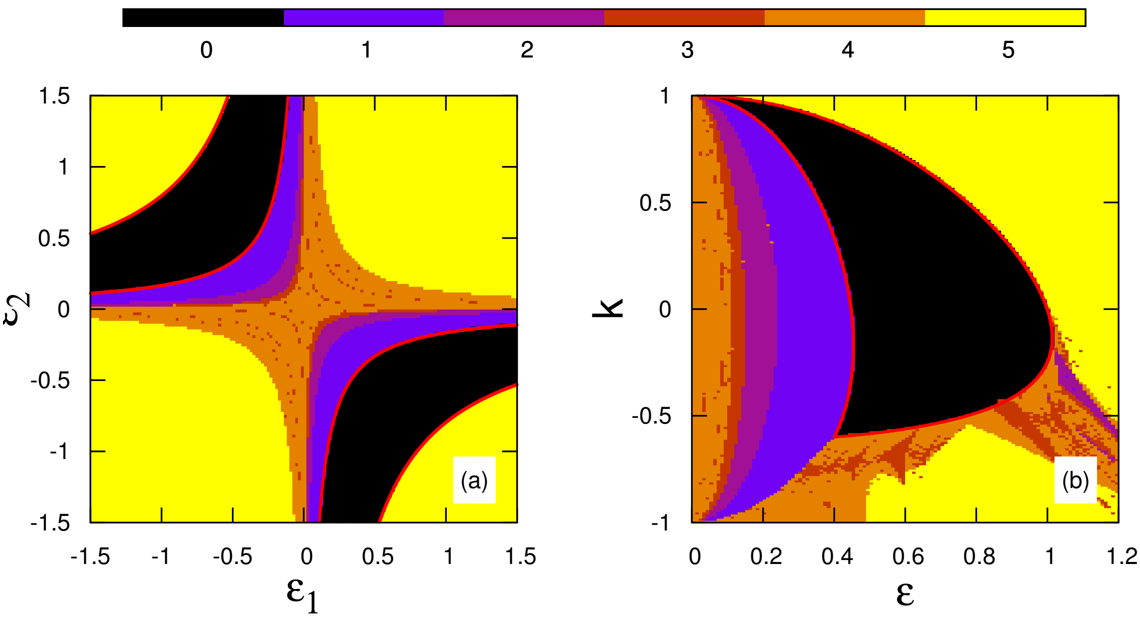

Figure 3.3: Parameter planes for a chaotic logistic map ($r = 3.6$) coupled to an external map showing regions of different dynamical behavior. Color coding is as follows, **0**: steady state, **1**: 2-cycle, **2**: 4-cycle, **3**: higher cycles, **4**: chaos and **5**: instability (a) ε_1-ε_2 plane for $k = 0.3$, (b) ε-k plane where $\varepsilon_1 = -\varepsilon_2 = \varepsilon$. The red boundary surrounding the region of steady state behavior (black region) in both the plots is obtained analytically.

As a second example we consider the Hénon map as the site dynamics. It is a 2-d map given by:

$$\begin{aligned} x(n+1) &= 1 + y(n) - ax(n)^2 \\ y(n+1) &= bx(n) \end{aligned} \tag{3.13}$$

Then the dynamics of the coupled system is given by:

$$\begin{aligned} x(n+1) &= 1 + y(n) - ax(n)^2 + \varepsilon_1 z(n) \\ y(n+1) &= bx(n) \\ z(n+1) &= kz(n) + \varepsilon_2 x(n) \end{aligned} \tag{3.14}$$

The intrinsic dynamics of Hénon map is chaotic with parameters chosen as $a = 1.4$ and $b = 0.3$. It is clear from time series given in Fig. 3.5 that the coupled system in Eq.(3.14),

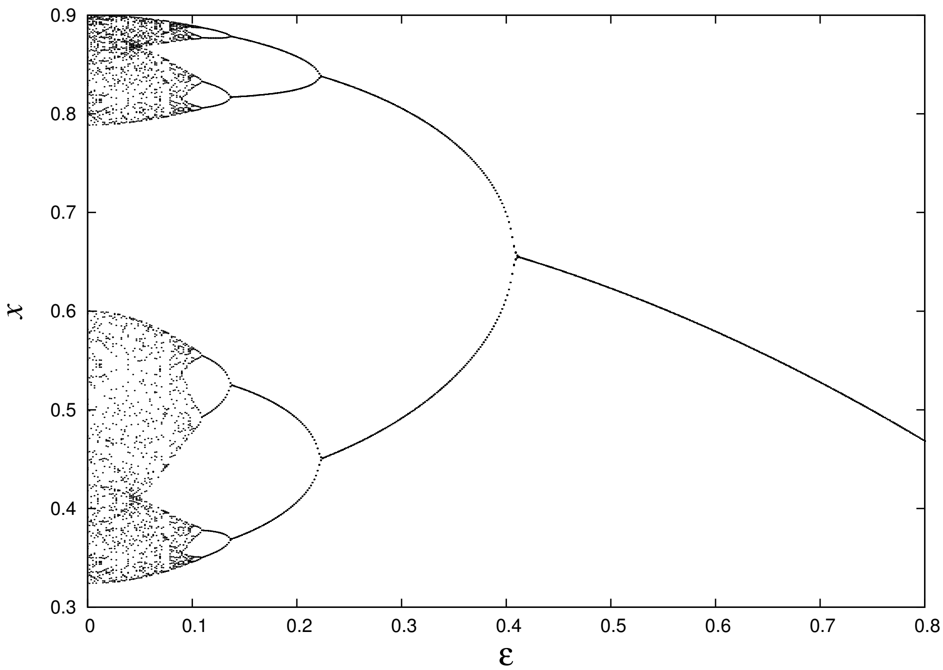

Figure 3.4: Bifurcation diagram for a single logistic map with $r = 3.6$ coupled to an external map with $k = 0.3$ as the control parameter ε is varied. As the plot shows, the map reaches a steady state through a sequence of reverse period doubling bifurcations.

can be controlled to periodic state or fixed point state by varying the parameters ε_1, ε_2 and k.

The 3-d dynamical system in (3.14) has a pair of fixed points given by:

$$\begin{aligned} x^* &= \frac{1}{2a}\left[-c \pm \sqrt{c^2+4a}\right] \\ y^* &= \frac{b}{2a}\left[-c \pm \sqrt{c^2+4a}\right] \\ z^* &= \frac{\varepsilon}{2a(1-k)}\left[-c \pm \sqrt{c^2+4a}\right] \end{aligned} \tag{3.15}$$

where,

$$c = 1 - b - \frac{\varepsilon_1\varepsilon_2}{1-k} \tag{3.16}$$

The stability of these fixed points is decided by the Jacobian matrix J evaluated at that fixed point:

$$J = \begin{pmatrix} -2ax^* & 1 & \varepsilon_1 \\ b & 0 & 0 \\ \varepsilon_2 & 0 & k \end{pmatrix} \tag{3.17}$$

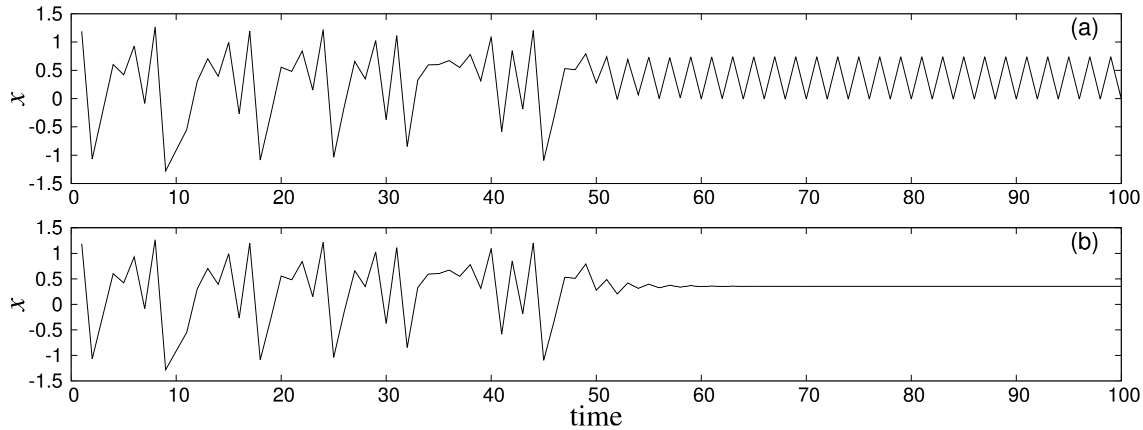

Figure 3.5: Time series, $x(n)$ of the system in Eq.(3.14) for 2 different values of coupling strength with $\varepsilon_1 = -\varepsilon_2$ and $k = 0.5$. Initially Hénon map is in the chaotic regime and the coupling with external system is switched on at time $n = 50$. (a) $\varepsilon_1 = 0.7$, chaotic dynamics is controlled to periodic dynamics of period two, (b) $\varepsilon_1 = 0.8$, the system is controlled to a fixed point.

The characteristic polynomial equation for the eigenvalue λ, in this case, is given by:

$$\lambda^3 + c_1\lambda^2 + c_2\lambda + c_3 = 0 \tag{3.18}$$

where

$$\begin{aligned} c_1 &= 2ax^* - k \\ c_2 &= -(b + 2akx^* + \varepsilon_1\varepsilon_2) \\ c_3 &= bk \end{aligned} \tag{3.19}$$

Similar to the case of logistic map, the absolute values of all eigenvalues given by Eq.(3.18) are less than 1 if the following conditions are satisfied [113]:

$$\begin{aligned} b_0 &= 1 + c_1 + c_2 + c_3 > 0 \\ b_1 &= 3 + c_1 - c_2 - 3c_3 > 0 \\ b_2 &= 3 - c_1 - c_2 + 3c_3 > 0 \\ b_3 &= 1 - c_1 + c_2 - c_3 > 0 \end{aligned} \tag{3.20}$$

Here also, one of the solutions in Eq.(3.15) (with negative sign) is unstable while the other is stable for regions in parameter planes ε_1-ε_2 and ε-k as shown in Fig. 3.6. The color codes and details are as given in Fig. 3.3. For any particular value of parameter k, the nature of transition in this case is also through a sequence of reverse period doubling bifurcations as shown in Fig. 3.7

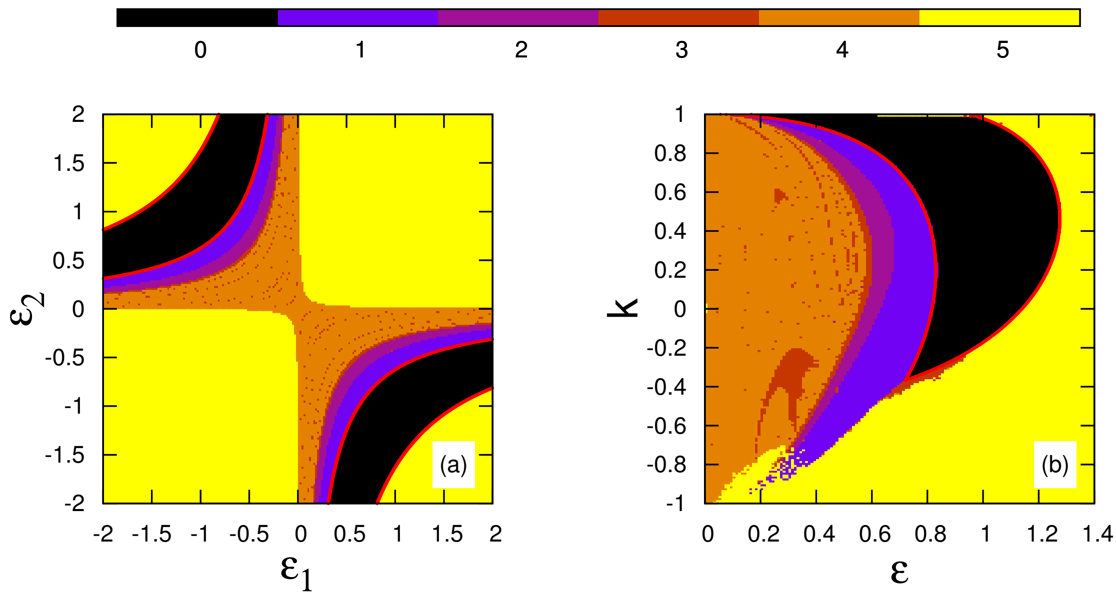

Figure 3.6: Parameter planes for a coupled system of Hénon map and external map. (a)ε_1-ε_2 plane for $k = 0.5$, (b)ε-k plane. Color coding is same as that for Fig. 3.3

3.2.2 Analysis of control in 1-d coupled map lattice

In this section, we consider control of dynamics on a ring of discrete systems. For this, as mentioned in section 3.2, we construct a ring of external maps which are coupled to each other diffusively and then couple it to the ring of discrete systems in one-to-one fashion with feedback type of coupling. With logistic map as on-site dynamics, the dynamics at the i^{th} site of the coupled system is given by:

$$\begin{aligned} x_i(n+1) &= f(x_i(n)) + D(f(x_{i-1}(n)) + f(x_{i+1}(n)) - 2f(x_i(n))) + \varepsilon_1 z_i(n) \\ z_i(n+1) &= g(z_i(n)) + D_e(g(z_{i-1}(n)) + g(z_{i+1}(n)) - 2g(z_i(n))) + \varepsilon_2 x_i(n) \end{aligned} \tag{3.21}$$

where

$$f(x) = rx(1-x) \tag{3.22}$$

Numerically, we find that the system in Eq.(3.21) can be controlled to a periodic state and a state of fixed point or amplitude death by adjusting the coupling strengths ε_1 and

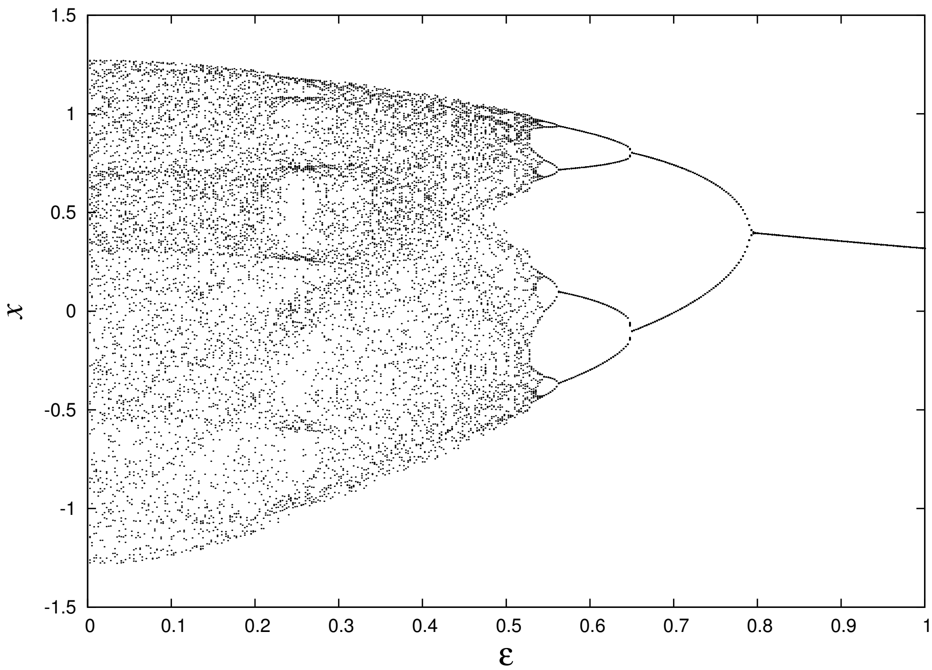

Figure 3.7: Bifurcation diagram for a Hénon map coupled to an external map as the control parameter ε is varied. As the plot shows, transition to the steady state is through a sequence of reverse period doubling bifurcations.

ε_2. Fig. 3.8 shows two such cases, where in (a) lattice is controlled to a temporal 2-cycle and in (b) temporal fixed point state.

To analyze the stability of the controlled and synchronized fixed point, we consider the system in Eq.(3.21) as a 1-d lattice of single units considered in section 3.2.1 coupled diffusively through x and z. Because of the synchronized nature of the fixed point and periodic boundary conditions, Jacobian of this system is block circulant matrix as given below.

$$J = \begin{pmatrix} a_0 & a_1 & 0 & . & . & 0 & a_1 \\ a_1 & a_0 & a_1 & . & . & . & 0 \\ . & . & . & . & . & . & . \\ . & . & . & . & . & . & . \\ a_1 & 0 & . & . & . & a_1 & a_0 \end{pmatrix} \tag{3.23}$$

For the case of logistic maps, a_0 and a_1 are 2×2 matrices and 0 denotes 2×2 zero matrix. In explicit form, these matrices are given by:

$$a_0 = \begin{bmatrix} (1-2D)r(1-2x^*) & \varepsilon_1 \\ \varepsilon_2 & (1-2D_e)k \end{bmatrix} \tag{3.24}$$

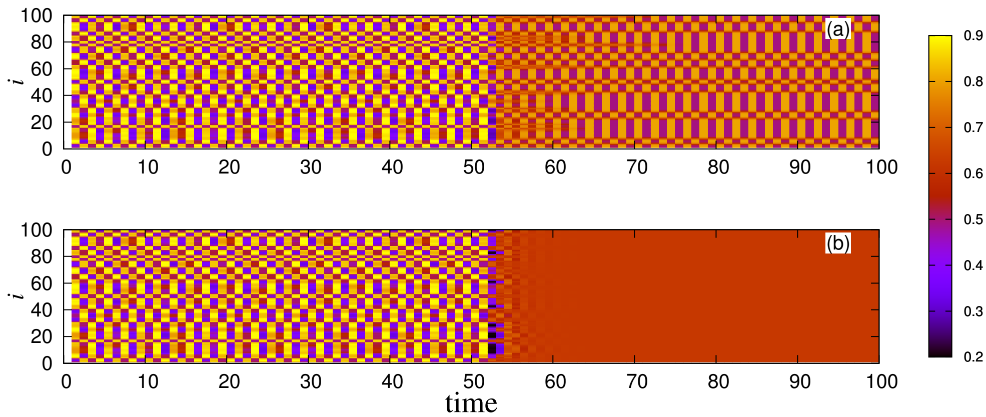

Figure 3.8: Space-time plots for a ring of logistic maps coupled to an external ring. The coupling is switched on at time 60. Parameter values of the system are: $r = 3.6$, $D = 0.1$, $D_e = 0.1$, $k = 0.3$. (a) For $\varepsilon_1 = -0.3$; $\varepsilon_2 = 0.3$, the dynamics is controlled to a 2-cycle state and (b) for $\varepsilon_1 = -0.5$; $\varepsilon_2 = 0.5$, the dynamics is controlled to a fixed point state. The color code is as per the value of $x(n)$

and

$$a_1 = \begin{bmatrix} Dr(1-2x^*) & 0 \\ 0 & D_e k \end{bmatrix} \tag{3.25}$$

Following the analysis given in [114] for eigenvalues of the general block circulant matrix as given below:

$$\begin{pmatrix} a_0 & a_1 & a_2 & . & . & a_{N-2} & a_{N-1} \\ a_{N-1} & a_0 & a_1 & . & . & a_{N-3} & a_{N-2} \\ a_{N-2} & a_{N-1} & a_0 & . & . & a_{N-4} & a_{N-3} \\ . & . & . & . & . & . & . \\ . & . & . & . & . & . & . \\ a_1 & . & . & . & . & a_{N-1} & a_0 \end{pmatrix} \tag{3.26}$$

We construct N blocks each of order 2×2 as follows :

$$H_j = a_0 + a_1\rho_j + a_2\rho_j^2 + ... + a_{N-1}\rho_j^{N-1} \tag{3.27}$$
$$j = 0, 1, ..., N-1$$

where ρ is a complex N'th root of unity:

$$\rho_j = exp\left(\frac{2\pi j}{N} i\right) \tag{3.28}$$

with $i = \sqrt{-1}$
For our problem, $a_1 = a_{N-1}$ and $a_2, a_3, ..., a_{N-2} = 0$. Thus we get,

$$H_j = a_0 + a_1(\rho_j + \rho_j^{N-1}) = a_0 + 2\theta_j a_1 \tag{3.29}$$

where

$$\theta_j = cos\left(\frac{2\pi j}{N}\right)$$

Thus, in this case, H_j is given by:

$$H_j = \begin{pmatrix} a_{11} & a_{12} \\ a_{21} & a_{22} \end{pmatrix} \tag{3.30}$$

where,

$$\begin{aligned} a_{11} &= (1 - 2D + 2D\theta_j)r(1 - 2x^*) \\ a_{12} &= \varepsilon_1 \\ a_{21} &= \varepsilon_2 \\ a_{22} &= (1 - 2D_e + 2D_e\theta_j)k \end{aligned} \tag{3.31}$$

Now we make use of the fact that eigenvalues of Jacobian when evaluated at the synchronized fixed point are the same as eigenvalues of these H_j matrices since the Jacobian is block circulant matrix [114]. This means that, to check the stability of the fixed point of the two coupled rings, instead of directly calculating eigenvalues of Jacobian matrix of size $2N \times 2N$, we can calculate eigenvalues of all H_j matrices, each of which is 2×2 matrix, which is a much simpler task. The characteristic equation for H_j is given by:

$$\lambda^2 + c_1\lambda + c_2 = 0 \tag{3.32}$$

where

$$c_1 = -(a_{11} + a_{22}) \tag{3.33}$$

$$c_2 = a_{11}a_{22} - a_{12}a_{21} \tag{3.34}$$

In this case, the corresponding fixed point with coordinates given by Eq.(3.7) or Eq.(3.8) is stable when the conditions given in Eq.(3.12) are satisfied for each H_j. These conditions then give us the regions in parameter space where the fixed point state of the whole system is stable i.e. the regions where the control of the original dynamics to the steady state is possible. Similar to the case of single unit, the fixed point with coordinates given by Eq.(3.7) turns out to be unstable for all values of control parameters. The other fixed point is stable for a range of parameter values. These amplitude death regions obtained numerically in ε-k and D-D_e planes for this system of coupled rings are shown in Fig. 3.9. In each of these plots, the steady state region is shown with black color while the red boundary around that region is obtained analytically. From Fig. 3.9(b), it is clear that the amplitude death can happen even when the logistic maps are not coupled to each other directly (corresponding to $D = 0$) or when external maps are not coupled to each other (corresponding to $D_e = 0$).

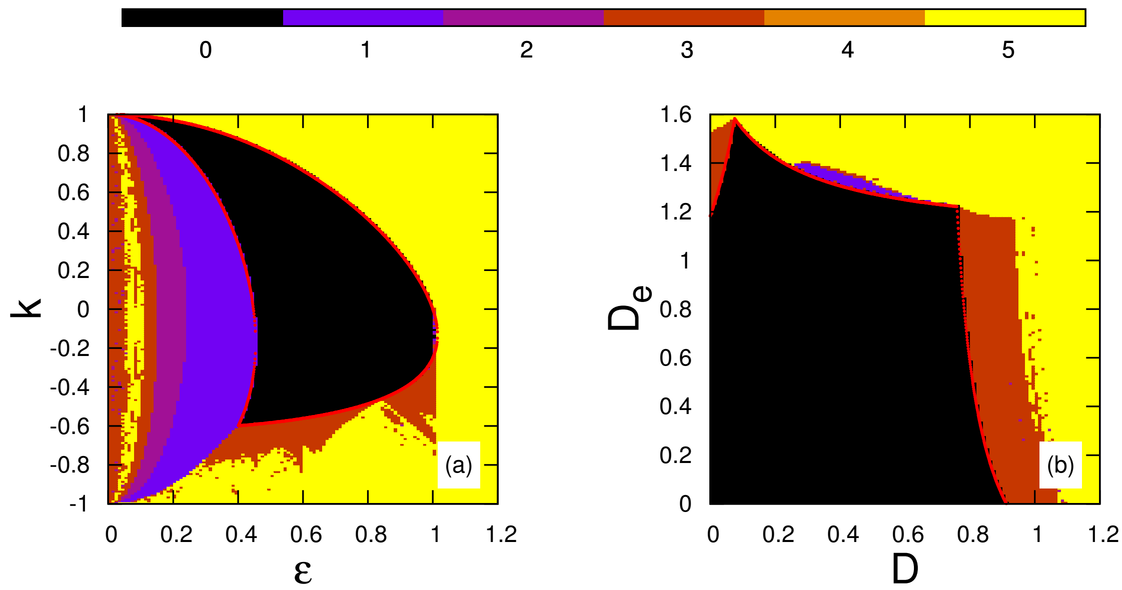

Figure 3.9: Parameter planes for a ring of logistic maps coupled to an external ring: (a) ε-k plane when $D = 0.3$ and $D_e = 0.3$, (b) D-D_e plane when $\varepsilon = 0.6$ and $k = 0.3$. We find that in the chaotic regime, the maps are in desynchronized state. Color coding is same as that for Fig. 3.3

As our next example, we illustrate the control scheme for a ring of Hénon maps. The coupled system in this case can be represented as follows:

$$\begin{aligned} x_i(n+1) &= f(x_i(n), y_i(n)) + D(f(x_{i-1}(n), y_{i-1}(n)) + f(x_{i+1}(n), y_{i+1}(n)) - 2f(x_i(n), y_i(n))) \\ &\quad + \varepsilon_1 z_i(n) \\ y_i(n+1) &= b x_i(n) \\ z_i(n+1) &= g(z_i(n)) + D_e(g(z_{i-1}(n)) + g(z_{i+1}(n)) - 2g(z_i(n))) + \varepsilon_2 x_i(n) \end{aligned} \tag{3.35}$$

where

$$f(x, y) = 1 + y - ax^2 \tag{3.36}$$

Here also the system can be controlled to a synchronized fixed point and because of the periodic boundary conditions and because of the synchronized nature of fixed point, Jacobian becomes block circulant as given in Eq.(3.23). In this case, a_0 and a_1 are 3×3

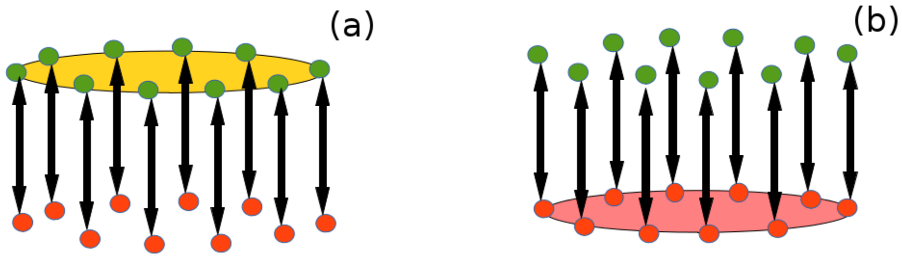

Figure 3.10: Schematic showing the two extreme cases of control. (a) with $D_e = 0$ and $D \neq 0$ individual systems are coupled to each other while external systems are not connected to each other (b) with $D = 0$ and $D_e \neq 0$, the external systems are coupled to each other while systems to be controlled are not coupled among themselves.

matrices and 0 represents 3×3 zero matrix. In explicit form, a_0 and a_1 are given by:

$$a_0 = \begin{pmatrix} (1-2D)(-2ax^*) & (1-2D) & \varepsilon_1 \\ b & 0 & 0 \\ \varepsilon_2 & 0 & (1-2D_e)k \end{pmatrix}$$

and

$$a_1 = \begin{pmatrix} D(-2ax^*) & D & 0 \\ 0 & 0 & 0 \\ 0 & 0 & D_e k \end{pmatrix}$$

Let

$$\begin{aligned} 1 - 2D + 2D\theta_j &= \eta_1 \\ 1 - 2D_e + 2D_e\theta_j &= \eta_2 \end{aligned} \tag{3.37}$$

Then,

$$H_j = \begin{pmatrix} \eta_1(-2ax^*) & \eta_1 & \varepsilon_1 \\ b & 0 & 0 \\ \varepsilon_2 & 0 & \eta_2 k \end{pmatrix} \tag{3.38}$$

The characteristic equation for H_j is given by:

$$\lambda^3 + c_1\lambda^2 + c_2\lambda + c_3 = 0 \tag{3.39}$$

where

$$\begin{aligned} c_1 &= 2ax^*\eta_1 - \eta_2 k \\ c_2 &= -(b\eta_1 + 2ax^*k\eta_1\eta_2 + \varepsilon_1\varepsilon_2) \\ c_3 &= bk\eta_1\eta_2 \end{aligned} \tag{3.40}$$

Using these parameters c_1, c_2, c_3, we define b_0, b_1, b_2, b_3 and $\triangle$ as in the case of single unit in Eq.(3.20). This allows us to check stability for each of the H_j matrices which in turn gives us regions in parameter space where the control of the dynamics is possible for a ring of Hénon maps. In Fig. 3.11 we show these regions in ε-k parameter plane, for $D_e = 0$ and for $D = 0$. The schematic for these cases is shown in Fig. 3.10.

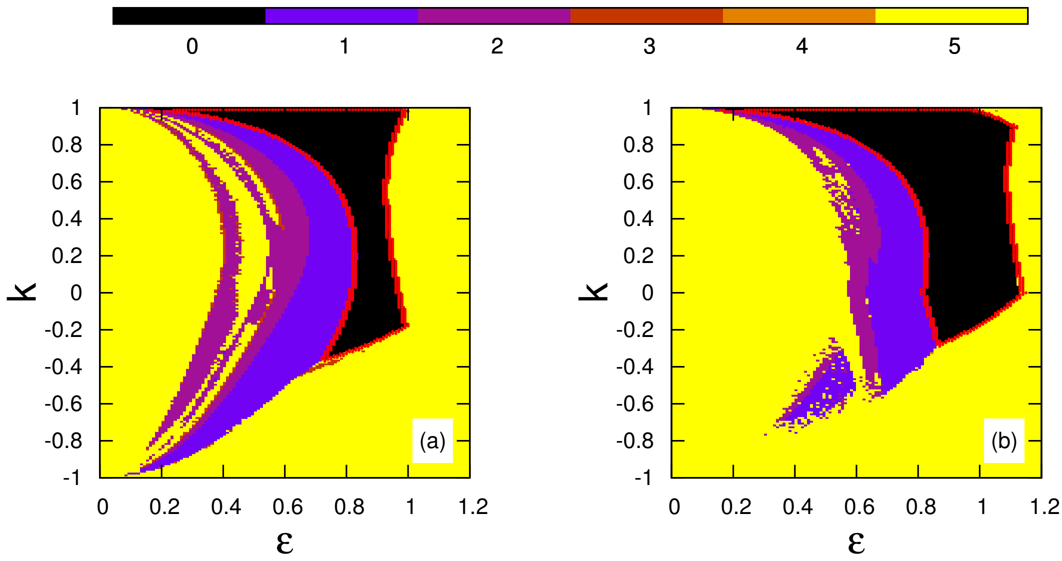

Figure 3.11: ε-k parameter planes for a ring of Hénon maps coupled to an external ring: (a) when $D = 0.3$, $D_e = 0$, (b) when $D = 0$, $D_e = 0.3$. Similar to the case of ring of logistic maps, in the chaotic regime, the maps are in the desynchronized state. Color code is same as that for Fig. 3.3

3.3 Control with random inter-connections

In the control scheme described so far for a ring, we considered only a very regular type of interconnections between the system ring and the external ring. It is an interesting question to ask whether the control can still be achieved even if the interconnections are randomized so that the node i in the system ring does not necessarily interact with the node i in the external ring. In such random topology of interconnections, nodes which are neighbors of each other in the external ring in general would try to control nodes in system ring that are not neighbors of each other. Hence, it is not a priori obvious that external ring would be able to control the system ring's dynamics.

To address this, we simulate an ensemble of 100 random realizations of interconnections with logistic map as the nodal dynamics. The logistic map is kept in a fully chaotic regime ($r = 4$) in this case. This system can be represented mathematically in the following fashion.

$$\begin{aligned} \mathbf{x}_i(n+1) &= \mathbf{f}(\mathbf{x}_i(n)) + D\zeta(\mathbf{f}(\mathbf{x}_{i-1}(n)) + \mathbf{f}(\mathbf{x}_{i+1}(n)) - 2\mathbf{f}(\mathbf{x}_i(n))) + \varepsilon_1 \xi \sum_{j=1}^{N} X_{ij} z_j(n) \\ z_i(n+1) &= g(z_i(n)) + D_e(g(z_{i-1}(n)) + g(z_{i+1}(n)) - 2g(z_i(n))) + \varepsilon_2 \xi^T \sum_{j=1}^{N} X_{ij} \mathbf{x}_i(n) \end{aligned} \tag{3.41}$$

where X_{ij} is the $(i,j)^{\text{th}}$ element of the adjacency matrix of interconnections which we take to be a random matrix such that inter-degree of every node is equal to 1.

We find that in each of these realizations, system ring gets controlled to a desired steady or periodic state depending upon the value of the control parameter. This shows that the applicability of the proposed method of control is quite general. To characterize the control in this randomized case, we calculate a quantity $\langle A \rangle_{\mathrm{r}}$ which we define as follows:

$$\langle A \rangle_{\mathrm{r}} = \frac{\sum_{i,j} (x_{j,\max} - x_{j,\min})}{n_r N} \tag{3.42}$$

where the index i runs over the realizations in the ensemble of random interconnections and the index j runs over the individual systems in the given ring. The quantities $x_{j,\max}$ and $x_{j,\min}$ respectively represent the maximum and the minimum values among the asymptotic values of the individual systems in the ring. Also, N is the number of systems in one ring and n_r is the number of realizations in the ensemble. When the steady state is achieved, the average amplitude $\langle A \rangle_{\mathrm{r}}$ should become zero. We plot $\langle A \rangle_{\mathrm{r}}$ as a function of control parameter ε which is shown in Fig. 3.12. As we can see from this figure, steady state is achieved for a sufficiently high value of control parameter ε. Also, as is clear from the same figure, there is a sufficient range of values of ε for which control can be achieved.

3.3.1 Control of chimera states in non-locally coupled 1-d lattice

As an application of our scheme, we present the control of chimera states produced on a 1-d lattice with non-local couplings. The chimera states have been observed in many

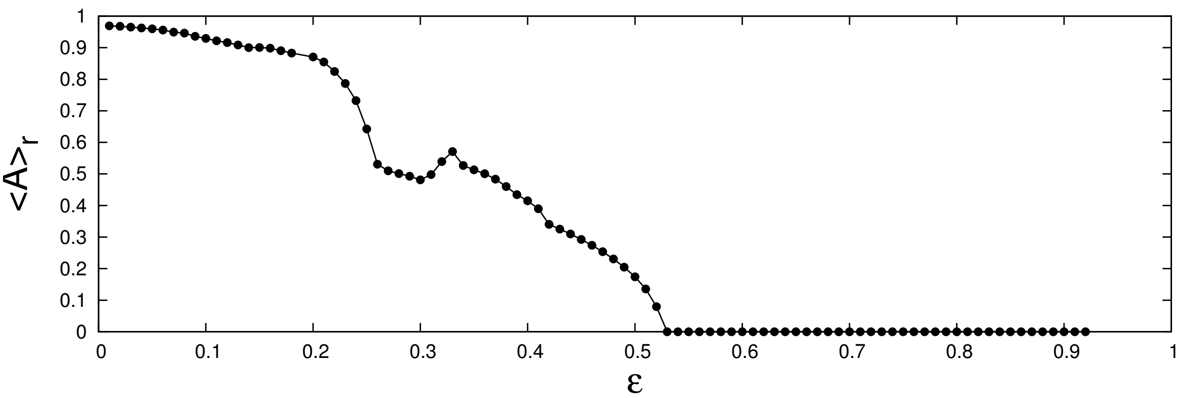

Figure 3.12: Controlling the dynamics on a ring of logistic map using external ring with random interconnections. The logistic maps are fully chaotic with $r = 4$. The figure shows the asymptotic average amplitude (Eq.(3.42)) as a function of control parameter ε with $k = 0.3$. Zero value of $\langle A\rangle_{\rm r}$ corresponds to the controlled steady state for the ring. For every value of ε, averaging is done over 100 random realizations.

spatially extended systems and coupled oscillators with non-local couplings [115–117]. These states, which correspond to the coexistence of spatial regions with synchronized and incoherent behavior, may not be desirable in many systems like power grids. Here we specifically consider the chimera states experimentally realized using liquid-crystal spatial light modulator [80]. This system corresponds to a 1-d lattice with each node diffusively coupled to R of its nearest neighbors. In this case the phase of each node ϕ_i is the dynamical variable whereas a physically important quantity is the output intensity I, related to phase as:

$$I(\phi) = (1 - \cos\phi)/2 \tag{3.43}$$

The coupled map lattice is then represented by the following set of equations [80]:

$$\phi_i^{n+1} = 2\pi a \left\{ I(\phi_i^n) + \frac{D}{2R} \sum_{j=-R}^{R} \left[I(\phi_{i+j}^n) - I(\phi_i^n) \right] \right\} \tag{3.44}$$

For the coupling radius $r = R/N = 0.41$ and $D = 0.44$ as shown in [80], the spatial profile of ϕ has two distinct synchronized domains which are separated by small incoherent domains confirming the existence of chimera states as shown in Fig. 3.13(a). When chimera state exists in the lattice, individual maps exhibit a 2-cycle behavior. However, the dynamics of two maps taken from two different domains are different as shown in Fig. 3.14(b).

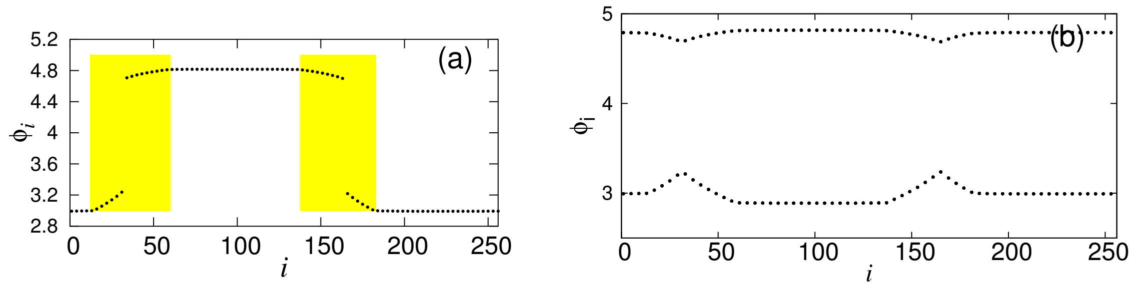

Figure 3.13: (a) Chimera state developed in a 1d coupled map lattice of size $N = 256$ represented by Eq.(3.44) shown with a dotted black line. The yellow regions in the plot highlight the regions of incoherent behavior. (b) Plot showing last 100 values after discarding the transients for each map in the lattice. From this, it is clear that because of the coupling, each map individually goes into 2-cycle state but the values of 2-cycle are different for different maps in the lattice.

To control this chimera state, the coupling with external lattice is done as:

$$\begin{aligned}\phi_i(n+1) &= 2\pi a \left\{ I(\phi_i(n)) + \frac{D}{2R}\sum_{j=-R}^{R}[I(\phi_{i+j}(n)) - I(\phi_i(n))] \right\} \\ &\quad +\varepsilon_1 z_i(n) \\ z_i(n+1) &= kz_i(n) + D_e(z_{i-1}(n) + z_{i+1}(n) - 2z_i(n)) + \varepsilon_2\phi_i(n)\end{aligned} \tag{3.45}$$

We find that with this control scheme, spatial as well as temporal control of chimera state can be achieved. To illustrate it, we plot the time series of a typical node from the lattice in Fig.3.14(a). In Fig. 3.14(b), we also plot 100 post-transient values for each of the maps in the system for two high values of control parameter ε. This plot is thus analogous to the bifurcation diagram of a dynamical system except that the horizontal axis is now a 1-d space instead of a parameter of the system. From this plot, it is seen that the initial spatial heterogeneity depicted in Fig. 3.13(b) disappears and all the maps oscillate between same values.

To study the control of chimera state in this case as a function of control parameter ε, we calculate synchronization index S for the lattice and plot it as a function of ε as shown in Fig. 3.15. As it shows, just below $\varepsilon = 0.3$ all the maps in the lattice get synchronized. Thus, at this point, chimera state in the lattice present initially completely disappears resulting in a state of chimera death.

The complete nature of transition from chimera state to uniform state can also be visualized by plotting the two types of bifurcation diagrams shown in Fig. 3.16. In the first diagram, we plot the usual bifurcation diagram for one of the nodes in the system as the control parameter is varied. We see that the transition to a fixed point state happens through a reverse period doubling route. In the second diagram, we plot all the values on each of the nodes in the ring after discarding the transients as a function of ε. This spatial bifurcation diagram shows the inter-relation between the values of the various

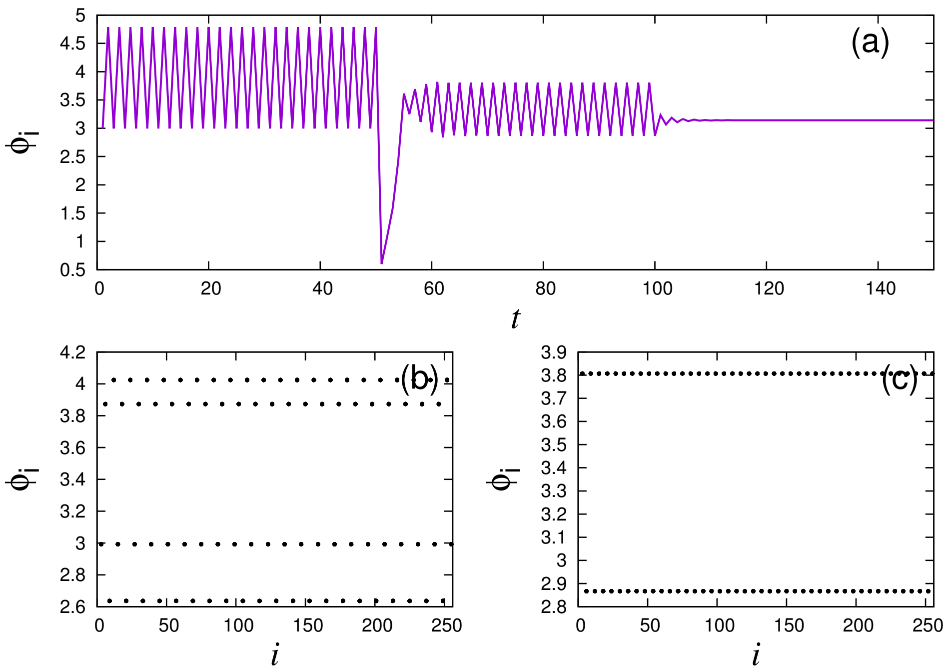

Figure 3.14: (a) Time series of a typical node of the CML. When chimera state is present, individual node is in 2-cycle state. At time $n = 50$ control is switched on with $k = 0.5$, $\varepsilon_1 = -\varepsilon_2 = -0.5$ which results in the shortening of the 2-cycle for a map. Further increase in coupling with $\varepsilon_1 = -\varepsilon_2 = -0.7$ at time $n = 150$ results in a stabilization of a fixed point of the system. (b) Plot showing 100 post-transient values for $\varepsilon_1 = -\varepsilon_2 = -0.41$ (with each map in the similar 4-cycle) and (c) for $\varepsilon_1 = -\varepsilon_2 = -0.5$ (with each map in the similar 2-cycle).

nodes in the system for a given value of the control parameter.

3.4 Control of dynamics on a 2d-Lattice

Now we consider controlling the dynamics on 2-d lattice of discrete systems by coupling to an external lattice as follows:

$$\begin{aligned}
\mathbf{x}_{i,j}(n+1) &= \mathbf{f}(\mathbf{x}_{i,j}(n)) + D\zeta(\mathbf{f}(\mathbf{x}_{i-1,j}(n)) + \mathbf{f}(\mathbf{x}_{i+1,j}(n)) + \mathbf{f}(\mathbf{x}_{i,j-1}(n)) + \mathbf{f}(\mathbf{x}_{i,j+1}(n)) - 4\mathbf{f}(\mathbf{x}_{i,j}(n))) \\
&\quad + \varepsilon_1 \xi z_{i,j}(n) \\
z_{i,j}(n+1) &= g(z_{i,j}(n)) + D_e(g(z_{i-1,j}(n)) + g(z_{i+1,j}(n)) + g(z_{i,j-1}(n)) + g(z_{i,j+1}(n)) - 4g(z_{i,j}(n))) \\
&\quad + \varepsilon_2 \xi^T \mathbf{x}_{i,j}(n)
\end{aligned} \tag{3.46}$$

Here, ξ is the $m \times 1$ matrix which determines the components of state vector $\mathbf{x}$ which take part in the coupling with an external system. In Fig. 3.18, we show the numerically obtained time series from a typical node of a 100×100 lattice of logistic maps coupled to

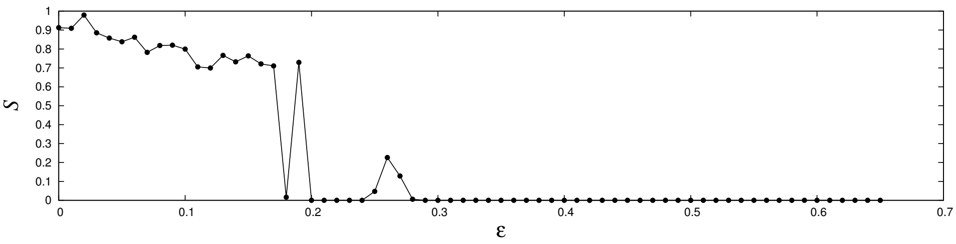

Figure 3.15: Synchronization index S for maps in the lattice as the control parameter ε is varied with $k = 0.5$. Just before $\varepsilon = 0.3$ maps get completely synchronized which marks the point of chimera death.

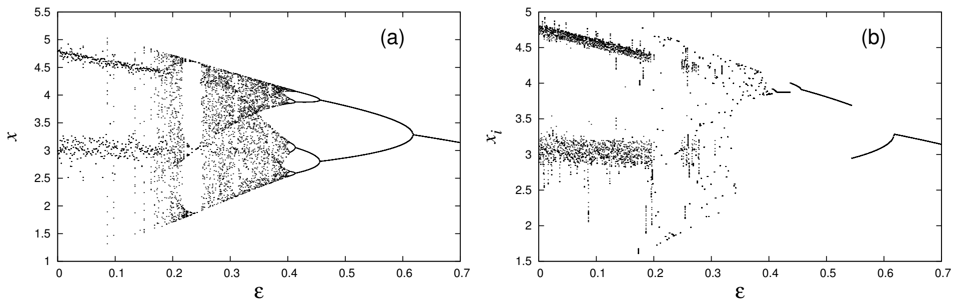

Figure 3.16: Nature of the transition to the controlled state from the chimera state as the control parameter ε is varied keeping $k = 0.5$ fixed. (a) bifurcation diagram for one of the nodes in the system showing a reverse period doubling route to a controlled state (b) spatial bifurcation diagram for the whole system. For every value of ε, values of all the nodes in the system are plotted on the y-axis after neglecting the transients. It can be seen that for sufficiently high value of ε, all maps become completely synchronized and the chimera state disappears.

an external lattice for 3 different coupling strengths ε. In all three cases, coupling with an external lattice is switched on at time 50.

In Fig. 3.19, we show space-time plots of 2-d lattice of logistic maps with and without coupling with an external lattice. Here the time series from nodes along one of the main diagonals of the lattice are plotted on the y-axis and time on the x-axis. The coupling strength with the external lattice is adjusted so that lattice of logistic maps is controlled to a 2-cycle state temporally.

The stability of the synchronized steady state of coupled 2-d lattices can be analyzed in exactly similar fashion to the coupled rings discussed in detail in previous section by re-indexing lattice site (i, j) with a running index l defined as $l = i + (j - 1)N$. Then Jacobian for the whole system becomes $N^2 \times N^2$ block circulant matrix with each block's order being $(m+1) \times (m+1)$. The intersection of regions satisfying the stability conditions for all the H_l matrices will then give the region of amplitude death in the corresponding

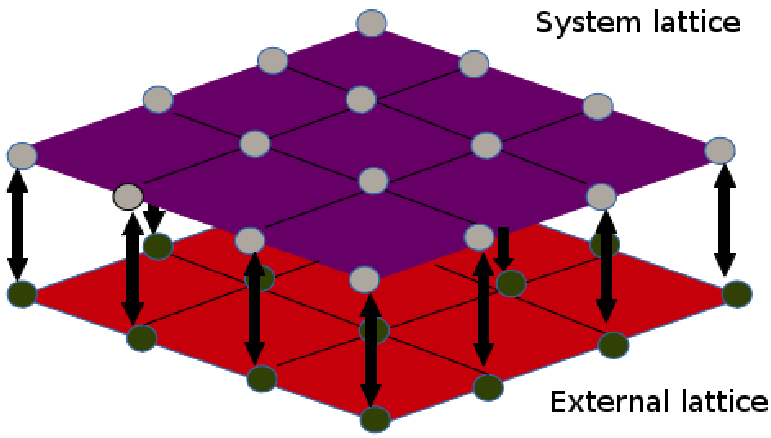

Figure 3.17: Schematic of a system lattice coupled to an external lattice. The black arrows between the lattices represent feedback coupling.

parameter planes. The results thus obtained are qualitatively similar to the case of the ring and therefore not included here.

3.4.1 Control of patterns in coupled neurons

In this section we show how the present scheme can provide a phenomenological model for the role of external medium in controlling the dynamics of coupled neurons. It is established that neurons can cause fluctuations in the extra cellular medium which when fed back to the neurons can affect their activity via ephaptic coupling [118]. In this context, we take the 2-d control lattice as the discrete approximation to the medium and the dynamics of individual neuron, to be the Rulkov map model [61] given by the following equations:

$$\begin{aligned} x(n+1) &= \frac{\alpha}{1+x(n)^2} + y(n) \\ y(n+1) &= y(n) - \beta x(n) - \gamma \end{aligned} \tag{3.47}$$

Here x, represents the membrane potential of the neuron and y is related to gating variables. α , β and γ are intrinsic parameters of the map. We take $\beta = \gamma = 0.004$ and for $\alpha < 2$, there exists a stable fixed point for the map given by $x^* = -1$ and $y^* = -1 - \frac{\alpha}{2}$. In the range $\alpha = 2$ to $\alpha = 3.1$, the map shows periodic behavior. We model the system of coupled neurons as a 2-d lattice which is in a feedback loop with the external lattice

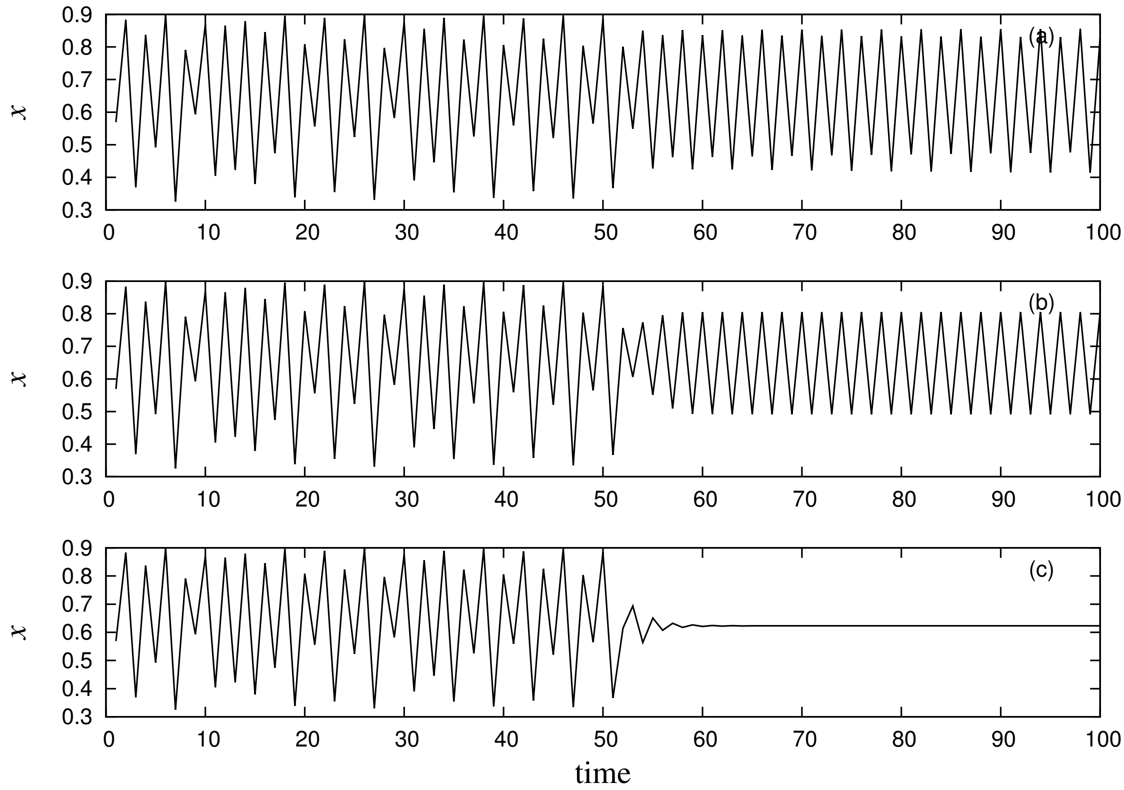

Figure 3.18: Time series $x(n)$ of a typical node from a 100×100 lattice of logistic maps coupled to an external lattice when $\varepsilon_1 = -\varepsilon_2$. Parameter values are: $D = 0.1$, $D_e = 0.1$ and $r = 3.6$. In all the cases coupling with external lattice is switched on at time $n = 50$. (a) For $\varepsilon_2 = 0.2$, the chaotic dynamics is controlled to 4-cycle state. (b) For $\varepsilon_2 = 0.3$, it is a 2-cycle state. (c) For $\varepsilon_2 = 0.5$, the dynamics is quenched to fixed point state or amplitude death state.

as given by:

$$\begin{aligned}
x^{i,j}(n+1) &= \alpha^{i,j}/(1+x^{i,j}(n)) + y^{i,j}(n) + D(x^{i-1,j}(n) + x^{i+1,j}(n) + x^{i,j-1}(n) + x^{i,j+1}(n) - 4x^{i,j}(n)) \\
&\quad + \varepsilon_1 z^{i,j}(n) \\
y^{i,j}(n+1) &= y^{i,j}(n) - \beta x^{i,j}(n) - \gamma \\
z^{i,j}(n+1) &= kz^{i,j}(n) + D_e(z^{i-1,j}(n) + z^{i+1,j}(n) + z^{i,j-1}(n) + z^{i,j+1}(n) - 4z^{i,j}(n)) + \varepsilon_2 x^{i,j}(n)
\end{aligned}$$

For a realistic modeling of the system, we take the values of the parameter α distributed uniformly and randomly between 2.1 and 2.3 among all the maps and the extra cellular medium as the external lattice of same size with a spread in k values distributed randomly in $[0.2 : 0.4]$. In the absence of coupling with medium, the neurons can form dynamical patterns of the type shown in Fig. 3.20(a) obtained by iterating the lattice for 50000 time steps with $D = 0.04$ and initial conditions for x and y randomly and uniformly distributed in $[-2 : 2]$. When coupling with the external lattice is switched on, the

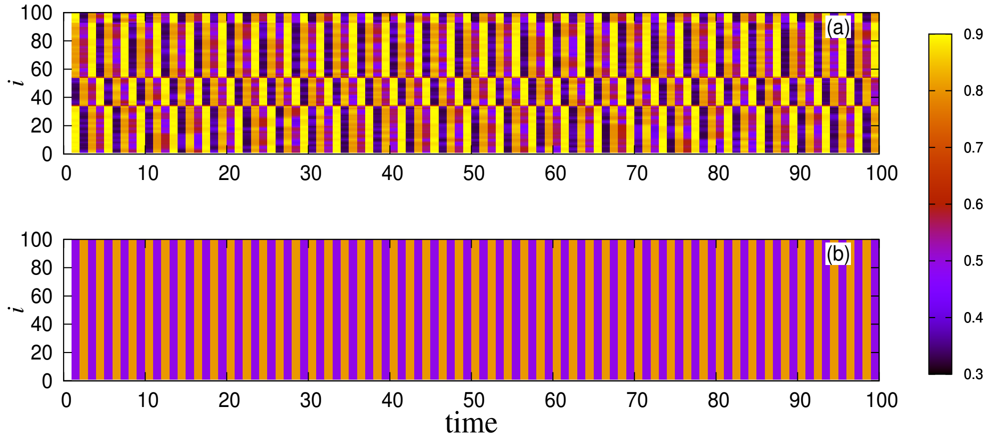

Figure 3.19: (a) Space-time plot of patterns formed on 2-d lattice of logistic maps when the individual maps are in chaotic regime, $r = 3.6$ and $D = 0.1$ (b) When this lattice is coupled to the external lattice with $\varepsilon_1 = -0.3$, $\varepsilon_2 = 0.3$, $D_e = 0.1$, the dynamics is controlled to a 2-cycle state temporally. Also, spatially pattern on the lattice becomes regular. Color coding in the plot is according the values of $x(n)$.

patterns get suppressed giving steady and synchronized states. In Fig. 3.20(b) we show the space time plot for the lattice with and $D_e = 0.1$, $\varepsilon_1 = -0.5$ and $\varepsilon_2 = 0.5$ and the coupling is switched on at time 49000. The horizontal axis represents the systems on the main diagonal of the lattice and vertical axis is time. As is clear from the plot, the external lattice suppresses the pattern on the lattice.

We note that dynamical spatio-temporal patterns can arise in the neuronal lattice because of defect neurons that are different from others. We illustrate this by considering a lattice of neurons in which all neurons have α in the range 1.95 to 1.98 except one neuron which is in the excited state with $\alpha = 2.2$. The patterns produced are shown in Fig. 3.21(a). Such patterns of propagating excitation waves can be pathological unless suppressed. The coupling with the external medium presented here can effectively suppress them as shown in Fig. 3.21(b),(c),(d) which display the snapshots of the lattice after coupling with the external lattice.

3.5 Control scheme for random networks

Now we generalize the control scheme given above to control the dynamics on random networks of discrete systems. As a first instance, we construct external network with the same topology as the system network and then we couple these networks in one to one fashion with feedback type of coupling. This coupled system of two networks, when the coupling between the nodes of the same network is of diffusive type, can be represented

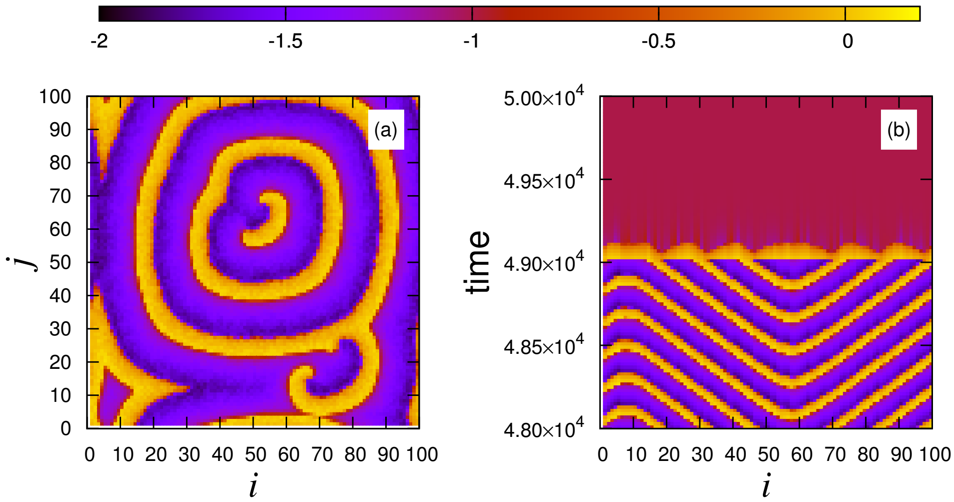

Figure 3.20: (a) Typical pattern formed on 100×100 lattice of Rulkov neurons at $D = 0.04$ for $\alpha = [2.1 : 2.3]$ starting from random initial conditions shown after 50000 time steps. (b) Space time plot for the same lattice with horizontal axis representing the main diagonal of the lattice. Here coupling with external lattice is switched on at time step 49000 and the pattern gets suppressed.

by:

$$\begin{aligned} \mathbf{x}_i(n+1) &= \mathbf{f}(\mathbf{x}_i(n)) + D\sum_{j=1}^{N} B_{ij}\zeta(\mathbf{f}(\mathbf{x}_j(n)) - \mathbf{f}(\mathbf{x}_i(n)) + \varepsilon_1\xi z_i(n) \\ z_i(n+1) &= g(z_i(n)) + D_e\sum_{j=1}^{N} B_{ij}(g(z_j(n)) - g(z_i(n))) + \varepsilon_2\xi^T\mathbf{x}_i(n) \end{aligned} \tag{3.48}$$

In this equation, intrinsic m-dimensional dynamics on the nodes of the network is given by $\mathbf{x}_i(n+1) = \mathbf{f}(\mathbf{x}_i(n))$ and the same function $\mathbf{f}(\mathbf{x})$ is used to couple nodes in the network diffusively. Also, B_{ij} is the $(i,j)^{th}$ entry of the adjacency matrix B of the network, ζ is the $m \times m$ matrix which determines the components of state vector $\mathbf{x}$ to be used in the coupling with the other nodes and ξ is the $m \times 1$ matrix which determines the components of state vector $\mathbf{x}$ to be used in the coupling with nodes of the external network. Fig. 3.22 shows a schematic of the system represented by these equations.

We perform numerical simulations for a network of 50 nodes for 5 different random topologies which include three realizations of Erdős-Rényi network with average degree equal to 4 and two realizations of Barabási-Albert scale-free network. The dynamics on the nodes is of logistic map in all these simulations with $\varepsilon_1 = -\varepsilon_2 = \varepsilon$. We find that for all topologies, as the coupling strength ε is increased both networks reach synchronized fixed point of the single unit given in Eq.(3.6). This synchronized steady sate or fixed point

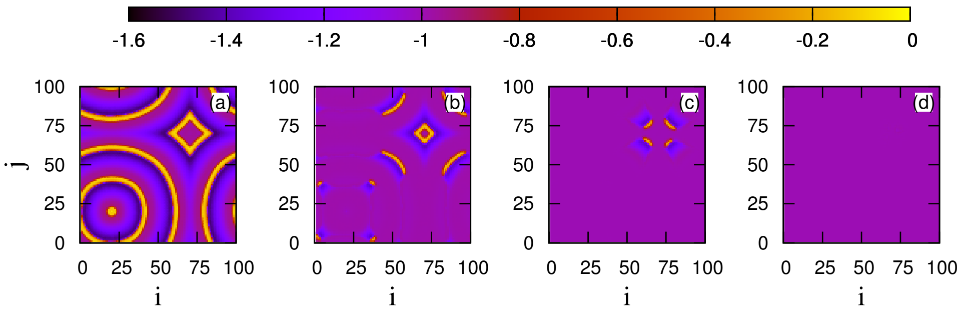

Figure 3.21: (a)Excitation waves generated on Rulkov lattice after iterating for 50000 time steps with periodic boundary conditions when all maps are in fixed point state and only one of them (here $(20, 20)$) is active ($\alpha = 2.2$) which acts as a defect. (b),(c) and (d) show the state of lattice after 250, 500 and 750 time steps respectively with coupling with external lattice is switched on. In this case, $D_e = 0.1, \varepsilon_1 = -0.15$ and $\varepsilon_2 = 0.15$. The values of k are distributed uniformly randomly in $[0.2 : 0.4]$.

can be considered as amplitude death state of the network and to analyze its stability, we invoke the master stability analysis for this fixed point [119].

Since the external network has exactly the same topology as the original network and since nodes of two networks are coupled in one to one fashion, this system of two coupled networks can be considered as a single network of the single units considered in section 3.2.1. Then if $\varepsilon_\mu^i(n)$ represents μ'th component of perturbation to the synchronized fixed point of the network at node i, we expand this perturbation as:

$$\varepsilon_\mu^i(n) = \sum_r c_\mu^r(n) v_r^i \tag{3.49}$$

where v_r^i is i^{th} component of r'th eigenvector of Laplacian matrix of the network. Following the analysis given in [1] we then get:

$$\boldsymbol{c}^r(n+1) = [\boldsymbol{\alpha} + \lambda_r \boldsymbol{\beta}]\boldsymbol{c}^r(n) \tag{3.50}$$

for logistic map as nodal dynamics and for diffusive coupling among the nodes, matrices $\boldsymbol{\alpha}$ and $\boldsymbol{\beta}$ are given by:

$$\boldsymbol{\alpha} = \begin{pmatrix} r(1-2x^*) & \varepsilon_1 \\ \varepsilon_2 & k \end{pmatrix} \tag{3.51}$$

and

$$\boldsymbol{\beta} = \begin{pmatrix} -rD(1-2x^*) & 0 \\ 0 & -D_e k \end{pmatrix} \tag{3.52}$$

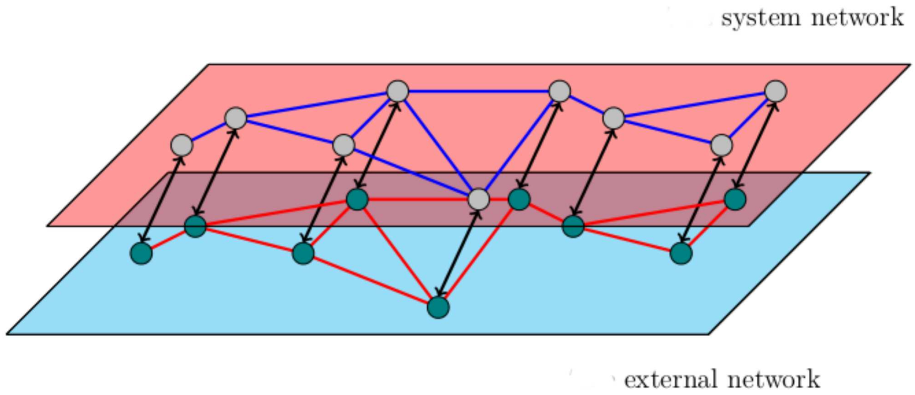

Figure 3.22: Schematic of a random network coupled to an external network. The arrows represent the feedback coupling connections between the two networks.

This gives,

$$\boldsymbol{\alpha} + \lambda_r \boldsymbol{\beta} = \begin{bmatrix} r(1-\lambda_r D)(1-2x^*) & \varepsilon_1 \\ \varepsilon_2 & k(1-\lambda_r D_e) \end{bmatrix} \tag{3.53}$$

Then for the synchronized fixed point state of the system of coupled networks to be stable, for every eigenvalue λ_r of the Laplacian matrix of the network, absolute values of all the eigenvalues of the matrix $(\boldsymbol{\alpha} + \lambda_r \boldsymbol{\beta})$ should be less than 1. We now consider λ_r in $(\boldsymbol{\alpha} + \lambda_r \boldsymbol{\beta})$ as a parameter λ and for a range of λ, find eigenvalue with largest absolute value and use this eigenvalue as master stability function (MSF). The results are shown in Fig. 3.23 where for 3 different values of ε, the master stability curves are shown. We see that all the curves are continuous over the whole range of λ. The region of the curve for which $-1 \leq MSF \leq 1$ is the stable region for that curve. If all the eigenvalues of Laplacian matrix for a given topology fall inside this region, then the state of synchronized fixed point is stable. Since the smallest eigenvalue of Laplacian matrix for unweighted and undirected network is always 0, we need to worry about the largest eigenvalue only. Hence if both $MSF(\lambda = 0)$ and $MSF(\lambda = \lambda_{max})$ are inside this region then fixed point for the network is stable.

The red curve in Fig. 3.23 is for $\varepsilon = 0.41$ which is the minimum coupling strength required for any topology for fixed point of the whole network to be stable. For any coupling strength less than this, absolute value of $MSF(\lambda = 0)$ is greater than 1 and hence fixed point of the network cannot be stable. To illustrate this, we plot the master stability curve for $\lambda = 0.3$ shown in the figure as a violet curve. The third curve (black) is for $\varepsilon = 0.5$. In the figure we mark largest eigenvalues of Laplacian matrices of 5 different networks for which numerical simulations are performed.

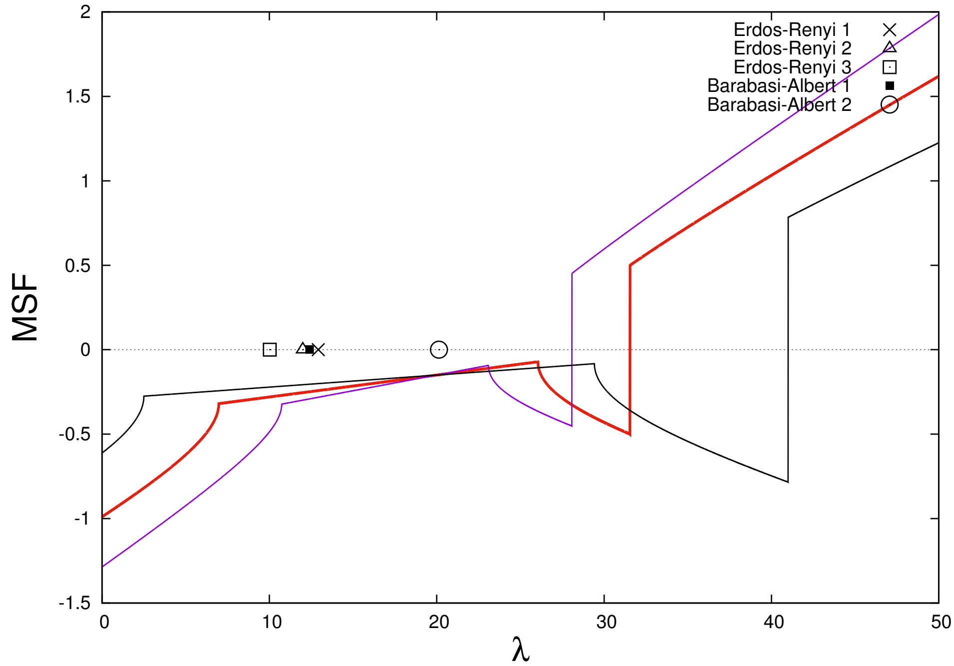

Figure 3.23: Master stability functions for a network of logistic maps coupled to an external network for three values of coupling strengths ε with $D = 0.05$ and $D_e = 0.1$. The red curve (thick) is for critical value of $\varepsilon = 0.41$ which is the minimum coupling strength necessary for the fixed point state of the network to be stable when all other parameters are kept constant. The violet curve is for $\varepsilon = 0.3$ and it is clear from the figure that for all topologies, fixed point state is unstable at this coupling strength. The black curve is for $\varepsilon = 0.5$. For a network of 50 nodes, with different random topologies (3 Erdős-Rényi topologies and 2 Barabási-Albert topologies), the largest eigenvalue is marked on the graph.

To support the master stability analysis, we present numerical results for one particular realization of Erdős-Rényi network. We calculate an index $\langle A \rangle$ to characterize the synchronized fixed point by taking the difference between global maximum and global minimum of the time series of x at each node of the network after neglecting the transients and averaging this quantity over all the nodes. For parameter values corresponding to the controlled state of amplitude death, this index has value 0 [112]. In Fig. 3.24, we show variation of $\langle A \rangle$ with ε and it is clear that $\langle A \rangle$ goes to 0 at $\varepsilon = 0.41$ indicating that amplitude death happens as predicted by master stability analysis.

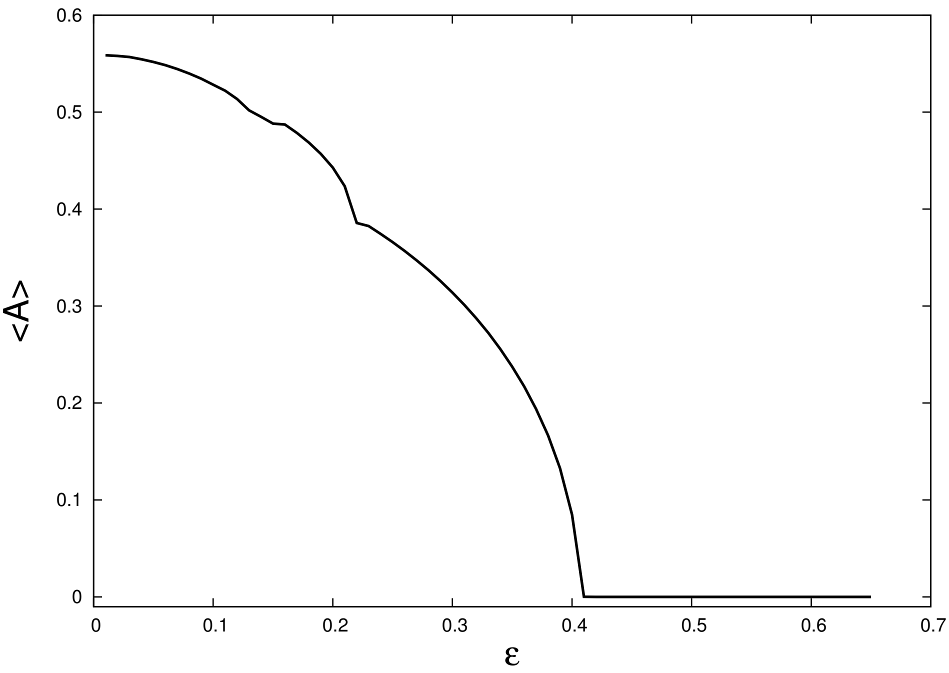

Figure 3.24: Index $\langle A \rangle$ obtained numerically as a function of coupling strength ε for a system of logistic network coupled to an external network. The topology of both networks in this case is of Erdős-Rényi type. For $\varepsilon \sim 0.41$, control to steady state happens.

3.6 Control of a network using structurally different networks

In the previous section, we discussed how the dynamics on a random network can be controlled using an external network, having exactly the same structure as that of the system network. This allows one to apply the master stability formalism to this system of two coupled networks. However, in a general case, the external network need not be identical to the system network for controlling the dynamics on the later.

We start with two structurally non-identical Erdős-Rényi networks each with $N = 100$ nodes. For both networks, the connection probability is $p = 0.3$. The interconnections between these two networks are then made in such a way that exactly one node in the external network is connected to one node in the system network. This system of two coupled networks is represented by the following equations:

$$\begin{aligned} \mathbf{x}_i(n+1) &= \mathbf{f}(\mathbf{x}_i(n)) + \frac{D}{k_i^s}\sum_{j=1}^{N} B_{ij}^s \zeta(\mathbf{f}(\mathbf{x}_j(n)) - \mathbf{f}(\mathbf{x}_i(n)) + \varepsilon_1 \xi z_i(n) \\ z_i(n+1) &= g(z_i(n)) + \frac{D_e}{k_i^e}\sum_{j=1}^{N} B_{ij}^e (g(z_j(n)) - g(z_i(n))) + \varepsilon_2 \xi^T \mathbf{x}_i(n) \end{aligned} \tag{3.54}$$

This equation is identical to Eq.(3.48) except for the fact that the adjacency matrices B^s and B^e of the system network and external network are not in general identical and we divide the total input received by a given node by its degree (k_i^s in system network and k_i^e in external network). We find that even in such a system of two non-identical networks, control of the system network can be achieved for sufficiently high value of the control parameter ε.

We repeat the same analysis with non-identical Barabási-Albert networks grown in such a way that a new node joining the network connects to two of the different existing nodes preferentially. We find that here also, the control is achieved for a sufficiently high value of control parameter.

To characterize these results about non-identical networks, for every value of ε, we generate such 100 random realizations of two networks and then calculate the index $\langle A\rangle_{\rm r}$ given in Eq.(3.42). The plots of $\langle A\rangle_{\rm r}$ as a function of ε for both types of networks are shown in Fig. 3.25.

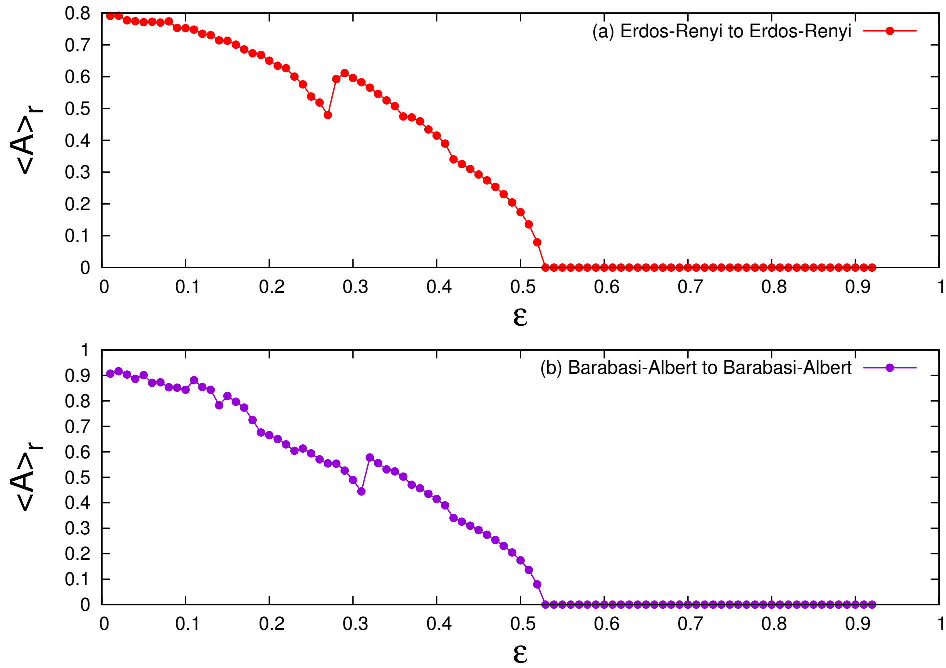

Figure 3.25: Index $\langle A\rangle_{\rm r}$ as a function of control parameter ε for coupled non-identical networks: (a)Erdős-Rényi network coupled to Erdős-Rényi network and (b)Barabási-Albert network coupled to Barabási-Albert network. For every value of control parameter α, 100 random realizations of two networks each with size 100 have been taken. Nodal dynamics in each case is that of fully chaotic logistic map ($r = 4$) and intra-coupling strengths for two networks are: $D = 0.1$ and $D_e = 0.1$. The damping parameter k is kept fixed at value 0.3.

3.7 Control scheme for continuous time dynamical systems

We now briefly demonstrate how the control scheme described so far can be extended to control the continuous time dynamics on networks. We consider a ring of continuous time dynamical systems and use external ring to control it similar to the case of ring of discrete systems. The resulting system can be represented by the following equations.

$$\begin{aligned}\dot{\mathbf{x}}_i(t) &= \mathbf{f}(\mathbf{x}_i(t)) + D\zeta(\mathbf{x}_{i-1}(t) + \mathbf{x}_{i+1}(t) - 2\mathbf{x}_i(t)) + \varepsilon_1 \xi w_i(t) \\ \dot{w}_i(t) &= -kw_i(t) + D_e(w_{i-1}(t) + w_{i+1}(t) - 2w_i(t)) + \varepsilon_2 \xi^T \mathbf{x}_i(t)\end{aligned} \tag{3.55}$$

where $\mathbf{x}_i \in \mathbb{R}^m$ is a state vector of the i^{th} node in the system ring, w_i is the state variable of the i^{th} node in the external ring, $k \in [0, \infty)$ is the damping parameter, D is the coupling strength among the nodes of the system ring, D_e is the coupling strength among the nodes of the external ring, ε_1 and ε_2 are the control parameters, ζ is an $m \times m$ matrix which decides which variables from the system vectors are coupled to each other inside the ring and ξ is a $m \times 1$ matrix which selects appropriate variables from the system dynamics to be coupled to the dynamics in the external ring.

3.7.1 Control of coupled Rössler systems

We start with Rössler system in the chaotic regime as the nodal dynamics for a system ring. The resulting system of two coupled rings then takes the following form:

$$\begin{aligned}\dot{x}_i &= -y_i - z_i + D(x_{i-1} + x_{i+1} - 2x_i) + \varepsilon_1 w_i \\ \dot{y}_i &= x_i + ay_i \\ \dot{z}_i &= b + z_i(x_i - c) \\ \dot{w}_i &= -kw_i + D_e(w_{i-1} + w_{i+1} - 2w_i) + \varepsilon_2 x_i\end{aligned} \tag{3.56}$$

The parameters of Rössler system are chosen to have values $a = 0.2$, $b = 0.2$ and $c = 5.7$ so that the intrinsic dynamics of the system is chaotic. Also, we take $\varepsilon = -\varepsilon_1 = \varepsilon_2$ henceforth.

We find that the ring of chaotic Rössler systems can be controlled to a fixed point state when the coupling parameter ε is sufficiently high while for smaller values of ε, Rössler system gets controlled to various limit cycle behaviors through reverse period doubling sequences. The phase plots of one of the nodes in the ring for different values of control parameter ε are shown in Fig. 3.26

We also explore the behavior of the system in Eq.(3.56) in the $\varepsilon - k$ parameter plane and find that there exists a significant region of control in this parameter plane. This plane is shown in Fig. 3.27

The transition to amplitude death in this case can be observed in a better way by looking at the bifurcation diagram of x variable of one of the nodes in the ring as ε is varied as shown in Fig. 3.28.

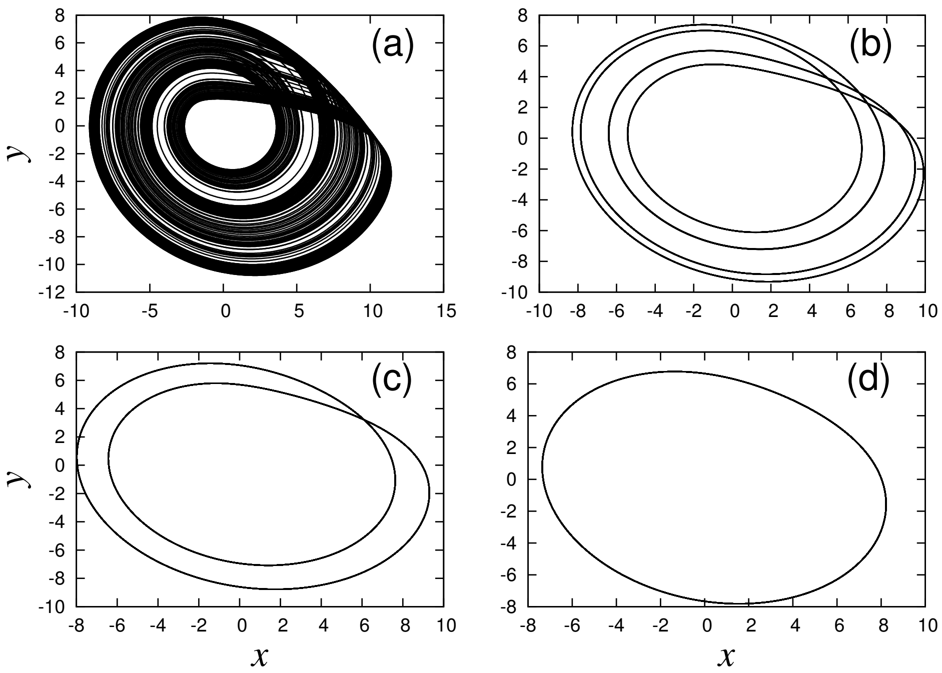

Figure 3.26: Phase plots for one of the nodes in the ring of Rössler systems coupled to an external ring represented by Eq.(3.56). For various values of control parameter ε with $k = 3$ fixed, different controlled states are observed: (a)$\varepsilon = 0$, (b)$\varepsilon = 0.42$, (c) $\varepsilon = 0.5$ and (d)$\varepsilon = 0.6$

3.7.2 Control of coupled Hindmarsh-Rose neurons

As our second example, we apply the control scheme to a ring of Hindmarsh-Rose neuron model (HR model) which is given by the following set of equations.

$$\begin{aligned} \dot{x} &= y - ax^3 + bx^2 - z + I \\ \dot{y} &= c - dx^2 - y \\ \dot{z} &= r[s(x - x_R) - z] \end{aligned} \tag{3.57}$$

The system of ring of HR neurons coupled to an external ring is then given by:

$$\begin{aligned} \dot{x}_i &= y_i - ax_i^3 + bx_i^2 - z_i + I + D(x_{i-1} + x_{i+1} - 2x_i) + \varepsilon w_i \\ \dot{y}_i &= c - dx_i^2 - y_i \\ \dot{z}_i &= r[s(x_i - x_R) - z_i] \\ \dot{w}_i &= -kw_i + D_e(w_{i-1} + w_{i+1} - 2w_i) - \varepsilon x_i \end{aligned} \tag{3.58}$$

The various parameters in this model have these values: $a = 3, b = 5, I = 2, r = 0.005, x_R = -8/5$ and $s = 4$. These values correspond to the bursting behavior of the neuron. We find that similar to the case of Rössler system, for a certain value of ε, all the

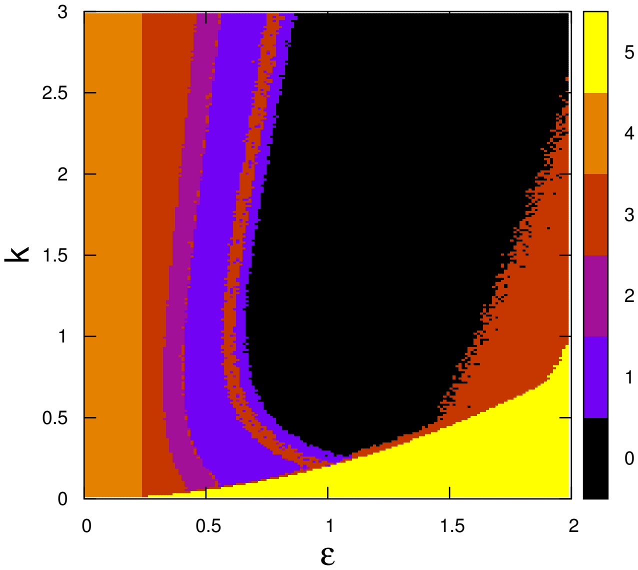

Figure 3.27: $\varepsilon - k$ parameter plane for a ring of Rössler systems coupled to an external ring (Eq.(3.56)). Direct coupling strength values are $D = 1$ and $D_e = 0.5$ and with these values, all systems in the ring remain completely synchronized for all values of ε. The color coding is as follows, **0**: amplitude death, **1**: one-cycle, **2**: two-cycle, **3**: higher-limit cycles, **4**: chaos, **5**: instability

systems in the ring go from bursting behavior to spiking behavior. When ε is increased further, the system gets controlled to a fixed point state. This behavior is shown in Fig. 3.29 which shows the time series of one of the systems in the ring for different values of ε.

The behavior of the system as the control parameter ε is varied can be visualized by plotting the bifurcation diagram shown in Fig. 3.30(a) for one of the systems in the ring. It can also be seen that from Fig. 3.30(b) that when these systems are controlled to a periodic state, they synchronize even though without control their dynamics is desynchronized.

3.8 Conclusion

The suppression of unwanted or undesirable excitations or chaotic oscillations in systems is essential in a variety of fields and therefore mechanisms for achieving this suppression in connected systems are of great relevance. In the specific context of neurons, it is known that exaggerated oscillatory synchronization or propagation of some excitations can lead to pathological situations and hence methods for their suppression are very important.

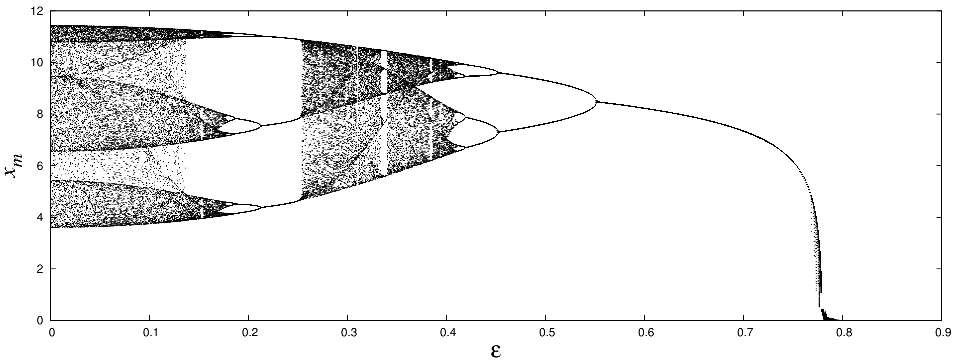

Figure 3.28: Bifurcation diagram for one of nodes in the ring of chaotic Rössler systems (Eq.(3.56)) as the control parameter ε is varied with damping parameter $k = 3$. Direct coupling strengths are $D = 1$ and $D_e = 0.5$.

Methods to avoid oscillations by design of system controls such as power system stabilizers are important in engineering too.

In this chapter, we present a novel scheme where suppression of dynamics can be induced by coupling the system with an external system. Our study is mostly on extended systems like rings and lattices in interaction with similar systems with different dynamics. However the method is quite general and is applicable to other such situations also where control and stabilization to steady states are desirable. Even in the case of single systems, as illustrated here for Hénon and logistic maps, this method can be thought of as a control mechanism for targeting the system to a steady state.

We develop the general stability analysis for the coupled systems using the theory of maps and circulant matrices and identify the regions where suppression is possible in the different cases considered. The results from direct numerical simulations carried out using two standard discrete systems, logistic amp and Hénon map, agree well with that from the stability analysis. Our method will work even with a single external system as control; however, extended or coupled external system enhances the region of effective suppression in the parameter planes. Our study indicates that by tuning the parameters of the external control system, we can regulate the dynamics of the original system to desired periodic behavior with consequent spatial order. We also show the generality of the scheme for rings by randomizing the connections between the two rings and showing that the control is still achieved.

We also report how the present coupling scheme can be extended to suppress dynamics on random networks by connecting the system network with an external similar network in a feedback loop. In this context the stability analysis using Master stability function, gives the critical strength of feedback coupling required for suppression. We also show that same scheme works even when the two networks in question are structurally non-identical.

Finally, we extend the scheme to coupled continuous systems and show that ring

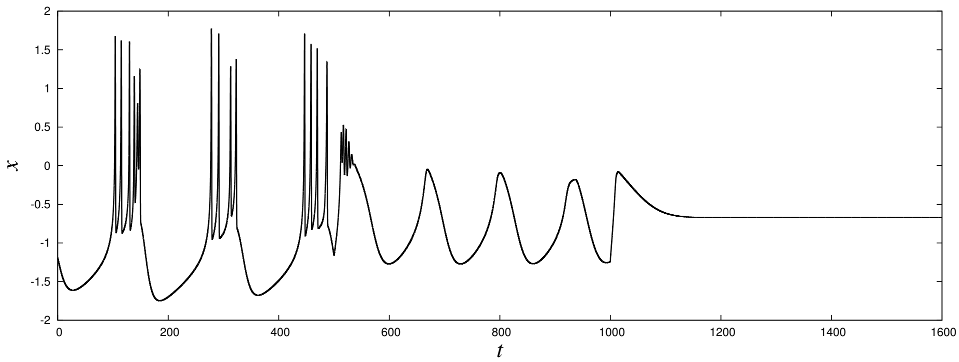

Figure 3.29: Time series of one of the systems from a ring of HR systems coupled to an external ring (Eq.(3.58)). Initially $\varepsilon = 0$. Around $t = 500$, control is switched on with $\varepsilon = 1$ and then systems go to spiking behavior. When ε is further increased to 1.4, system ring goes to fixed point state. The damping parameter k is kept fixed at value 1 while direct coupling strengths are $D = 1$ and $D_e = 0.5$.

of chaotic systems like Rössler system and Hindmarsh-Rose system can be controlled to periodic or steady state using this scheme. Our analysis leads to the interesting result that control to steady state occurs even when the systems are not coupled among themselves but coupled individually to the connected external systems. So also, individual external systems, which are not connected among themselves but each one connected to one node in the system, can suppress the dynamics of the connected nodes in the system. This facilitates flexibility in the design of control through connected or isolated external systems depending on the requirement.

The scheme of external and extended control, introduced here, has relevance in understanding and modeling controlled dynamics in real systems due to interaction with external medium. We illustrate this in the context of coupled neurons where the suppression of dynamical patterns is achieved by coupling with the extra cellular medium. We also indicate how the same scheme can be applied to control chimera states in non-locally coupled systems. Until recently, CML was considered as an idealized theoretical model for studies related to spatio-temporal dynamics. However the recent works on a physically realizable CML system using liquid-crystal spatial light modulator [80] and based on digital phase-locked loop [120] have opened up many interesting possibilities in studying their control schemes also experimentally. In this context we note that the scheme presented in the paper is suitable for a physical realization using optical instruments or electronic hardware.

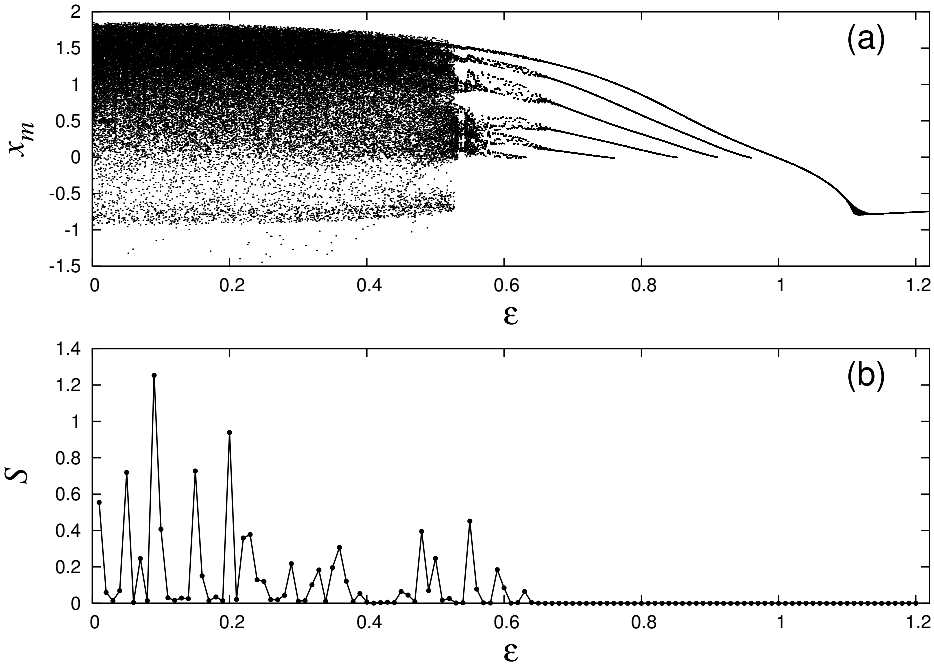

Figure 3.30: (a) Bifurcation diagram for one of the systems in the ring of HR neurons in burst regime with $k = 1$, $D = 1$ and $D_e = 0.5$. As is clear from the diagram, for sufficiently high value of ε, systems go to spiking and fixed point behavior. (b) The corresponding plot of the synchronization index S. Systems are seen to synchronize when they are controlled to a periodic state.

Chapter 4

Mediated attachment in complex networks

4.1 Introduction

One of the most important topics of study in the theory of complex networks is related to understanding the physical mechanisms which give rise to various structural features seen in real-world networks [1,2,42,121,122]. The analysis of empirically observed data of real networks reveals a very interesting fact that apart from system dependent details, there exist structural features in these networks which are common in large number of systems [1,2]. This universality suggests that robust organizing principles which are almost system independent must be at work in these systems [121]. The *generative network models* use such principles or physical mechanisms to simulate networks [39, 42, 121, 123]. If the networks so constructed have similar structural features as that of the real networks, then this suggests that similar mechanisms could be at work in real networked systems also [1].

The most important structural features of real networks which set them apart from completely random networks like Erdös-Rényi graph, include their scale-free structure [2, 121], small-world nature [2, 42], modularity or community structure [22, 124] and non-zero degree correlations [1, 25]. Many generative models have been proposed to explain the structure of real networks [39,42,121,123,125,126]. The real networks are essentially random since it is not always possible to say whether given two nodes will be connected to each other with certainty. Hence the first step in modelling real networks is to model them as random networks. Such a model for random networks or random graphs was put forth by Erdös and Rényi [127] and the networks constructed using this model are called as Erdös-Rényi networks or simply ER networks. To explain the high clustering and small average path length of real networks, Watts and Strogatz proposed what is now known as the Watts-Strogatz model or WS model [42]. The more important issue of emergence of power-law in the degree distribution of real networks was first addressed by Price [128] and then by Barabási and Albert [121]. These models fall into the category of preferential attachment models where network keeps growing by the addition of new nodes and new node connects to old nodes preferentially with respect to their degree values. Thus, the probability that a new node will connect to an existing node i k_i is:

$$\Pi(k_i) = \frac{k_i}{\sum_j k_j} \tag{4.1}$$

To explain specific cases of scale-free networks in real world systems, many modifications of basic preferential attachment have been suggested. For example, creation of links between the pre-existing nodes has been considered in [129]. In preferential attachment models, the effect of removal of nodes while the network is growing has been shown to have no effect on the scale-free structure of the network when there is a net increase in the size of the network [130]. When vertices of varying intrinsic fitness or attractiveness are considered, the model may or may not lead to power-law type of degree distribution depending upon the details [131, 132].

More general models with nonlinear preferential attachment have also been studied. In one such model [133], the connection probability is taken to be:

$$\Pi(k_i) = \frac{k_i^\gamma}{\sum_j k_j} \tag{4.2}$$

such that the Barabási-Albert model is then a special case of this model with $\gamma = 1$. It has been shown that for $\gamma < 1$, this model produces networks with a stretched exponential type of degree distribution while for $\gamma > 1$, the networks produced contain a super-hub with almost all other nodes connected to this particular node.

The preferential attachment models usually employ global mechanisms to develop a network and hence the local properties like clustering and finite degree-correlations are not explained well by these models. Also the mechanisms behind the emergence of modular structure of networks is not explained by these models. Thus, it is important to investigate the local mechanisms responsible for the emergence for these structures along with scale-free structure. An important mechanism in this respect that has been proposed is that of "triadic closure" [123, 125, 126, 134] that results in scale-free networks with modular structure as well as finite degree correlations.

In the present chapter, we introduce a generative network model based on "triadic closure" with an additional principle that "Hubs are weak mediators". We call this model as "mediated attachment model" to distinguish it from the other models involving triadic closure. We show that the networks generated with this mechanism exhibit both scale-free nature and hierarchical community structure. The work has been published in *Eur. Phys. J. B (2015)* **88***:227*.

4.2 Triadic closure in real networks

The triadic closure is proposed as one of the local processes that seem to be present in many real networks [126, 134]. This involves the formation of links between a pair of nodes of the networks which share one or more neighbors in the network (See Fig. 4.1(a)). We now indicate the existence of mechanisms analogous to triadic closure in various real networks.

4.2.1 Social networks

Nodes in social networks are human beings or their user accounts on social networking sites like Facebook. The acquaintance is usually considered as a definition of a link in these networks; however, the definition of acquaintance itself varies such that one can define various social networks like simple acquaintance, friendships, co-authors, Facebook etc. Social networks present perhaps the most prominent example where the process of triadic closure is at work because people get to know each other through other people or common neighbors.

4.2.2 Networks in linguistics

Various relations existing in human languages can be used to construct complex networks in linguistics where individual words are nodes. For example, significant co-occurrence of words in a sentence has been used to construct a network of words from British National Corpus [135]. Similarly, dependency grammar formalism has been used to construct and analyze networks of words from corpora in Czech, Romanian and German languages [136]. During the evolution of a particular language, when words A and B start appearing together in a sentence and if the same happens for words B and C, with a fairly high probability words A and C would appear in the same sentence. Thus, there exists triadic closure connecting words A and C through word B.

4.2.3 World Wide Web

World Wide Web is a man made network in which individual webpages are nodes connected by hyperlinks [12,137]. Most web pages keep evolving by the addition and modification of their content and hence new hyperlinks are usually added to the page. Suppose a web page A has hyperlink to another page B, which itself contains hyperlink to page C, then A can know about C through B and can connect to C.

4.2.4 Scientific Papers

The network of scientific papers, also known as citation network, consists of research articles as nodes [138, 139]. Two nodes in this network are said to be connected if one article cites the other article. Most of the time, researchers come to know about other research articles through bibliographies of the articles they are reading and hence might cite those articles. This phenomenon is very analogous to the triadic closure mechanism [123].

4.3 Internal links in the triadic closure models

All the network growth models involving triadic closure models assume that no direct preferential attachment is present while network is growing and preferential attachment is only an outcome of local process of triadic closure [123, 126, 140]. Such triadic closure models have been proved to be extremely successful in producing highly clustered scale-free networks.

However, most of the triadic closure models reported have restricted themselves to "external links". This means that in these models, only the new node is usually considered as a source of a triadic closure [123, 125, 126, 134]. This in some sense is unsatisfactory since it is obvious that many links generated in the network actually come from existing nodes. The "mediated attachment model" presented here tries to rectify this by including internal links created by triadic closure. However, as we will see in the next section, the inclusion of such internal links in these models actually leads to networks that are highly dense and do not possess scale-free structure as well as community structure. We save the situation by identifying a fundamental property of nodes of complex networks called "mediating capacity" and argue that its behavior is almost system independent. We show that this property can potentially explain the simultaneous existence of scale-free structure and hierarchical modularity even with inclusion of internal links.

4.4 Hubs as weak mediators

We now make an important observation about the nodes of all complex networks, especially scale-free networks. The capacity to mediate a triadic closure is a degree dependent property such that high degree nodes or hubs are weak mediators. We present a following argument in support of this. Usually hubs in scale-free networks are considered as most important nodes. At the same time, it is easy to see that the high degree nodes or hubs in complex networks have capability to interact with nodes of a wide range of properties. For example, if we consider Google web page which is a hub in World Wide Web, the web pages which link to it are related to very diverse topics like mathematics, history, sports, music and so on. Similarly, a hub in social network i.e. the person with many more friends than an average number, usually has interest in wide variety of topics and hence develops the connections to people from highly diverse fields. In the network of words of a particular language. In this network, hub is usually a word that is capable of appearing with words belonging to diverse range of contexts. For example, the word "THE" in English can appear with many different words. In the jargon of network theory, we can thus say that hubs are usually connected mostly to nodes that are dissimilar to each other. On the other hand, a low degree node (a Wikipedia page about a technical topic from mathematics) would have links only to nodes similar to it and hence usually its neighbors are also similar with each other.

In all these cases the probability that such diverse or dissimilar nodes will get connected is very low. This leads to the observation that hubs should function as weak mediators in such networks. For example, a hub in social network may introduce two of his contacts with each other but those two contacts would usually share different interests and hence the link may not get established between them. This implies that the mediating capacity of a node decreases with increase in degree. As we will see, this insight naturally unifies the emergence of hierarchical community structure with scale-free nature in such networks.

4.5 Mediated attachment model

We present a generative mechanism in the growth of networks with the property of mediating capacity for the nodes as discussed in the previous section. To incorporate this, we conjecture that the average number of links mediated by a node with degree k decreases with k. Therefore we take the probability that a node i with degree k_i connects two of its neighbors at a given time to be $1/k_i^n$ where n is a parameter. For a node of degree k, maximum ${}^kC_2 \sim k^2$ links are possible among its k neighbors. Hence a node with degree k will form approximately $k^2(1/k^n) = (1/k^{n-2})$ links at any given time. Thus we must have $n > 2$ if hubs are to behave as weak mediators. However, we also describe the effect of $n < 2$ (i.e. the effect of hubs not being weak mediators) later in the section.

Since real networks operate locally, usually what happens in one part of the network doesn't directly affect the processes like addition of links and nodes in the other part of the network. This means that both the number of links and number of nodes that join the network is an increasing function of the size of the network. To incorporate this type of increase in the number of nodes, at each discrete time t we add approximately $pN(t)$ number of nodes to the network where p is the parameter with value between 0 and 1 and $N(t)$ is the number of nodes in the network at time t. The case of addition of fixed number of nodes at a time would then correspond to p value that decreases with time.

The growth of the network in this model thus involves two processes:

1. Starting from two connected nodes at time $t = 0$, $\lceil pN \rceil$ number of nodes are added to the network at each discrete time t where $\lceil\rceil$ denotes the ceiling function. Each new node connects to one of the old nodes randomly with uniform probability.

2. At the same time, every existing node i of degree $k_i(t)$ (> 1) connects every pair of its neighbors with probability:

$$w_i(t) = \frac{A}{k_i(t)^n} \tag{4.3}$$

where A and n are adjustable parameters with $n > 2$. The quantity $w_i(t)$ reflects the mediating capacity of node i at time t.

A small network generated under these processes is shown in Fig. 4.1(b).

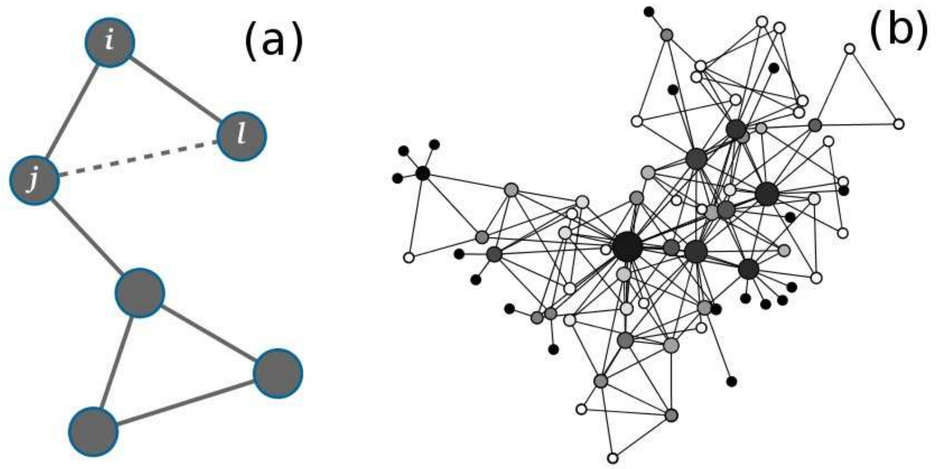

Figure 4.1: (a) Graphical representation of triadic closure process: node i acts as a mediator for nodes j and l and tries to connect them. (b) Mediated network at time $t = 25$ with $p = 0.1$, $A = 8$ and $n = 3$. The sizes of nodes are proportional to their degree values and the color of each node is graded according to its clustering coefficient, the darkest being the lowest.

It can be easily seen that since each node is allowed to connect its neighbors with each other, the number of new links added to the network is an increasing function of the network size. If the rate of increase of network size is low, this would produce a highly dense network whose average degree $\langle k \rangle$ would increase with time. However, in the present model, the total number of nodes also increases quite fast and as we will see below, these two factors can stabilize $\langle k \rangle$ of the network.

In general $\langle k \rangle$ of the network must stabilize if the degree distribution is to be stationary asymptotically. In Fig. 4.2, $\langle k \rangle$ is plotted as a function of time for different values of n. With $p = 0.1$, the results shown are for 100 realizations of the growth process. The values for $n = 1.5$ are divided by 5 for better visualization. Clearly, for $n < 2$, $\langle k \rangle$ is a very rapidly increasing function of time and hence the degree distribution is not stationary in this case whereas for $n > 2$, it always stabilizes leading to a stationary degree distribution.

Fig. 4.3 shows the behavior of average degree as a function of parameter n at two different times. The rapid increase in average degree with time (and hence the existence of non-stationary degree distribution) is evident. This behavior is understandable because for small n, the process of creation of links overtakes the process of creation of nodes.

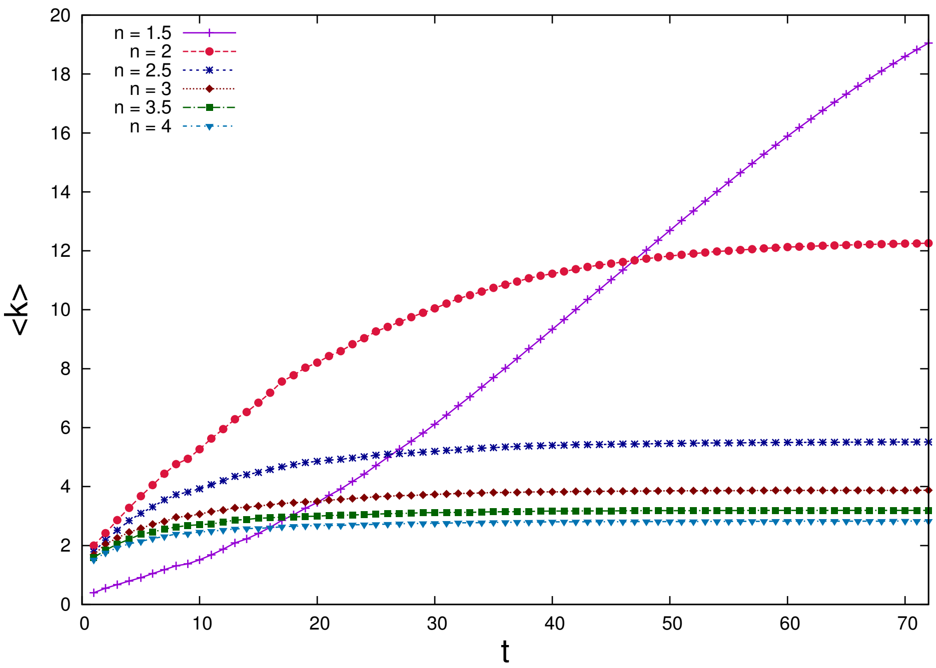

Figure 4.2: Average degree of the network as a function of time for various values of n with $A = 4$ and $p = 0.1$. For better visualization, for $n = 1.5$ the plotted values are equal to actual values divided by 5. For $n < 2$, $\langle k \rangle$ is a rapidly increasing function of time and hence leads to a non-stationary degree distribution. All cases with $n \geq 2$ lead to a stabilized averaged degree. In each case, network is grown up to size $N = 9525$ and results are averaged over 100 realizations.

For the mediating capacity chosen as in Eq.(4.3) from $n = 2$ onwards these two effects balance each other stabilizing $\langle k \rangle$.

Also when $n < 2$, the network is so dense that there are too many nodes with very high degree and hence the network does not exhibit a scale-free structure. To see this, we plot the degree distributions of the network for $n = 1.5$ and $n = 2.5$ in Fig. 4.5. For $n = 1.5$, there exists a peak in the tail and hence the network in this case is not scale-free.

4.6 Simultaneous occurrence of scale-free structure and hierarchical modularity

Many real networks are both scale-free and hierarchically modular. The simultaneous occurrence of scale-free structure and hierarchical modularity is a less explored topic in the context of generative network models. As we now show, the mediated attachment model based on the conjecture that the hubs are weak mediators naturally gives rise to networks with both these properties. To establish the scale-free structure of the resulting

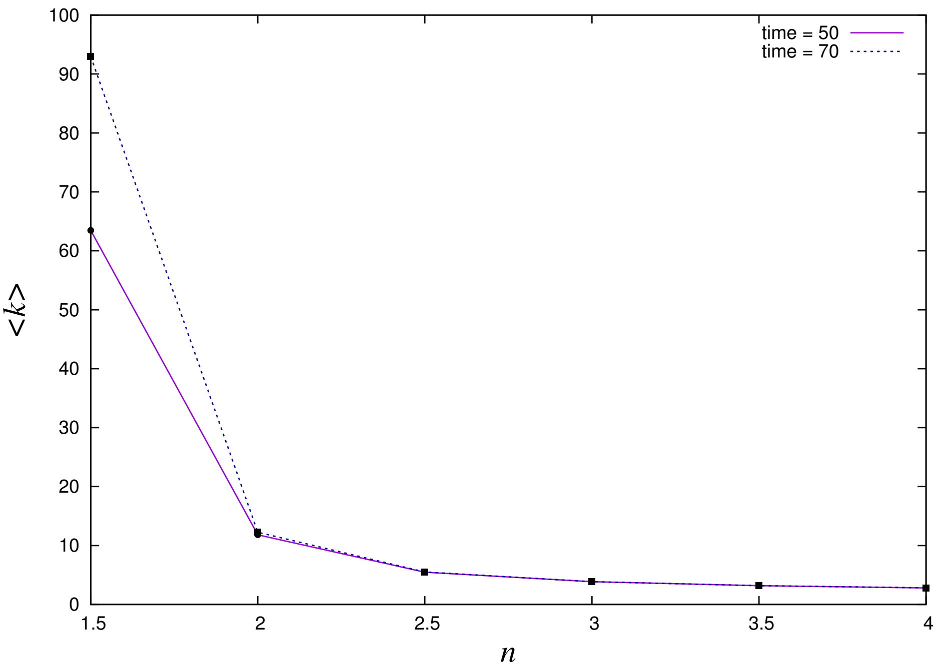

Figure 4.3: Average degree $\langle k \rangle$ as a function of parameter n at two different times $t = 50$ (a continuous line) and $t = 70$ (a solid line). It can be seen that when $n < 2$, $\langle k \rangle$ has tendency to increase rapidly while for $n > 2$ average degree saturates. The results are averaged over 100 random realizations.

network, in Fig. 4.5 we plot the degree distributions of the network for various values of n with $n > 2$ and all of them can be seen to follow a power-law behavior with a scaling index close to 3. Most of the real networks are usually seen to have scaling indices in the range $(2, 4)$ [1, 2] and hence the parameters of the model like A and n can be tuned to produce the actually observed distributions satisfactorily.

A necessary (but not sufficient) indicator of existence of hierarchical modularity in the given network is the dependence of local clustering coefficient on the degree (Eq.(1.4)).

For the networks with hierarchical modularity, c_i shows a systematic decrease with degree k with $c(k) \sim k^{-1}$ [141]. For the model presented here, we compute the local clustering coefficient for different values of n using Eq.(1.4) and plot it as a function of k in Fig. 4.6. The decrease of $c(k)$ with degree is clear in all cases. This happens because the mediating capacity of a node decreases with increase in its degree and which in turn reduces its clustering coefficient when degree is large.

To confirm that the mediated network does possess the hierarchical modularity, we use hierarchical Infomap (http://www.mapequation.org/code.html). We find that for all $n > 2$, the mediated network is hierarchically modular but the number of modular levels depends on the value of n and in fact is an increasing function of n. Thus, for the network size $N = 9525$ used here, for $n = 2.5$, the generated network has 4 to 5 levels of hierarchy

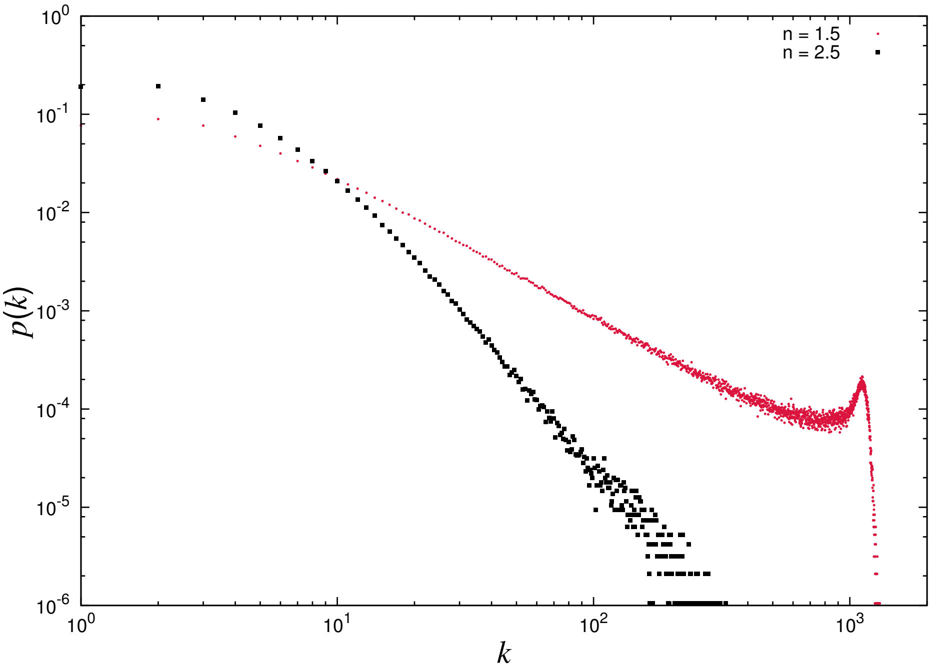

Figure 4.4: Comparison of degree distributions for mediated network with $n < 2$ and $n > 2$. Here for $n < 2$ ($n = 1.5$ in this case), the distribution completely deviates from the power law in the tail and is also non-stationary as shown in Fig. 4.2. Both cases correspond to $N = 9525$ and results are averaged over 100 realizations.

while for $n = 4$, it has 8 to 9 levels of hierarchy.

4.7 Characteristics measures and their scaling

Now we look at the various important network characteristics like clustering coefficient, path length and degree correlations for the mediated network.

4.7.1 Clustering coefficient

!Clustering coefficient!of mediated network

In the present context, we use Watts-Strogatz clustering coefficient C_{WS} (also called as average clustering coefficient) defined in Eq.(1.5) as the quantifier for the clustering in the network. Fig. 4.7 shows the Watts-Strogatz clustering coefficient of the mediated network as a function of time for various values of n. It can be seen that all C_{WS} values settle asymptotically to values in the range $(0.4, 0.7)$. Almost all the real networks like film actors, coauthorships, citations, Internet, WWW, metabolic networks, protein interactions, ecological food webs and neural networks show such high values of C_{WS} [122].

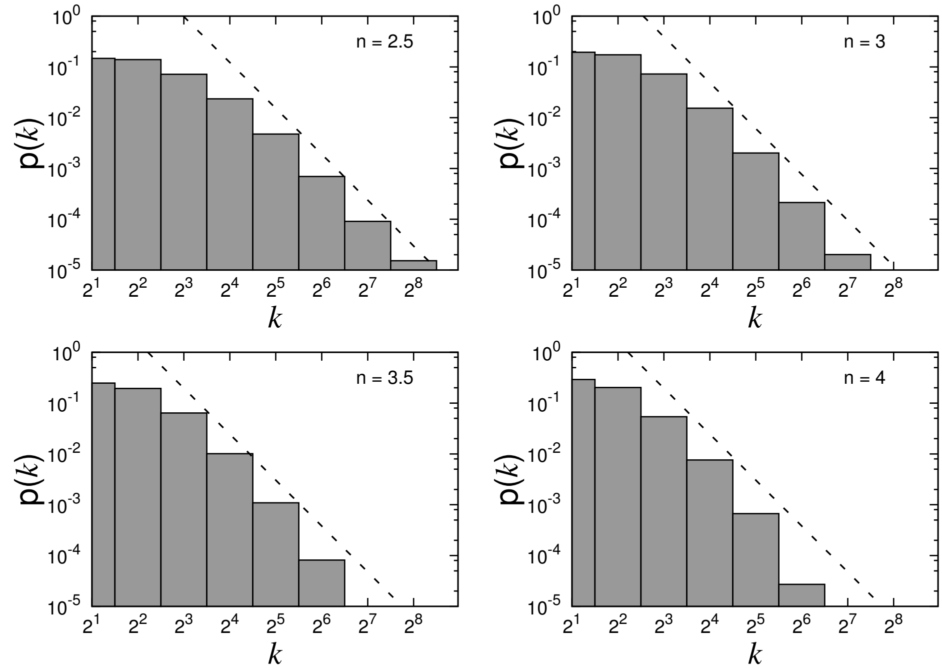

Figure 4.5: Degree distributions of mediated network of size $N = 9525$ for different values of n with $A = 8$ and $p = 0.1$. A logarithmic binning is used to plot the histograms. The dotted line in each plot has slope -3 which is close to the actual scaling indices of real networks. All the results are averaged over 1000 random realizations.

This agreement with the empirical observations further supports the relevance and utility of the model presented here.

4.7.2 Degree correlations

Apart from the properties discussed so far, many real networks show non-zero degree correlations. Assortative or dissortative nature of networks can be quantified by calculating the assortativity coefficient defined in Eq.(1.8)

Interestingly, social networks are always seen to possess positive degree correlations i.e they are assortative [25]. In Fig. 4.8 we show the assortativity coefficient of the mediated network as a function of time for different n. It is clear that our model with $n > 2$ leads to positive degree correlations.

Though the present model doesn't reproduce networks with negative value of the correlation coefficient, modifications are possible. For example, the model doesn't include the fitness for the nodes which has been considered as an important quality of the nodes in the previous works [131, 132]. We think that such important modifications of the present model would lead to even more realistic model of the network formation and would allow one to tune the degree correlations.

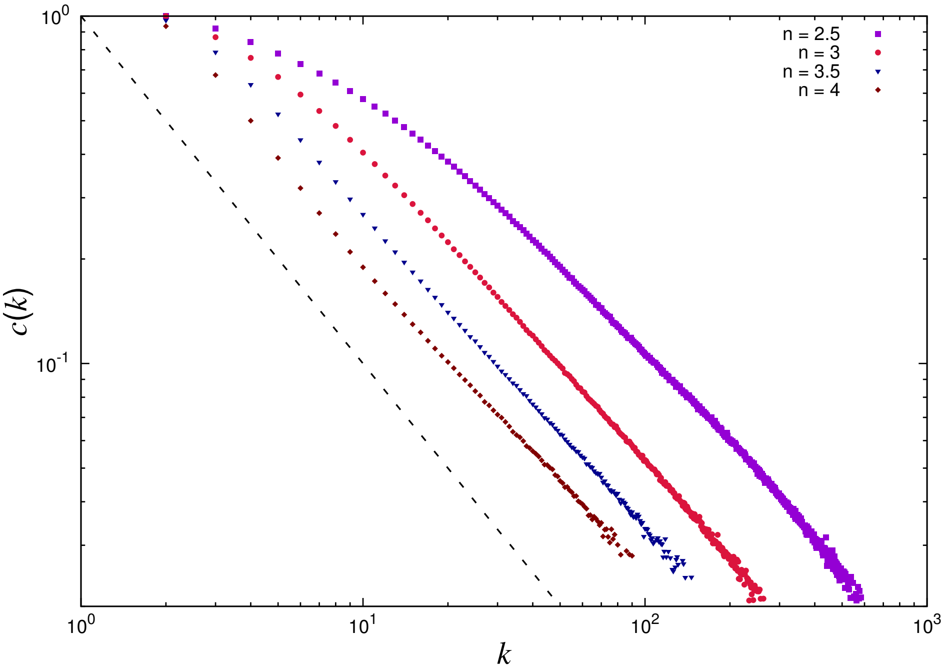

Figure 4.6: Local clustering coefficient c as a function of degree k for mediated network. The parameters are same as for Fig. 4.5. The black dotted line has slope -1. Results are averaged over 1000 random realizations.

4.7.3 Average path length

Most of the real networks are found to have a small-world property which means that the average path length $< l >$ of these networks varies very slowly with size and also they have high clustering coefficient [42]. We also calculate the $< l >$ of mediated network as a function of its size for different n. It is clear that $< l >$ increases logarithmically with size (see Fig. 4.9). Such logarithmic scaling with size has been reported earlier for many real networks [2]. This along with the observed high clustering, makes the mediated network a small-world network.

4.8 Conclusion

Understanding the physical mechanisms which lead to the emergence of various structural properties seen in real networks is an important aspect of the network science. Since the discovery of small-world nature and scale-free nature of various real networks, several models of network formation have been proposed over the years. It has been observed that many real networks exhibit both scale-free nature and hierarchical modularity. However, the generic mechanisms which lead to their simultaneous occurrence in real networks are not yet very clear. In the present work we show that the weakness of hubs in mediating

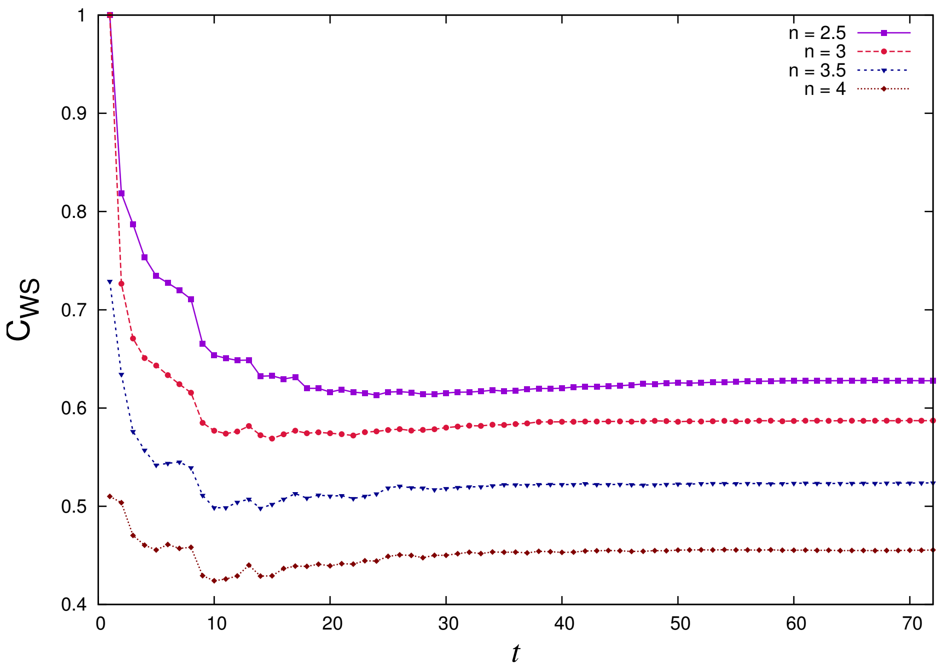

Figure 4.7: Watts-Strogatz clustering coefficient C_{WS} of the network as a function of time for various values of parameter n. All the parameter values are same as in Fig. 4.6

the connections between their neighbors is the underlying property that produces both of these structures simultaneously. This property in fact follows from the more fundamental fact that hubs are usually connected to dissimilar nodes in the network. We feel that a more careful use of this idea in the context of specific networks will lead to many novel insights into the structure and function of various real networks like social network, World Wide Web and citation networks.

The model presented here comes with tunable parameters p, A and n that can be adjusted to get desired values of network characteristics. For $n > 2$ we show that the average degree of the network stabilizes and can be tuned to a desired value by tuning parameters A and n. Apart from scale-free nature and hierarchical modularity, we also show that the mediated network is highly clustered and its path length scales logarithmically with size. This shows that the small-world nature is also an emergent property of this model. These networks show positive degree correlations as observed in case of social networks. We anticipate that detailed investigations to understand the intrinsic mechanisms that generate this property in different cases, can reveal interesting processes underlying the complexity of such systems.

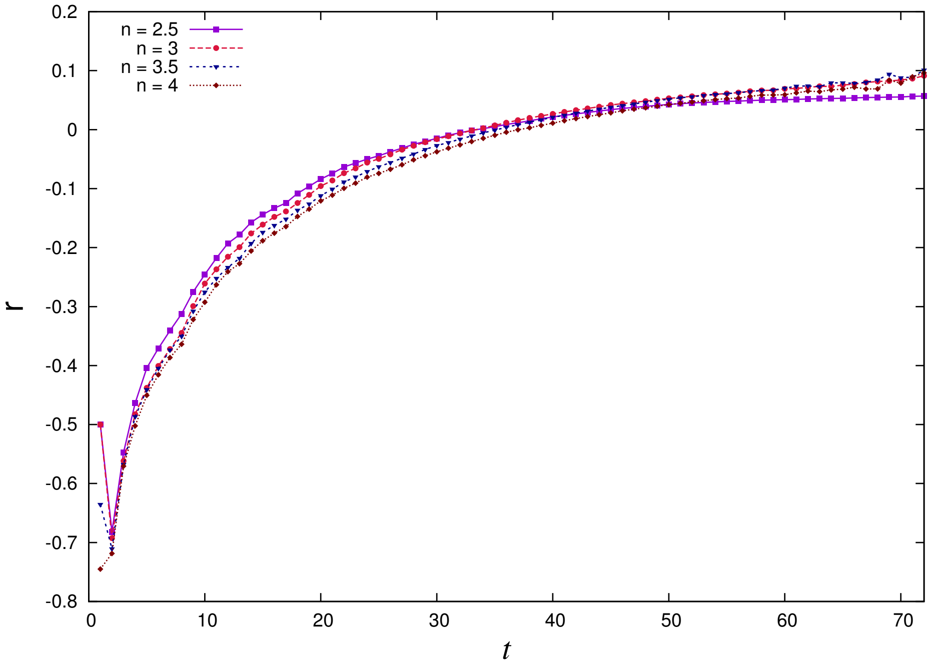

Figure 4.8: Assortativity coefficient r of the mediated network as a function of time for different values of parameter n. It can be seen that r stabilizes to positive values asymptotically and hence the mediated network is assortative. All the parameter values are as in Fig. 4.6

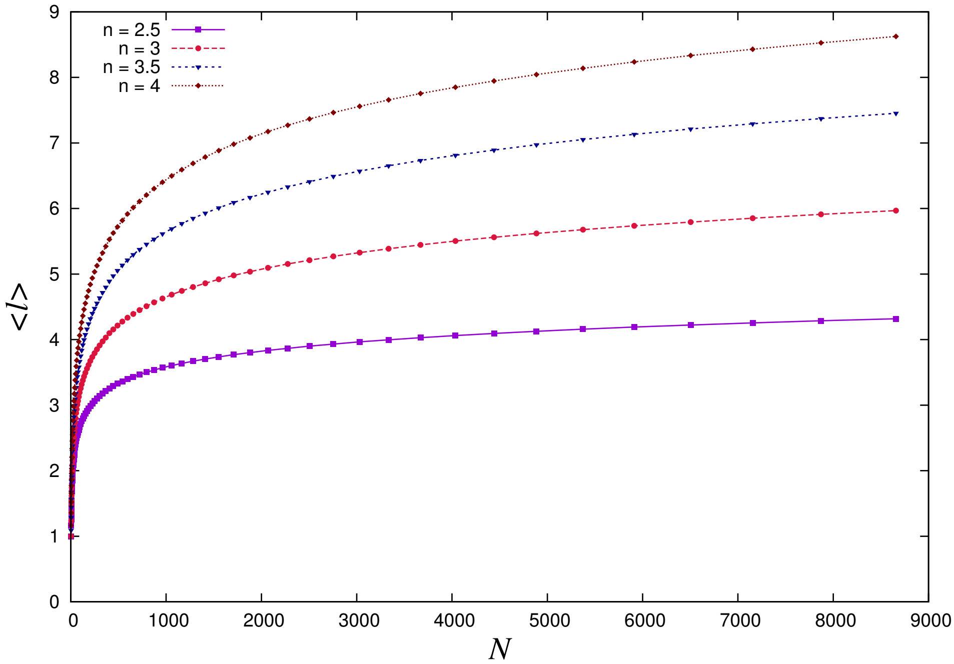

Figure 4.9: Average path length $< l >$ of the network as a function of size $N(t)$ of the network for different n. The parameter values are as given in Fig. 4.6. Each curve in the plot follows a logarithmic increase.

Chapter 5

Complex network of natural numbers

5.1 Introduction

Apart from being used as an important tool to model physical complex systems, complex networks can also be used to understand interesting results from pure mathematics by constructing appropriate networks of mathematical objects based on their mathematical relations [142–147]. In most of these networks, usually the deterministic rules give rise to apparently irregular structure and such irregular deterministic networks can be treated as complex networks.

In the present work, we discuss the analysis for a particular deterministic network that resembles real networks in many aspects. This network consists of natural numbers $1, 2, 3, \cdots$ as nodes and if a given number divides another, then their corresponding nodes are connected by an undirected link. In this context we note that, a similar network with nodes as composite numbers has already been studied [20]. A network of natural numbers with decomposition by primes as the definition of the link has also been studied and analytical results have been obtained [142, 143]. Also, a directed network of natural numbers based on the divisibility which includes only the multiples in the pattern has been reported by Ding-hua et al [148]. A network with prime numbers with links created with the help of Goldbach's conjecture has been studied in [144]. Finally, a bipartite structure separating composite and prime numbers with weighted links between them based on divisibility has been analyzed by García-Pérez et al [147].

Here we consider a more general set up where we put all the natural numbers on a complex network with their divisibility relations as the underlying deterministic rule of connections. This network is undirected with links to both divisors and multiples. As compared to other complex networks, this network is unique since each node has an identity which is the natural number on it resulting in a specific ordering of the nodes in the network.

Using tools from statistical inference, we confirm that this network is scale-free and show that average degree, global clustering coefficient and assortativity coefficient vary smoothly with the size of the network. This is surprising in view of the fact that distribution of primes is quite irregular in the sequence of natural numbers. We provide analytical results for the asymptotic behavior of average degree and global clustering coefficient for this network. In particular, we show that the global clustering coefficient of this network decays to zero whereas average degree increases logarithmically. We also report an interesting and novel similarity exhibited by local clustering coefficients of nodes in this network which we call "stretching similarity". The work presented in this chapter is published in *Scientific Reports, 5:14280*.

5.2 Construction of the network

The nodes of the present network are natural numbers $1, 2, 3, \cdots$ and there is a link between two nodes if either divides the other. We avoid self-links and all the links are undirected. Since the sequence of natural numbers has natural ordering, it is helpful to view this network as a growing network with the addition of a new node at each discrete time as follows:

1. At time $t = 1$ network starts with a single node $n = 1$ and at every time t, a node with the number $n = t$ is added to the network.

2. This node connects to all the existing nodes whose numbers divide it.

The network thus constructed is shown in Fig. 5.1 at two different times $t = 16$ and $t = 32$ which would correspond to networks of size $N = 16$ and $N = 32$ respectively.

5.3 Scaling properties of the network

5.3.1 Degree distribution

We start by growing the network till the size reaches $N = 2^{25} = 3,35,54,432$. To plot the degree distribution, we use logarithmic binning as advised in [149] in which the bin widths of successive bins are taken to be successive powers of 2 and the count in each bin is normalized by diving by the bin width. The resulting distribution is shown in Fig. 5.2.

The shape of the degree distribution of the network in Fig. 5.2 indicates the existence of asymptotic power law in the distribution ($p(k) \sim k^{-\alpha}$ for $k \geq k_{min}$). However a visual inspection to find k_{min} and least square fit and related methods to find the exponent α of the power law are known to produce very poor estimates [150]. Hence we use the method of maximum likelihood for the degree sequence of the network to find scaling index α of the power-law distribution [151]. For this, we initially assume that the sequence is drawn from a distribution that follows a power law $k^{-\alpha}$ for all k after $k \geq k_{min}$. To find this k_{min}, we use the approach proposed by Clauset et al. [152]. The idea behind this method

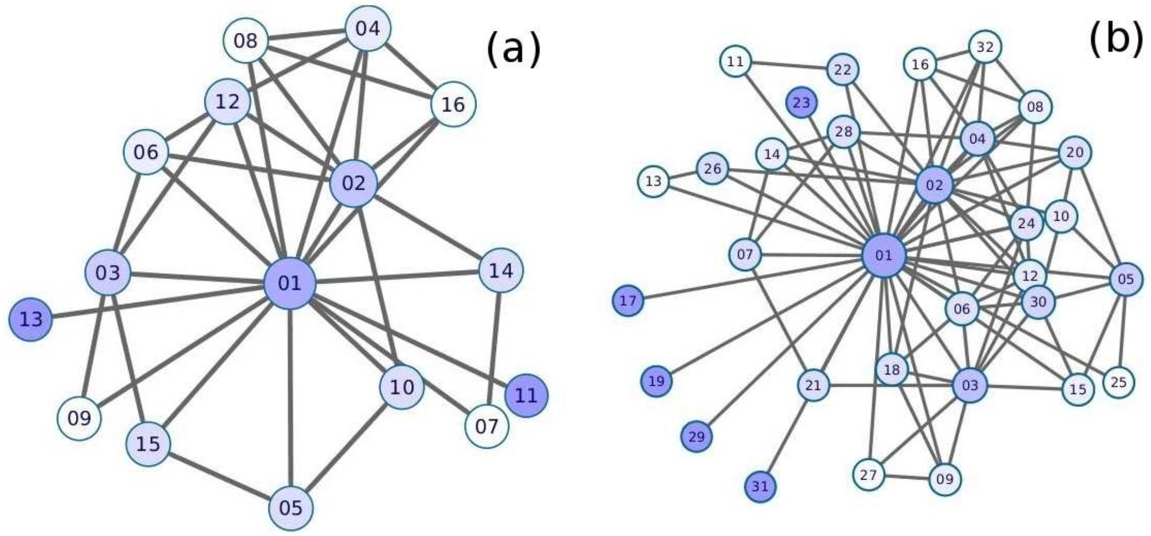

Figure 5.1: **Network of natural numbers with two different sizes.** (a) $t = 16$ nodes and (b) $t = 32$ nodes. In each panel, the size of each node is proportional to its degree and color of each node is graded according to its clustering coefficient with more white nodes as nodes with higher value of local clustering.

is to choose that value of k as k_{min} which makes the probability distribution of the data and best-fit power-law model as similar as possible above k_{min} where we use Kolmogorov-Smirnov statistic as the distance between two distributions [151]. After finding k_{min} using this method, the best estimation for scaling exponent $\hat{\alpha}$ is given by [1, 151]:

$$\hat{\alpha} = 1 + N \left[\sum_{i=1}^{N} \ln \frac{k_i}{k_i - \frac{1}{2}} \right]^{-1} \tag{5.1}$$

where k_i, $i = 1, \cdots, N$ are values of k such that $k_i \geq k_{min}$. For the network of size 2^{15}, the value α is obtained here as ~ 2.

Using the method of maximum likelihood we find that the scaling-index $\alpha \sim 2$. The standard error in the value of α in this case is given by [151]:

$$\sigma = \frac{\hat{\alpha} - 1}{\sqrt{N}} + O(1/N) \tag{5.2}$$

Thus the error in the estimation of the scaling index rapidly goes to zero and is negligible for the network size that we consider here.

However, this type of estimation does not “prove” that the distribution really follows a power-law and hence we need to rigorously establish that the distribution is most probably a power-law. We establish the existence of power-law in this distribution (and hence the fact that this network is scale-free) using the approach described in Clauset et al [151]. In this approach, we generate many synthetic data sets from a true power-law distribution and measure how far they fluctuate from the power-law type of behavior. We then compare the results of similar measurements on the observed data. If the observed data set is much further from the power-law form than the synthetic one, the power-law is rejected. The $p-$value is defined as the fraction of the synthetic distances that are larger than the empirical distance. A large $p-$value is indicative of existence of power law in the data. In the present work we calculate the $p-$values for three different sizes of the network: $N = 256$, $N = 512$ and $N = 1024$. For this, we generate 2500 synthetic data sets which gives $p-$values accurate up to two decimal places as 0.62, 0.95 and 0.98 respectively. The existence of power-law degree distribution for this network is thus confirmed by the fact that $p-$values rapidly converge to 1 as the network size increases.

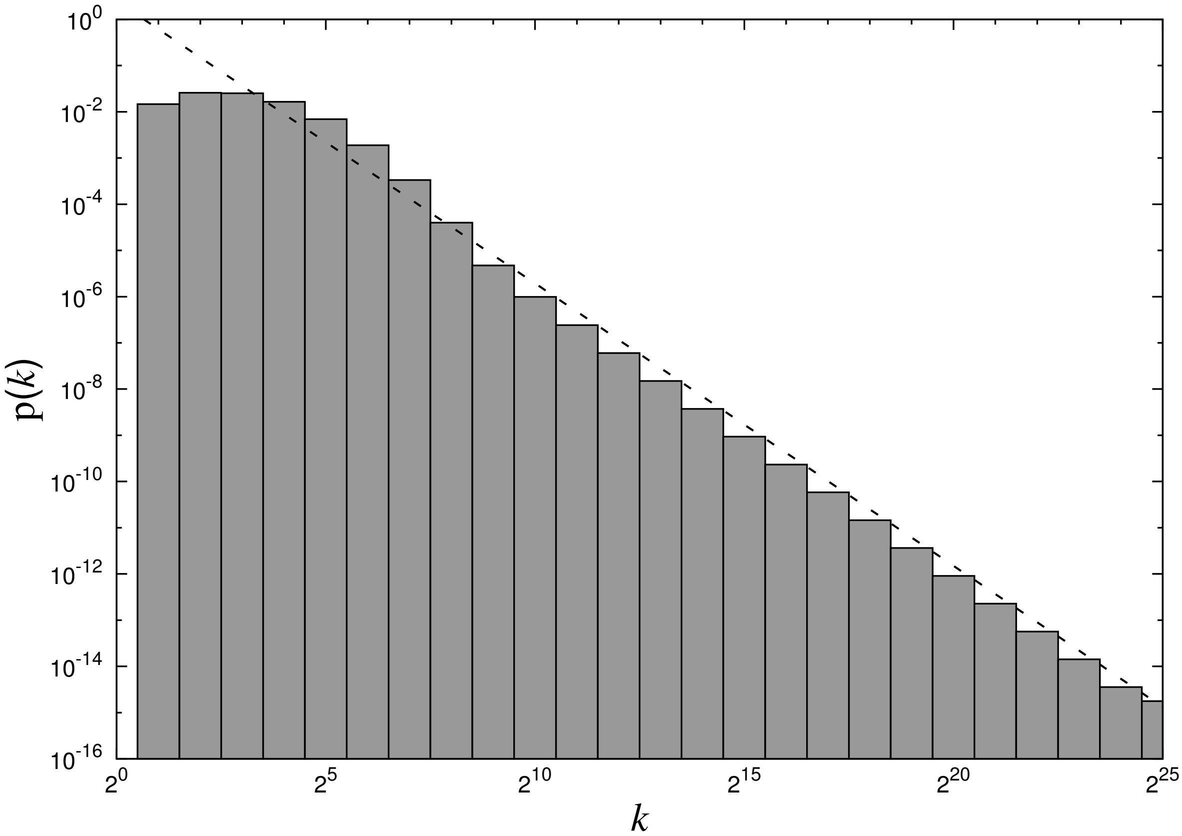

Figure 5.2: **Degree distribution of network of natural numbers with logarithmic binning.** Sizes of successive bins are equal to successive positive powers of 2 and count in each bin is normalized by dividing by a bin width. The dotted line in the graph has slope $\alpha = -2$ and it is calculated using the *method of maximum likelihood* [151]. The existence of the underlying power law is established by calculating p-value using Kolmogorov-Smirnov statistic for smaller sizes of the same network.

5.3.2 Local clustering coefficient

We also study the scaling behavior of the local clustering coefficient as given in Eq.(1.4) with degree. In Fig. 5.3 we show the dependence of local clustering coefficient of nodes in the network on the degree. It can be seen that the asymptotic behavior is compatible with a power law with exponent 1. This behavior is similar to one that is usually observed in real networks [141]; however when tested with Infomap, this network does not exhibit hierarchical community structure.

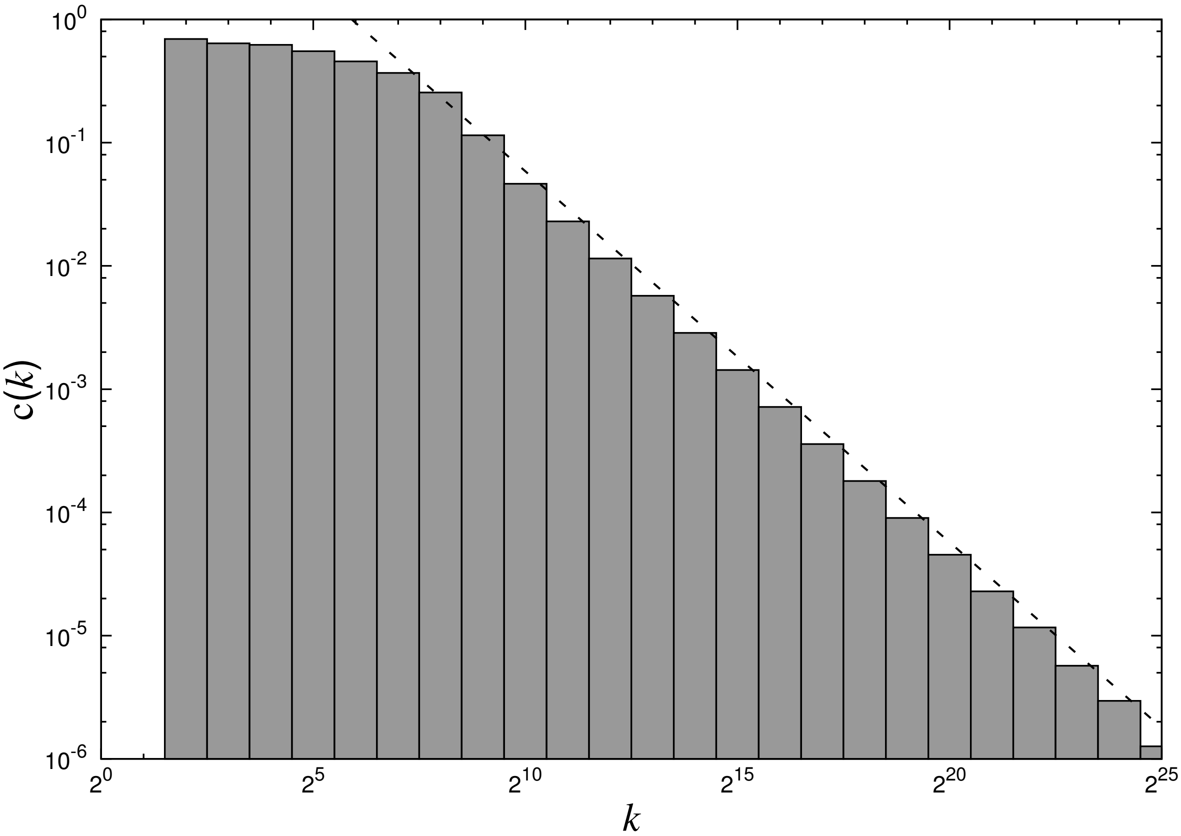

Figure 5.3: **Dependence of local clustering coefficient on degree.** The plot is created using a logarithmic binning. Asymptotically, the local clustering is seen to follow a power law with exponent ~ 1.

5.4 Stretching similarity of local clustering

We now discuss an interesting behavior that sets network of natural numbers apart from other complex networks. In the network presented here, each node has an identity which is the number attached to it and this defines a natural order on the nodes. This means that we can study various properties of nodes as a function of their labels. This is not possible for other networks because no such unique labeling exists for the nodes. Here we specifically consider local clustering coefficient of nodes and study its behavior as a function of node index. We find that the clustering coefficient c_i of node i varies seemingly irregularly. However, when c_i is plotted against i, a global pattern is seen. In Fig. 5.4 we show this pattern for three different network sizes. For better visualization, the plots are shown only for relatively small network sizes.

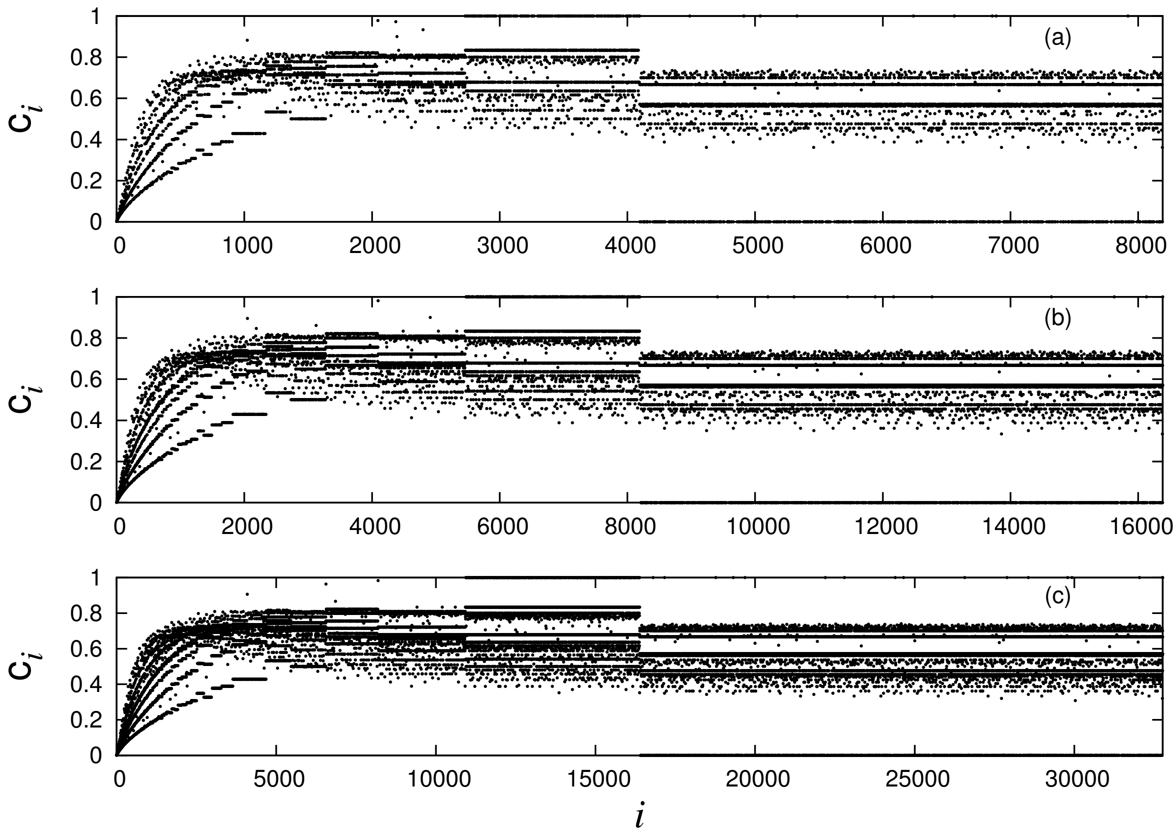

Figure 5.4: **Local clustering coefficient as a function of node index for three different sizes of network.** (a) $N = 2^{13}$, (b) $N = 2^{14}$ and (c) $N = 2^{15}$. In any local region of the plot, the values c_i seem to be scattered irregularly. However, with the increase in the network size, the whole pattern is stretched on a global scale. We call this similarity as "stretching similarity".

From the figure, it is clear that the global pattern of the local clustering coefficient gets stretched as the size of the network increases such that the nature of the pattern remains the same. We call this new kind of similarity as **"stretching similarity"** and this seems to be a unique feature of this network, not so far reported for any other complex network. We note from plots in Fig. 5.4 that for a network with size N some discontinuous vertical steps occur approximately at values $N/2, N/3, N/4, \cdots$. Also, we observe a band of numbers with clustering coefficient 1 between $N/3$ and $N/2$ and these numbers correspond to prime numbers and their powers in that range. This can be seen by the following argument. Consider any prime number p in the interval $(N/3, N/2)$. On the lower side, it is connected only to 1 while on the upper side, it would be connected only to its multiples. However, all the numbers in this range would have only one multiple $2p$ up to N. Thus, three numbers $1, p, 2p$ form a triangle and hence clustering coefficient of number p must be 1. A similar argument for prime powers in this range tells that they also have clustering coefficient 1. There is another band of numbers with clustering coefficient exactly 0 between $N/2$ and N which are also prime numbers. This is because all the primes in this range are connected only to 1 making their clustering 0.

Now we discuss the local clustering coefficient for the composite numbers between $N/2$ and N. For a vertex n, the only neighbors are the proper divisors of n i.e. m such that $1 \leq m < n$ and n is divisible by m.

Let $n = \prod_{i=1}^{k} p_i^{j_i}$ be the factorization of n as the product of (distinct) prime powers. The fundamental theorem of arithmetic states that such a factorization is unique up to a reordering of the primes p_i's [153]. Thus, the number of neighbours or degree of n is equal to its number of divisors which is equal to:

$$s = (j_1 + 1)(j_2 + 1) \cdots (j_k + 1) \tag{5.3}$$

Let $E(n)$ be the set of all edges among the neighbors of node n. Then this set is given by:

$$E(n) = \{(m, m') : m \text{ divides } m', \quad m' \text{ divides } n, \quad m \text{ divides } n\} \tag{5.4}$$

If $|E(n)|$ is the size of this set, then the local clustering coefficient of node n is given by:

$$c_n = \binom{s-1}{2}^{-1} |E(n)| \tag{5.5}$$

To find out the size of this set, we observe that every divisor m of n is of the form $m = \prod_{i=1}^{k} p_i^{\ell_i}$ where $0 \leq \ell_i \leq j_i$ for every $1 \leq i \leq k$.

Any two neighbors $m = \prod_{i=1}^{k} p_i^{\ell_i}$ and $m' = \prod_{i=1}^{k} p_i^{\ell_i'}$ such that $m < m'$ are adjacent to each other if and only if $\ell_i \leq \ell_i'$ for all i.

Thus the clustering coefficient of n in the network of size N is given by,

$$c_n = \binom{s-1}{2}^{-1} \left[\left(\sum_{\ell_1=0}^{j_1} \sum_{\ell_2=0}^{j_2} \cdots \sum_{\ell_k=0}^{j_k} [(\ell_1+1)(\ell_2+1)\cdots(\ell_k+1) - 1] \right) - [s-1] \right]. \tag{5.6}$$

where we subtract the quantity $(s-1)$ because we are only counting the proper divisors of n.

Since the individual sums in the above expression are independent, we can write the sums of the product as the product of the individual sums:

$$\therefore\ c_n = \binom{s-1}{2}^{-1}\left(\prod_{i=1}^{k}\binom{j_i+2}{2} - 2s + 1\right) \tag{5.7}$$

From the above expression it follows that value of c_n depends only on the number of distinct prime factors of n and the powers j_i's which appear in the prime factorization of n; but not on the actual primes which appear there. Thus for any given $j_1, j_2, \ldots j_k$, the value c_n is constant for every n in the range $N/2 < n \leq N$ such that $n = \prod_{i=1}^{k} p_i^{j_i}$ for some set of k distinct primes $p_1, p_2, \cdots p_k$. This explains the occurrence of horizontal dotted lines in the plot for local clustering coefficients.

Similarly, the clustering coefficients for other n can be computed and it can be observed that they depend on the powers and the number of distinct prime factors of n as well as the range in which n belongs that is r such that $N/(r+1) < n \leq N/r$. Here one has to also consider the number of multiples of n in the range $1, 2, \cdots, N$. This leads to possibly different values of clustering coefficients. This explains the occurrence of demarked regions like $N/2$ to N, $N/3$ to $N/2$, $N/4$ to $N/3$ etc in the plot for local clustering coefficients. For any N there will be sufficient number of primes in the range $[1, N/2]$ and choices for j_i such that the pattern of horizontal lines between $N/2$ to N remains the same. Also, the demarked regions have similar structures. This provides a possible explanation for the observed stretching similarity in the clustering coefficients as N is changed (Fig. 5.4).

We also observe an interesting pattern when we plot the difference $\triangle c = c_i - c_{i+1}$ as a function of i in Fig. 5.5. We find that this pattern is symmetric about $\triangle c = 0$ which can be quantified by finding the local density of values in the plot. With increasing size of the network, this pattern also shows stretching similarity.

To establish the global symmetry of difference in local clustering values $\triangle c$ around the horizontal axis $\triangle c = 0$ (Fig. 5.5) for any value of N, we calculate the local density of points in the plot. For this, we divide the horizontal axis into $2^7 = 128$ cells and vertical axis into 200 cells. The whole plot then gets divided into pixels of dimension $0.01 \times 2^{N-7}$. We define density $\rho(x, y)$ of a particular pixel (x, y) as the ratio of the number of points present in the pixel to the maximum number that can be there which is equal to 2^{N-7} (all the points on y-axis with difference less than 0.01 are to be considered same so the vertical dimension of each pixel is just 1). For each x we calculate the absolute difference between the corresponding pixels on each side of the line $\triangle c = 0$. If the pattern is symmetric then these absolute differences are expected to be small. We calculate the average of such differences as:

$$\phi(x) = \frac{1}{100}\sum_{y=1}^{100} |\rho(x, y) - \rho(x, -y)| \tag{5.8}$$

In Fig. 5.6 we show $\phi(x)$ as a function of x and as is clear from the figure, all ϕ values

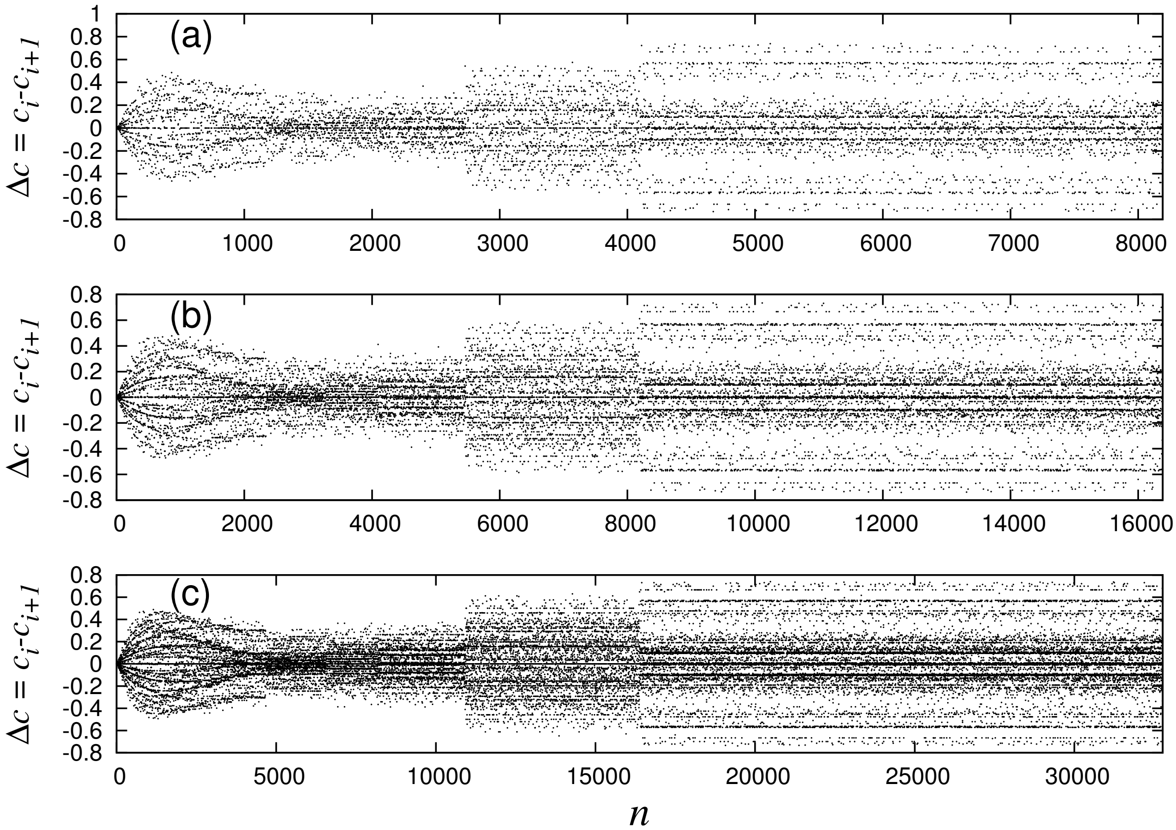

Figure 5.5: **Difference in clustering coefficients of successive nodes i and $i+1$ as a function of index i.** (a) $N = 2^{13}$, (b) $N = 2^{14}$, (c) $N = 2^{15}$. This pattern is symmetric about the line $\triangle c = 0$ and also shows stretching similarity as is evident from these plots.

are very close to 0 confirming that the pattern is indeed symmetric.

5.5 Topological characteristics of the network.

In the present section, we discuss how three of the most important quantities average degree, global clustering and assortativity coefficient vary with the size of the network.

5.5.1 Average degree

Here we derive an approximate expression for the average degree of the network as a function of its size. By definition, the average degree of the network is given by:

$$\langle k \rangle_n = \frac{2m}{n} \tag{5.9}$$

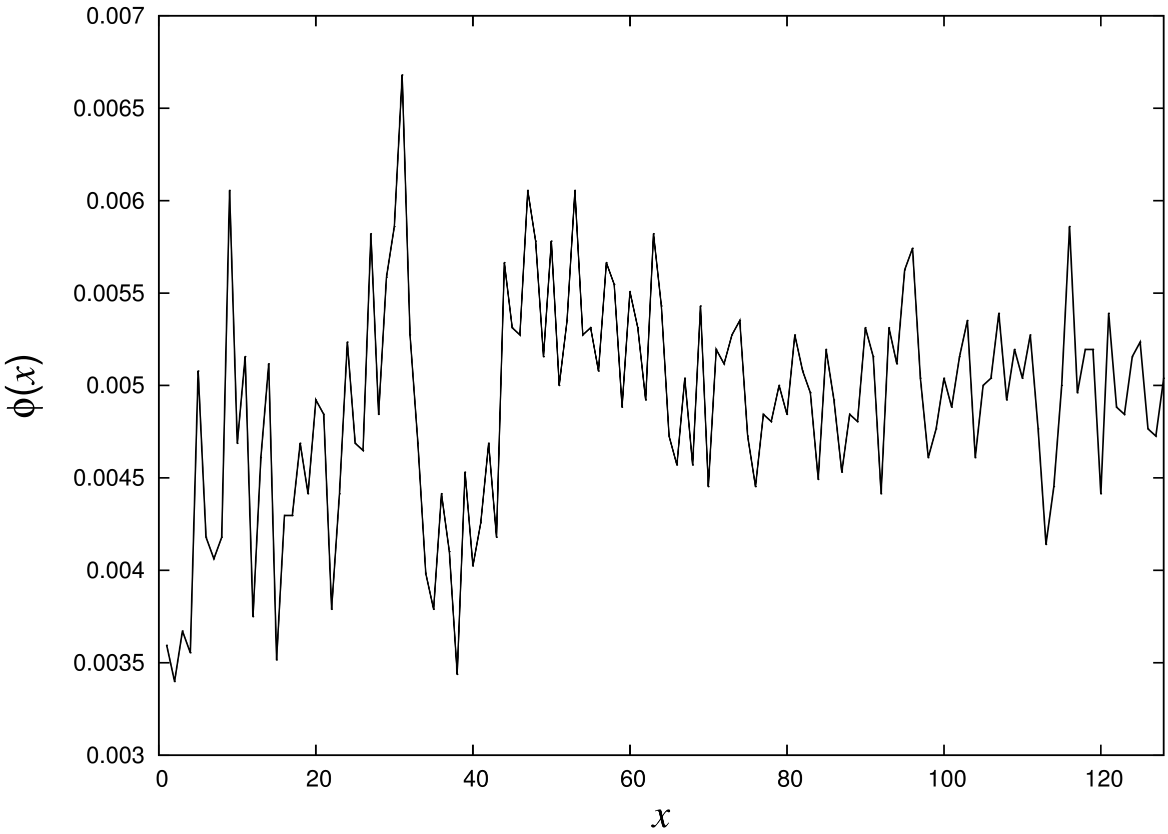

Figure 5.6: **Symmetry quantifier for Fig. 5.5 as given by Eq.(5.8).** The values of ϕ are very close to zero for all horizontal pixel indices establishing the approximate symmetry for the pattern.

where m is the total number of edges in the network and n is the size of the network. The value of m is also equal to the sum of the elements in lower (or upper) triangular part of the adjacency matrix. To find this sum, we interpret the second index of element A_{ij} of adjacency matrix to be the divisor of first index if $A_{ij} = 1$. In other words, let $A_{ij} = 1$ if and only if $i > j$ and $j|i$. Then the sum of the elements in the lower triangular part of the matrix is equal to the number of integers of the form kj with $k \geq 2$ and $kj \leq n$. However, whenever $j > \frac{n}{2}$ all the entries in the j^{th} column of the lower triangular part of A are zero. Let $\lfloor x \rfloor$ denote the greatest integer $\leq x$. Then m is given by:

$$\begin{aligned} m &= \sum_{j=1}^{n/2} \left(\left\lfloor \frac{n}{j} \right\rfloor - 1 \right) \\ &= \sum_{j=1}^{n} \left\lfloor \frac{n}{j} \right\rfloor - \sum_{n/2<j\leq n} \left\lfloor \frac{n}{j} \right\rfloor - \frac{n}{2} \end{aligned} \tag{5.10}$$

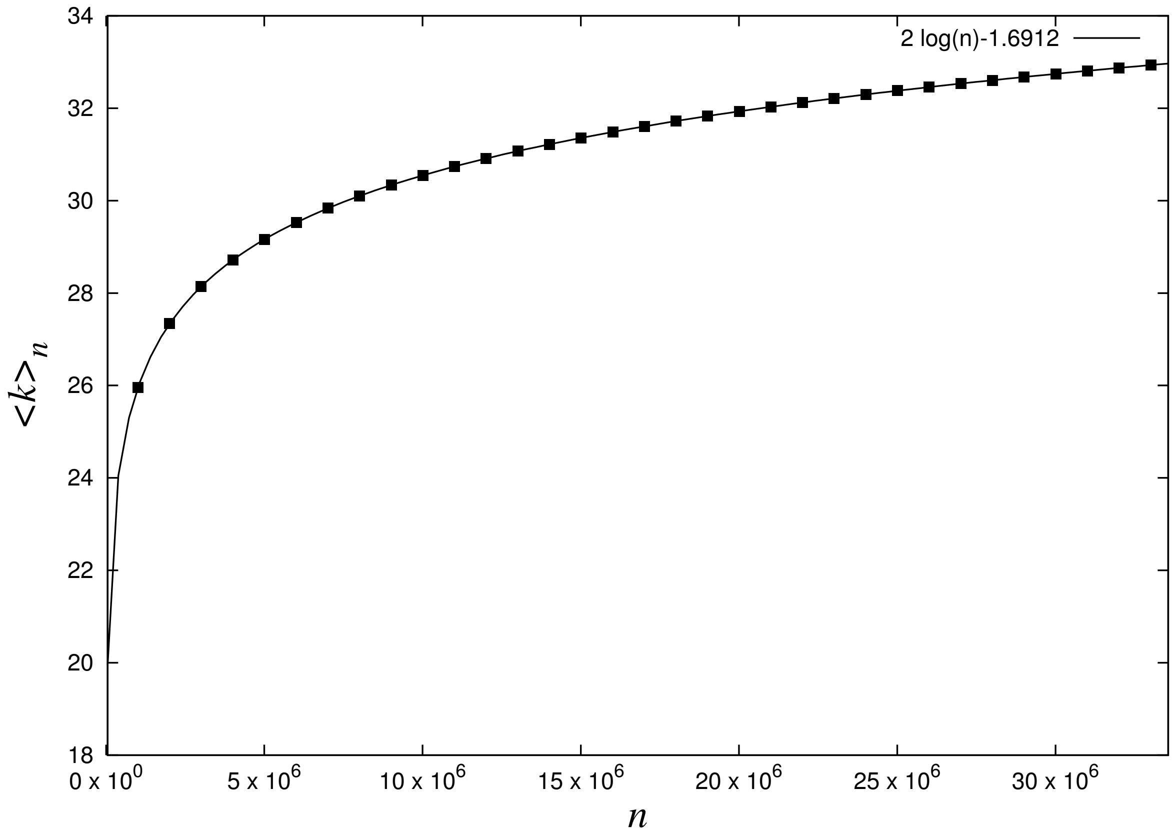

Figure 5.7: **Average degree of the network as a function of size.** The solid dots represent the actual values calculated by direct numerical simulations while the solid line is plotted using the analytic expression (5.14).

It is well known that the first term on the right satisfies an estimate as follows [154]:

$$\sum_{j=1}^{n} \left\lfloor \frac{n}{j} \right\rfloor = n \ln n + n(2\gamma - 1) + O(\sqrt{n}) \tag{5.11}$$

where γ is Euler-Mascheroni constant. Also we observe that:

$$\left\lfloor \frac{n}{j} \right\rfloor = 1 \quad \forall\ \frac{n}{2} < j \leq n \tag{5.12}$$

From Eqs.(5.9),(5.10),(5.11),(5.12), it follows that:

$$\langle k \rangle_n \;=\; 2 \ln n + 2(2\gamma - 1) - 2 + O(\frac{1}{\sqrt{n}}) \quad \text{as } n \to \infty \tag{5.13}$$

Since $\gamma \approx 0.5772$, in the limit of large n, we get,

$$\langle k \rangle_n \;\sim\; 2 \ln n - 1.6912 \tag{5.14}$$

This means that the average degree of the network increases logarithmically with the size and this variation is plotted in Fig. 5.7 (solid line) using Eq.(5.14). We calculate this numerically by growing the network up to $N = 2^{25}$ and the results obtained, shown by solid dots in Fig. 5.7, are found to agree exactly with analytic expression (5.14). Since the average degree of the network increases with size, the degree distribution of the network is not stationary though as shown in the previous section, the network is scale-free at each stage.

5.5.2 Global clustering coefficient

The global clustering coefficient of the network quantifies the density of closed triplets in the network. A connected triplet in the network is the set of 3 nodes connected to each other with exactly 2 links. A closed triplet is the set of 3 nodes connected to each other with exactly 3 links. A triangle in the network counts as three closed triplets (one centered at each node of the triangle). The global clustering coefficient of the network is then defined as:

$$C = \frac{3 \times \text{Number of triangles}}{\text{Number of connected triplets}} \tag{5.15}$$

We estimate the number of triangles T_n in the network using the following strategy. Let us fix a vertex i and calculate the number of triangles in which i is the smallest vertex. The number i has $\left\lfloor \frac{n}{i} \right\rfloor - 1$ proper multiples in the range $[1, n]$. Each of them is of the form ki where $k = 2, 3, ..., \left\lfloor \frac{n}{i} \right\rfloor$. Thus, T_n is given by:

$$T_n = \sum_{i=1}^{n} \sum_{k=2}^{\lfloor \frac{n}{i} \rfloor} \left\lfloor \frac{n}{ki} \right\rfloor \tag{5.16}$$

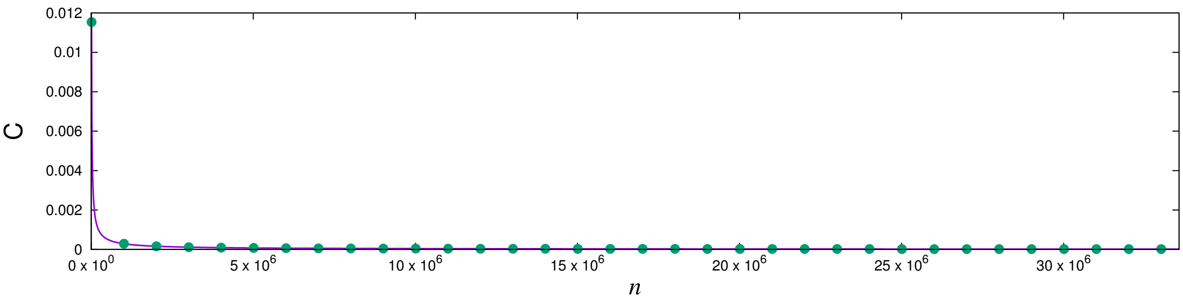

Figure 5.8: **Global clustering coefficient as a function of size of the network.** The global clustering coefficient (see Eq.(1.7)) decays to 0 as the size of network increases.

Using the integral approximation for the above:

$$T_n \sim n \sum_{i=1}^{n} \int_{x=2}^{n/i} \frac{1}{ix} dx \sim n \sum_{i=1}^{n} \frac{1}{i} \left(\ln \frac{n}{i} - A \right) \tag{5.17}$$

The above is bounded by,

$$n\sum_{i=1}^{n}\frac{1}{i}\left(\sqrt{\frac{n}{i}}-A\right)\sim n\sqrt{n}\int\limits_{x=1}^{n}\frac{dx}{x^{3/2}}-An\int\limits_{x=1}^{n}\frac{dx}{x}\sim Bn-An\ln n \tag{5.18}$$

Here A and B are constants. Hence we see that:

$$T_n \leq O(n)+O(n\ln n)+o(n^2) \tag{5.19}$$

Here, $f=O(g)$ implies that asymptotically, the quantity f is of the order of g while $f=o(g)$ implies that asymptotically, the quantity g dominates f.

In particular,

$$T_n = o(n^2) \tag{5.20}$$

Let $U(n)$ be the the number of connected triplets in the network after n^{th} stage. Then $U(n)$ is given by:

$$U_n=\sum_{i=1}^{n}(k_i^2-k_i)=n\left\langle k^2\right\rangle-n\left\langle k\right\rangle\sim O(n\left\langle k^2\right\rangle) \tag{5.21}$$

Since we have (Fig. 5.2) observed that the degree distribution of the network follows a power law $k^{-\alpha}$ with $\alpha\sim 2$, we see that the proportion $p(k)$ of nodes with degree k is $\sim k^{-2}$.

Thus, the expectation of the variable k^2 satisfies:

$$\left\langle k^2\right\rangle=\sum_{k=1}^{n}k^2p(k)\sim n$$

Hence we see that

$$U_n\sim n\left\langle k^2\right\rangle=O(n^2) \tag{5.22}$$

From Eqs.(5.15), (5.19) and (5.22), the global clustering coefficient, which is proportional to the ratio of T_n and U_n, decays to zero as the network size goes to infinity. We verify this by numerically computing the global clustering coefficient and this is shown in Fig. 5.8.

5.5.3 Average clustering coefficient as a function of size of the network

In Fig. 5.9 we show the variation of average clustering coefficient C_{WS} as a function of a network size n and as can be seen from the figure, the average clustering coefficient for this network has very high value as compared to the global clustering coefficient which goes to zero asymptotically. This is clear from Fig. 5.4 since the pattern repeats with stretching similarity as the network size increases. To the best of our knowledge, there is no other network in which C_{WS} saturates to a high non-zero value but the global clustering coefficient decays to 0.

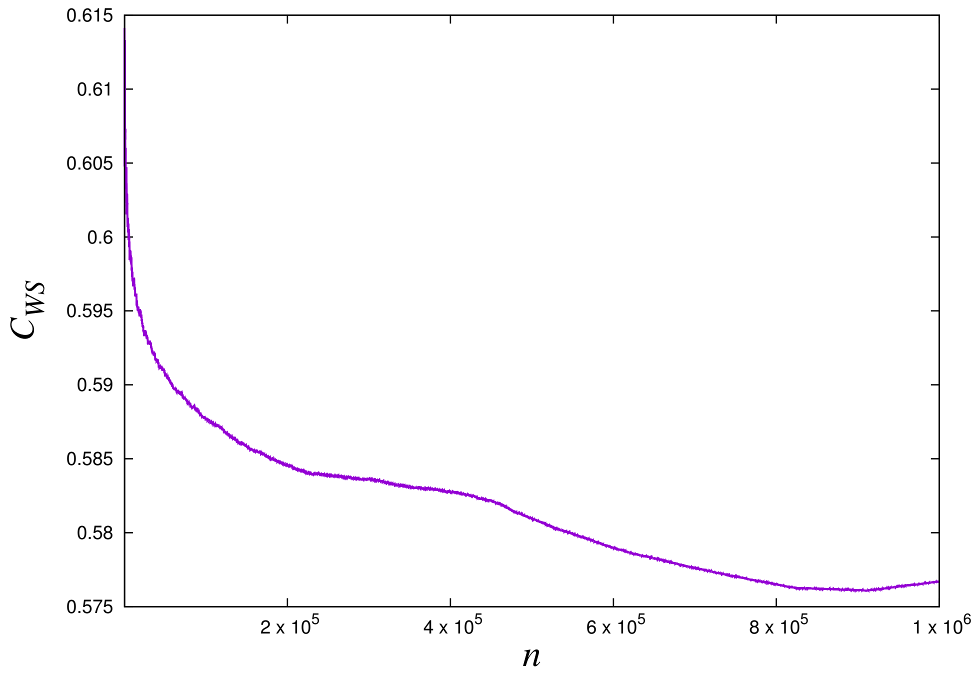

Figure 5.9: Watts-Strogatz clustering coefficient C_{WS} of the network of natural numbers as a function of its size n.

5.5.4 Assortativity coefficient

The correlation of degrees in the network is an important quantifier of the network structure [25]. All the real networks except social networks are seen to be dissortative [25] and this has been explained using the fact that the dissortative state is the most likely state of scale-free networks [155]. The assortative/dissortative nature of networks can be quantified using the assortativity coefficient [1]:

$$r = \frac{S_1 S_e - S_2^2}{S_1 S_3 - S_2^2} \tag{5.23}$$

with,

$$\begin{aligned} S_e &= 2 \sum_{\text{edges}(i,j)} k_i k_j \\ S_1 &= \sum_i k_i \\ S_2 &= \sum_i k_i^2 \\ S_3 &= \sum_i k_i^3 \end{aligned} \tag{5.24}$$

We use this expression to calculate r instead of Eq.(1.8) since we don't need adjacency matrix to calculate it.

In Fig. 5.10 we show the dependence of r on the size of the network and in spite of irregularity in the divisibility pattern, r has a smooth behavior with n. It can be seen that r always remains negative though asymptotically it seems to reach the value 0 implying that the network is dissortative. The dissortative nature of the network of natural numbers is understandable from the following argument. For any link in this network, the one end of the link is divisor (node A) and other is multiple (node B). Hence node A is also connected to all the nodes which are multiples of B but the reverse is not true. This means that the degree of node A always tends to be very high as compared to degree of node B for a given size of the network giving the negative value for the overall correlation coefficient.

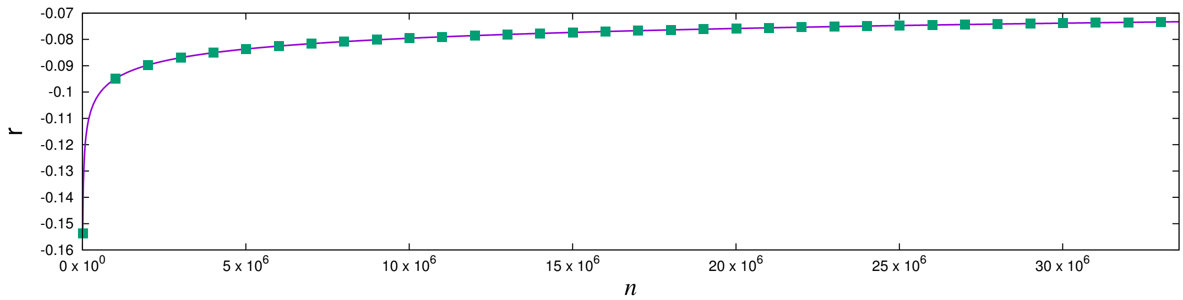

Figure 5.10: Assortativity coefficient r (see Eq.(1.8)) seems to reach 0 asymptotically though it always remains negative.

5.6 Number network with high degree nodes removed

The present network contains a succession of star motifs. For example, the number 1 is connected to all the remaining nodes in the network, the number 2 is connected to all the even numbered nodes in the network and so on. The natural question is whether the properties like scale-free structure and stretching similarity exist because of the existence of these very high degree nodes. To answer these questions, we calculate the statistical properties of the network by successively removing biggest hubs like numbers $1, 2, 3, \cdots$.

We simulate the network of natural numbers removing numbers 1 to 4 step by step. When number 1 is removed from the network, all the prime numbers between $N/2$ and N become isolated and these remain as the only isolated nodes. This means that in this case the network consists of a giant component along with many isolated nodes. We find that such a removal does not affect the degree distribution and clustering-degree correlation too much and qualitatively the network remains scale-free with the same power-law index as for the original network. The other properties like average degree, clustering coefficients and assortativity do change to some extent by this removal but

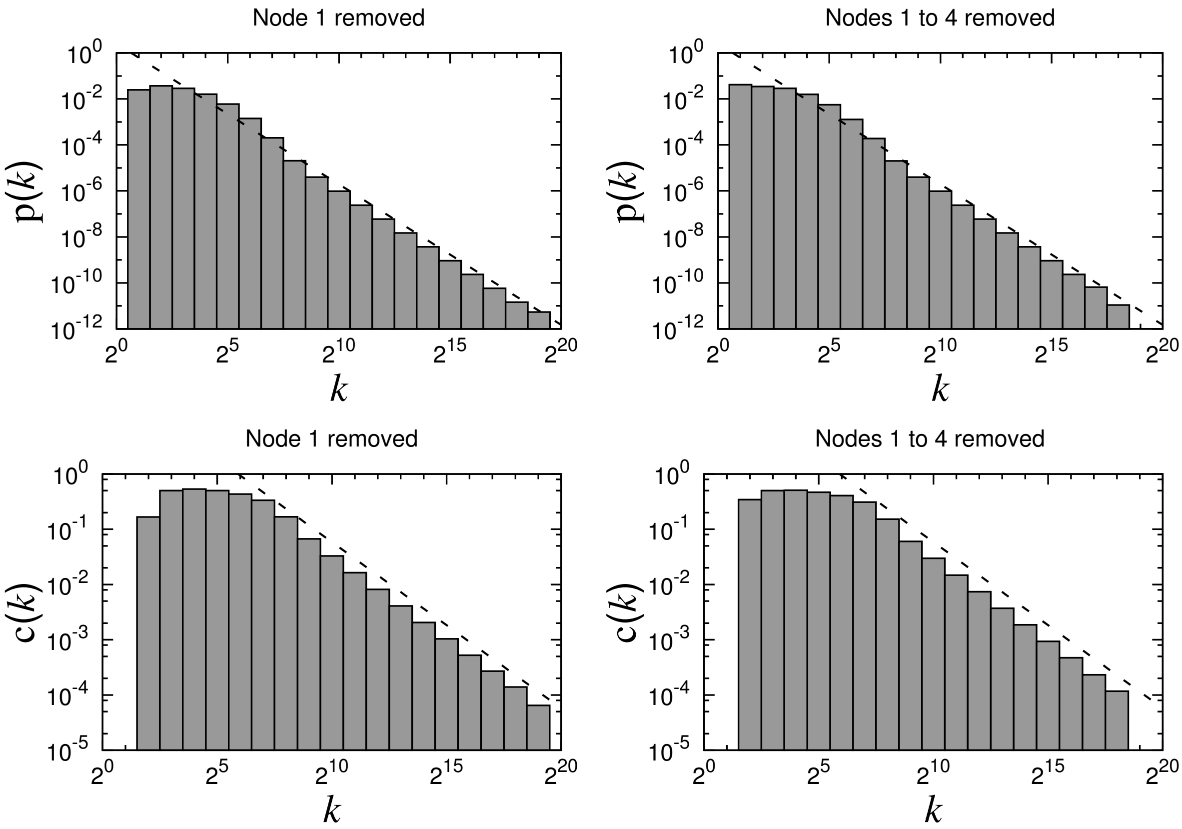

Figure 5.11: Degree distributions of the network of natural numbers after removing nodes from 1 to 4. The distributions follow a power-law similar to the original network.

qualitatively remain the same. The plot of degree distributions after removing hubs is shown in Fig. 5.11.

Thus, all the important statistical properties of the network like stretching similarity, degree distribution, clustering-degree correlation etc. are very robust to the removal of even these biggest hubs. This shows that the global divisibility pattern of natural numbers does not depend only on the few nodes but instead is built by contributions from all the nodes.

5.7 Conclusion

The deterministic network of natural numbers constructed using divisibility relations looks like real networks in many characteristics like degree distribution, clustering and degree correlations. We show how insights into the divisibility patterns of natural numbers can be obtained using the framework of complex networks, where we consider both composite and prime numbers in a single undirected network with links generated using both multiples and divisors. Some of the interesting results that we get are the scale-free nature of the network with a non-stationary distribution and the existence of stretching similarity. We validate the existence of power-law in the distribution and estimate the corresponding power-law index using rigorous techniques from statistical inference advocated by Clauset et al [151]. We find that the average degree of the network grows logarithmically with the size of the network and we find the exact formula for its behavior analytically. We also find that the global clustering coefficient of the network reaches to the value 0 while the average clustering coefficient C_{WS} saturates to a high value. All these results are validated by extensive numerical calculations for network up to size 2^{25}.

We also find that there exists a pattern in the local clustering coefficients that reflects universality in the organization of natural numbers in terms of their prime constituents. We observe that this pattern has a stretching similarity which is a reflection of the nature of prime factorization of natural numbers. Also, the behavior of characteristics like average degree, global clustering and assortativity coefficients for this network vary quite smoothly and hence may help us to understand better the divisibility relations between natural numbers. In conclusion, the work presented here describes an interesting perspective on the divisibility relations of natural numbers and has potential to become an important tool in the investigation of related properties of natural numbers.

Chapter 6

Conclusion

The study reported in the thesis was set out to explore two key aspects of complex networks, namely, their structure and dynamics. Both these aspects turn out to be very important for real world complex systems that can be modelled as networks. Since many natural and man made complex systems are meant to perform specific functions, it is important to be able to control them, analyze their structural and functional aspects and find the physical processes which shape these aspects. The function of a complex system as a whole is determined by the individual components or nodes which constitute it. The complex interactions between these nodes can give rise to a variety of emergent behaviors in complex systems and in situations where some of these behaviors may be undesirable, they need to be modified or controlled in an appropriate way. These emergent behaviors and the corresponding control mechanisms are almost always dictated by the structure of the underlying network. Thus, an equally important issue in this context is to find out the mechanisms which are responsible for the emergence of the existing structures of these systems. This framework of complex networks originally developed to probe the behavior of complex systems has turned out to be important to address many interesting problems from pure mathematics also and several important insights can be gained with this approach.

In the first two chapters of the thesis, we present a brief but comprehensive introduction to complex networks, then consider dynamical systems and possible emergent states of such systems on networks. In chapter 3 of the thesis, we study a mechanism of control of dynamics on networks and lattices proposed by us using a coupling scheme in which external network is used as a controller. We show that under appropriate conditions, such interaction can lead to a regularization or suppression of the possible chaotic behavior in the system. The actual implementation of this scheme does not need any a priori knowledge about the dynamics of the system or its parameter values. Thus, from an engineering point of view this provides a practically suitable control method that can be implemented easily since it is completely external to the system and works for several different dynamics and topologies without any modification. Also, for many extended systems, such external network provides an approximation of the external medium with which the system is interacting. This raises an interesting possibility that possibly such control mechanism might already be at work in real systems like neuronal networks to control unwanted or harmful excitations.

We first analyze this control scheme for single units of the system using logistic map and Hénon map. Using properties of circulant matrices and Routh-Hurwithz conditions for discrete systems, we then analyze the stability of controlled states for 1d lattice or ring of these systems. This leads to the identification of the regions of control in various parameter planes and we verify all these results by direct numerical simulations of the corresponding systems. We also show that randomization of connections between controller and the system does not hamper the control and hence that the scheme is much more general. We also extend the scheme to 2d lattices and random networks and showed that the scheme works for very different types of topologies like scale-free networks and completely random networks. We analyze the case of networks using master-stability approach and show that the stability of the controlled steady state in this case is related to the largest eigenvalue of the Laplacian of the network. We also show that even when the topology of the controller is different from that of the system network, the control can be achieved indicating the wide applicability of the scheme.

Also, we successfully apply the scheme to regular networks of continuous time systems like chaotic Rössler system and Hindmarsh-Rose system in burst regime. In the case of Rössler system, by extensive numerical computation, we isolate different regions of various dynamical behaviors like amplitude death and periodic behavior in a corresponding parameter space. In case of both of these systems, we show how a desired periodic or a steady state behavior can be obtained by adjusting the coupling strength between the system and the controller.

As an application of the proposed method, we show how the experimentally realizable chimera state can be controlled to synchronized periodic or steady state. In this case, we discuss the nature of transition to chimera death and to a controlled state of amplitude death in detail with the help of several quantifiers. We also show how a similar mechanism can suppress the unwanted patterns on the 2-d lattice of neuronal dynamics represented by a Rulkov map.

In chapter 4, we turn to the related topic of an understanding of the mechanisms which shape the structure of the real world networks. In this context, we propose a new model, called the 'mediated attachment model', of a growing network. This model incorporates two basic principles namely, triadic closure and weak mediating capacity of hubs. We argue that in the absence of a direct preferential attachment, these two principles in a growing network can reproduce many structural features observed in real networks including scale-free structure and hierarchical community structure. This is important since very few generative network models are known to produce both these important features seen in real networks. The networks so produced also have high clustering, low average path length and non-zero degree correlations. All of these properties are not reproduced by most of the preferential attachment models and hence the mediated attachment model reveals the importance of the local processes in the formation of real world networks.

In chapter 5, we apply the paradigm of complex networks to study the problem of divisibility patterns of natural numbers. This is considered as a very important problem in Mathematics because of its close association to the prime numbers. For this, we construct a growing network in which the natural numbers are nodes connected by undirected edges based on the divisibility. Using the rigorous methods from the area of statistical inference, we show that the resulting network has a non-stationary power-law degree distribution. We also find a very interesting similarity in this network which we call a "stretching similarity". We also derive some of the numerically observed results using analytical arguments in this case.

We note that the work presented in this thesis has opened several new directions for further investigations. Some of these directions are the following:

1. The control scheme presented here is sufficiently general and it would be interesting to look for the systems in nature in which this scheme is already prevalent as a mechanism for regularization. As an example, neurons in the brain interacting through extracellular fluid could be one such system and the role of such interactions on the dynamics of neurons could be investigated along the directions suggested here.

2. In the present work, the control scheme is applied to a particular type of chimera state. It would be interesting to see whether the coupling scheme can suppress all types of chimera states in general and the transition to chimera death can be analyzed for each such case.

3. Mediated attachment model presented in this thesis is still a very general model and does not take into consideration the specific system dependent properties. The more realistic models of real networks like social networks should include many more factors like age and fitness values apart from principles of mediated attachment model. It would be interesting to see the way the processes like random walks and synchronization are affected by a structure of the mediated network. This will open up number of interesting topics for further study.

4. For the natural number network presented in this thesis, no complete explanation of the numerically observed "stretching similarity" pattern is evident now. Such an explanation might reveal some of the interesting underlying properties of natural numbers. The investigation of spectral properties of natural number network is underway currently to understand this structure in a better way.

In conclusion, we report our research on three important aspects of the study of complex networks namely, control of emergent dynamics, structure and growth of networks and extending network theory to deterministic networks. We are confident that these studies will inspire further studies on similar and varied directions to unravel many of the intricacies observed in real world complex systems.

Bibliography

[1] Newman, M. E. J. *Networks: An Introduction* (Oxford University Press, 2010).

[2] Albert, R. & Barabási, A. L. Statistical mechanics of complex networks. *Rev. Mod. Phys.* **74**, 47–97 (2002).

[3] Newman, M. E. J. Scientific collaboration networks: I. network construction and fundamental results. *Phys. Rev. E* **64**, 016131 (2001).

[4] Newman, M. E. J. Why social networks are different from other types of networks. *Phys. Rev. E* **68**, 036122 (2003).

[5] Jeong, H., Tombor, B., Albert, R., Oltvai, Z. N. & Barabási, A. L. The large-scale organization of metabolic networks. *Nature* **407**, 651 (2000).

[6] Jeong, H., Mason, S., Barabási, A. L. & Oltvai, Z. N. Lethality and centrality in protein networks. *Nature* **411**, 41 (2001).

[7] Vázquez, A., Flammini, A., Maritan, A. & Vespignani, A. Modeling of protein interaction networks. *ComPlexUs* **1**, 38–44 (2002).

[8] Durek, P. & Walther, D. The integrated analysis of metabolic and protein interaction networks reveals novel molecular organizing principles. *BMC Systems Biology* **2**, 100 (2008).

[9] Lewis, A. C. F., Jones, N. S., Porter, M. A. & Deane, C. M. The function of communities in protein interaction networks at multiple scales. *BMC Systems Biology* **4**, 100 (2010).

[10] Montoya, J. M. & Solé, R. V. Small world patterns in food webs. *J. Theor. Biol.* **214**, 405 (2002).

[11] White, J. G., Southgate, E., Thompson, J. N. & Brenner, S. The structure of the nervous system of the nematode *Caenorhabditis Elegans*. *Phil. Trans. R. Soc. London* **314** (1986).

[12] Albert, R., Jeong, H. & Barabási, A. L. Diameter of the world-wide web. *Nature* **401**, 130 (1999).

[13] Pastor-Satorras, R., Vázquez, A. & Vespignani, A. Dynamical and correlation properties of the internet. *Phys. Rev. Lett.* **87**, 258701 (2001).

[14] Foschi, R., Riccaboni, M. & Schiavo, S. Preferential attachment in multiple trade networks. *Phys. Rev. E* **90**, 022817 (2014).

[15] Gozolchiani, A., Yamasaki, K., Gazit, O. & Havlin, S. Pattern of climate network blinking links follows El Niño events. *Europhys. Lett.* **83**, 28005 (2008).

[16] Donges, J. F., Zou, Y., Marvan, N. & Kurths, J. The backbone of the climate networks. *Europhys. Lett.* **87**, 48007 (2009).

[17] Amaral, L., Scala, A., Barthélémy, M. & Stanley, H. E. Classes of small-world networks. *Proc. Natl. Acad. Sci. USA* **97**, 11149–11152 (2000).

[18] Sen, P. *et al.* Small-world properties of the Indian railway network. *Phys. Rev. E* **67**, 036106 (2003).

[19] Gastner, M. T. & Newman, M. E. J. Optimal design of spatial distribution networks. *Phys. Rev. E* **74**, 016117 (2006).

[20] Zhou, T., Wang, B.-H., Hui, P. M. & Chan, K. P. Topological properties of integer networks. *Physica A: Statistical Mechanics and its Applications* **367**, 613–618 (2006).

[21] García-Pérez, G., Serrano, M. & Boguñá, M. Complex architecture of primes and natural numbers. *Physical Review E* **90**, 022806 (2014).

[22] Newman, M. E. J. Modularity and community structure in networks. *Proc. Natl. Acad. Sci. USA* **103**, 8577–8582 (2006).

[23] Newman, M. E. J. Communities, modules and large-scale structure in networks. *Nature physics* **8**, 25–31 (2011).

[24] Girvan, M. & Newman, M. E. J. Community structure in social and biological networks. *PNAS* **99**, 7821–7826 (2002).

[25] Newman, M. E. J. Assortative mixing in networks. *Phys. Rev. Lett.* **89**, 208701 (2002).

[26] Traub, R. D., Schmitz, D., Jefferys, J. G. R. & Draguhn, A. High-frequency population oscillations are predicted to occur in hippocampal pyramidal neuronal networks interconnected by axoaxonal gap junctions. *Neuroscience* **92**, 407–426 (1999).

[27] Traub, R. D. *et al.* Gap junctions between interneuron dendrites can enhance synchrony of gamma oscillations in distributed networks. *The journal of neuroscience* **21**, 9478–9486 (2001).

[28] Bennet, M. V. L. & Zukin, R. S. Electrical coupling and neuronal synchronization in the mammalian brain. *Neuron* **41**, 495–511 (2004).

[29] Moreno, Y., Nekovee, M. & Pacheco, A. F. Dynamics of rumour spreading in complex networks. *Phys. Rev. E* **69**, 066130 (2004).

[30] Goldenberg, J., Shavitt, Y. & Solomon, S. Distributive immunization of networks against viruses using the 'honey-pot' architecture. *Nature Physics* **1**, 184–188 (2005).

[31] Yang, L. X., Yang, X., Liu, J., Zhu, Q. & Gan, C. Epidemics of computer viruses: A complex network approach. *Appl.Math.Comput.* **219**, 3914–3922 (2012).

[32] Gan, C. *et al.* Propagation of computer virus both across the internet and external computers: A complex-network approach. *Commun Nonlinear Sci Numer Simul* **19**, 2785–2792 (2014).

[33] Newman, M. E. J. Spread of epidemic disease on networks. *Phys. Rev. E* **66**, 016128 (2002).

[34] Pastor-Satorras, R. & Vespignani, A. Epidemic spreading in scale-free networks. *Phys. Rev. Lett.* **86**, 3200–3203 (2001).

[35] Chen, S., Huang, W., Cattani, C. & Altieri, G. Traffic dynamics on complex networks: A survey. *Math. Probl. Eng.* **2012**, 732698 (2012).

[36] Mendes, G. A., da Silva, L. R. & Herrmann, H. J. Traffic gridlock on complex networks. *Physica A* **391**, 362–370 (2012).

[37] Strogatz, S. H. Exploring complex networks. *Nature* **410**, 268–276 (2001).

[38] Arenas, A., Díaz-Guilera, A., Kurths, J., Moreno, Y. & Zhou, C. Synchronization in complex networks. *Physics Reports* **469**, 93–153 (2008).

[39] Albert, R., Jeong, H. & Barabási, A. L. Error and attack tolerance of complex networks. *Nature* **406**, 378 (2000).

[40] Kishore, V., Santhanam, M. S. & Amritkar, R. E. Extreme events on complex networks. *Phys. Rev. Lett.* **106**, 188701 (2011).

[41] Kishore, V., Santhanam, M. S. & Amritkar, R. E. Extreme events and event size fluctuations in biased random walks on networks. *Phys. Rev. E* **85**, 056120 (2012).

[42] Watts, D. J. & Strogatz, S. H. Collective dynamics of 'small-world' networks. *Nature* **393**, 440–442 (1998).

[43] Hilborn, R. C. *Chaos and nonlinear dynamics* (Oxford University Press, 2001).

[44] Broer, H. W., Huitema, G. B. & Sevryuk, M. B. *Quasi-periodic motions in families of dynamical systems: order amidst chaos* (Springer, 2009).

[45] Broer, H. W. & Sevryuk, M. B. kam theory: quasi-periodicity in dynamical systems. *Handbook of Dynamical Systems* **3**, 249–344 (2010).

[46] Heagy, J. & Ditto, W. L. Dynamics of a two-frequency parametrically driven duffing oscillator. *Journal of Nonlinear Science* **1**, 423–455 (1991).

[47] Ditto, W. L. *et al.* Experimental observation of a strange nonchaotic attractor. *Physical review letters* **65**, 533 (1990).

[48] Grebogi, C., Ott, E. & Yorke, J. A. Fractal basin boundaries, long-lived chaotic transients, and unstable-unstable pair bifurcation. *Physical Review Letters* **50**, 935 (1983).

[49] McDonald, S. W., Grebogi, C., Ott, E. & Yorke, J. A. Fractal basin boundaries. *Physica D: Nonlinear Phenomena* **17**, 125–153 (1985).

[50] Zhang, D., Györgyi, L. & Peltier, W. R. Deterministic chaos in the belousov-zhabotinsky reaction: Experiments and simulations. *Chaos* **3**, 723 (1993).

[51] Sciamanna, M. & Shore, K. A. Physics and applications of laser diode chaos. *Nature Photonics* **9**, 151–162 (2015).

[52] Murali, K., Lakshmanan, M. & Chua, L. O. Bifurcation and chaos in the simplest dissipative non-autonomous circuit. *Int. J. Bifur. and Chaos* **4**, 1511 (1994).

[53] Ahlers, G., Grossmann, S. & Lohse, D. Heat transfer and large scale dynamics in turbulent rayleigh-bénard convection. *Rev. Mod. Phys.* **81**, 503 (2009).

[54] Chay, T. R., Fan, Y. S. & Lee, Y. S. Bursting, spiking, chaos, fractals, and universality in biological rhythms. *Int. J. Bifur. and Chaos* **05**, 595 (1995).

[55] Buchler, J. R., Serre, T. & Kolláth, Z. A chaotic pulsating star: The case of r scuti. *Phys. Rev. Lett.* **73**, 842–845 (1995).

[56] Sparrow, C. *The Lorenz equations: bifurcations, chaos, and strange attractors*, vol. 41 (Springer Science & Business Media, 2012).

[57] Mandel, P. & Erneux, T. Laser lorenz equations with a time-dependent parameter. *Phys. Rev. Lett.* **53**, 1818 (1984).

[58] Poland, D. Cooperative catalysis and chemical chaos: a chemical model for the lorenz equations. *Physica D* **65**, 86–99 (1993).

[59] Strogatz, S. *Nonlinear dynamics and chaos* (Perseus Books, 1994).

[60] Rulkov, N. F. Regularization of synchronized chaotic bursts. *Phys. Rev. Lett.* **86**, 183 (2001).

[61] Rulkov, N. F. Modeling of spiking-bursting neural behavior using two-dimensional map. *Phys. Rev. E* **65**, 041922 (2002).

[62] Franović, I. & Miljković, V. The effects of synaptic time delay on motifs of chemically coupled rulkov model neurons. *Commun Nonlinear Sci Numer Simulat* **16**, 623–633 (2011).

[63] Wolf, A., Swift, J., Swinney, H. L. & Vastano, J. A. Determining lyapunov exponents from a time series. *Physica D* **16**, 285–317 (1985).

[64] Harikrishnan, K., Mishra, R. & Ambika, G. Nonlinear time series analysis of the light curves from the black hole system 1915+105. *Research in Astronomy and Astrophysics* **11**, 71–90 (2011).

[65] Kantz, H. & Schreiber, T. *Nonlinear time series analysis*, vol. 7 (Cambridge university press, 2004).

[66] Feki, M., Robert, B., Gelle, G. & Colas, M. Secure digital communication using discrete-time chaos synchronization. *Chaos, Solitons and Fractals* **18**, 881–890 (2003).

[67] Saxena, G., Prasad, A. & Ramaswamy, R. Amplitude death: The emergence of stationarity in coupled nonlinear systems. *Physics Reports* **521**, 205–208 (2012).

[68] Koseka, A., Volkov, E. & Kurths, J. Oscillation queching mechanisms: Amplitude vs. oscillation death. *Physics Reports* **531**, 173–199 (2013).

[69] Abrams, D. M. & Strogatz, S. H. Chimera states in a ring of nonlocally coupled oscillators. *Int j bifurcat chaos* **16**, 21–37 (2006).

[70] Sethia, G. C. & Sen, A. Chimera states: The existence criteria revisited. *Phys. Rev. Lett.* **112**, 144101 (2014).

[71] Kuramoto, Y. & Battogtokh, D. Coexistence of coherence and incoherence in nonlocally copuled phase oscillators. *Nonlinear Phenom. Complex Syst.* **5**, 380 (2002).

[72] Bordyugov, G., Pikovsky, A. & Rosenblum, M. Self-emerging and turbulent chimeras in oscillator chains. *Phys. Rev. E* **82**, 035205(R) (2010).

[73] Zhu, Y., Zheng, Z. & Yang, J. Reversed two-cluster chimera state in non-locally coupled oscillators with heterogeneous phase lags. *Europhys. Lett.* **103**, 10007 (2013).

[74] Omelchenko, I., Maistrenko, Y., Hövel, P. & Schöll, E. Loss of coherence in dynamical networks: Spatial chaos and chimera states. *Phys. Rev. Lett.* **106**, 234102 (2011).

[75] Omelchenko, I., Riemenschneider, B., Hövel, P., Maistrenko, Y. & Schöll, E. Transition from spatial coherence to incoherence in coupled chaotic systems. *Phys. Rev. E* **85**, 026212 (2012).

[76] Zhu, Y., Zheng, Z. & Yang, J. Chimera states on complex networks. *Phys. Rev. E* **89**, 022914 (2014).

[77] Rattenborg, N. C., Amlaner, C. J. & Lima, S. L. Behavioral, neurophysiological and evolutionary perspectives on unihemispheric sleep. *Neurosci. Biobehav. Rev.* **24**, 817 (2000).

[78] Mathews, C. G., Lesku, J. A., Lima, S. L. & Amlaner, C. J. Asynchronous eye closure as an anti-predator behavior in the western fence lizard(sceloporus occidentalis). *Ethology* **112**, 286 (2006).

[79] Tinsley, M. R., Nkomo, S. & Showalter, K. Chimera and phase-cluster states in populations of coupled chemical oscillators. *Nature Physics* **8**, 662–665 (2012).

[80] Hagerstrom, A. M. *et al.* Experimental observation of chimeras in coupled-map lattices. *Nature Physics* **8**, 658–661 (2012).

[81] Lazarides, N., Neofotistos, G. & Tsironis, G. Chimeras in squid metamaterials. *Physical Review B* **91**, 054303 (2015).

[82] Boccaletti, S., Grebogi, C., Lai, Y. C., Mancini, H. & Maza, D. The control of chaos: Theory and applications. *Physics Reports* **329**, 103–197 (2000).

[83] Ott, E., Grebogi, C. & Yorke, J. A. Controlling chaos. *Phys. Rev. Lett.* **64**, 1196 (1990).

[84] Pyragas, K. Continuous control of chaos by self-controlling feedback. *Phys. Lett. A* **170**, 421–428 (1992).

[85] Lima, R. & Pettini, M. Suppression of chaos by resonant parametric perturbations. *Phys. Rev. A* **41**, 726–733 (1990).

[86] Braiman, Y. & Goldhirsch, I. Taming chaotic dynamics with weak periodic perturbations. *Phys. Rev. Lett.* **66**, 2545–2548 (1991).

[87] Grigoriev, R., Cross, M. & Schuster, H. Pinning control of spatiotemporal chaos. *Phys. Rev. Lett.* **79**, 2795 (1997).

[88] Schöll, E. & Schuster, H. G. *Handbook of chaos control* (Wiley-VCH, 2007).

[89] Resmi, V., Ambika, G., Amritkar, R. E. & Rangarajan, G. Amplitude death in complex networks induced by environment. *Phys. Rev. E* **85**, 046211 (2012).

[90] Klinger, T. *et al.* Chaos control and taming of turbulence in plasma devices. *Physics of Plasmas* **8**, 1961–1968 (2001).

[91] Córdoba, A., Lemos, M. & Jiménez-Morales, F. Periodical forcing for the control of chaos in a chemical reaction. *J. Chem. Phys.* **124**, 014707 (2006).

[92] Roy, R., Murphy, J. T. W., Maier, T. D., Gills, Z. & Hunt, E. R. Dynamical control of a chaotic laser: experimental stabilization of a globally coupled system. *Phys. Rev. Lett.* **68**, 1259 (1992).

[93] Wei, M. D. & Lun, J. C. Amplitude death in coupled chaotic solid-state lasers with cavity-configuration-dependent instabilities. *Appl. Phys. Lett.* **91**, 061121 (2007).

[94] Gang, H. & Zhilin, Q. Controlling spatiotemporal chaos in coupled map lattice systems. *Phys. Rev. Lett.* **72**, 68 (1994).

[95] Boccaletti, S., Bragard, J. & Arecchi, F. T. Controlling and synchronizing space time chaos. *Phys. Rev. E* **59**, 6574 (1999).

[96] Sharma, A. & Shrimali, M. D. Amplitude death with mean-field diffusion. *Phys. Rev. E* **85**, 057204 (2012).

[97] Banerjee, T. & Biswas, D. Amplitude death and synchronized states in nonlinear time-delay systems coupled through mean-field diffusion. *CHAOS* **23**, 043101 (2013).

[98] Zou, W. *et al.* Amplitude death in nonlinear oscillators with mixed time-delayed coupling. *Phys. Rev. E* **88**, 032916 (2013).

[99] Gjurchinovski, A., Zakharova, A. & Schöll, E. Amplitude death in oscillator networks with variable-delay coupling. *Phys. Rev. E* **89**, 032915 (2014).

[100] Hens, C. R., Olusola, O. I., Pal, P. & Dana, S. K. Oscillation death in diffusively coupled oscillators by local repulsive link. *Phys. Rev. E* **88**, 034902 (2013).

[101] Zakharova, A. *et al.* Time delay control of symmetry-breaking primary and secondary oscillation death. *Europhys. Lett.* **104**, 59901 (2013).

[102] Gjurchinovski, A., Jüngling, T., Urumov, V. & Schöll, E. Delayed feedback control of unstable steady states with high-frequency modulation of the delay. *Phys. Rev. E* **88**, 032912 (2013).

[103] Wang, X. F. & Chen, G. Pinning control of scale-free dynamical networks. *Physica A* **310**, 521–531 (2002).

[104] Dab, D., Boon, J.-P. & Li, Y.-X. Lattice-gas automata for coupled reaction-diffusion equations. *Phys. Rev. Lett.* **66**, 2535 (1991).

[105] Kessler, D. A., Levine, H. & Reynolds, W. N. Coupled-map lattice model for crystal growth. *Phys. Rev. A* **42**, 6125 (1990).

[106] Neiman, A., Schimansky-Geier, L., Cornell-Bell, A. & Moss, F. Noise-enhanced phase synchronization in excitable media. *Phys. Rev. Lett.* **83**, 4896 (1999).

[107] Perc, M. Spatial coherence resonance in excitable media. *Phys. Rev. E* **72**, 016207 (2005).

[108] Ito, H. & Glass, L. Spiral breakup in a new model of discrete excitable media. *Phys. Rev. Lett.* **66**, 5 (1991).

[109] Pedersen, M. G. Homogenization of heterogeneously copuled bistable ode's- applied to excitation waves in pancreatic islets of langerhans. *Journal of biological physics* **30**, 285–303 (2004).

[110] Yanagita, T. Coupled map lattice for boiling water. *Phys. Lett. A* **165**, 405 (1991).

[111] Yanagita, T. & Kaneko, K. Modeling and characterization of cloud dynamics. *Phys. Rev. Lett.* **78**, 4297 (1997).

[112] Resmi, V., Ambika, G. & Amritkar, R. E. General mechanism for amplitude death in coupled systems. *Phys. Rev. E* **84**, 046212 (2011).

[113] Sonis, M. Critical bifurcation surfaces of 3d discrete dynamics. *Discrete Dyn Nat Soc* **4**, 333–343 (2000).

[114] Tee, G. J. Eigenvectors of block circulant and alternating circulant matrices. *Res. Lett. Inf. Math. Sci.* **8**, 123–142 (2005).

[115] Dudkowski, D., Maistrenko, Y. & Kapitaniak, T. Different types of chimera states: An interplay between spatial and dynamical chaos. *Phys. Rev. E* **90**, 032920 (2014).

[116] Panaggio, M. J. & Abrams, D. M. Chimera states: Coexistence of coherence and incoherence in networks of coupled oscillators. *arXiv:1403.6204v2 [nlin.CD]* (2014).

[117] Yao, N., Huang, Z.-G., Lai, Y.-C. & Zheng, Z.-G. Robustness of chimera states in complex dynamical systems. *Sci. Rep.* **2013**, 3522 (2013).

[118] Anastassiou, C. A., Perin, R., Markram, H. & Koch, C. Ephaptic coupling of cortical neurons. *Nat. Neurosci.* **14**, 217–223 (2011).

[119] Pecorra, L. M. & Carroll, T. L. Master stability functions for synchronized coupled systems. *Phys. Rev. Lett.* **80**, 2109–2112 (1998).

[120] Banerjee, T., Paul, B. & Sarkar, B. C. Spatiotemporal dynamics of a digital phase-locked loop based coupled map lattice system. *Chaos* **24**, 013116 (2014).

[121] Barabási, A. L. & Albert, R. Emergence of scaling in random networks. *Science* **286**, 509–512 (1999).

[122] Newman, M. E. J. The structure and function of complex networks. *SIAM REVIEW* **45**, 167–256 (2003).

[123] Vázquez, A. Growing network with local rules: Preferential attachment, clustering hierarchy, and degree correlations. *Phys. Rev. E* **67**, 056104 (2003).

[124] Newman, M. E. J. Communities, modules and large-scale structure in networks. *Nat. Phys.* **8**, 25 (2012).

[125] Davidsen, J., Ebel, H. & Bornholdt, S. Emergence of a small world from local interactions: Modelling acquaintance networks. *Phys. Rev. Lett.* **88**, 128701 (2002).

[126] Bianconi, G., Darst, R. K., Iacovacci, J. & Fortunato, S. Triadic closure as a basic generating mechanism of communities in complex networks. *Phys. Rev. E* **90**, 042806 (2014).

[127] Bollobás, B. *Random Graphs* (Cambridge University Press, 2001).

[128] de S. Price, D. J. Networks of scientific papers. *Science* **149**, 510–515 (1965).

[129] Krapivsky, P. L., Rodgers, G. J. & Redner, S. Degree distributions of growing networks. *Phys. Rev. Lett.* **86**, 5401 (2001).

[130] Moore, C., Ghoshal, G. & Newman, M. E. J. Exact solutions for models of evolving networks with addition and deletion of nodes. *Phys. Rev. E* **74**, 036121 (2006).

[131] Bianconi, G. & Barabási, A. L. Bose-einstein condensation in complex networks. *Phys. Rev. Lett.* **86**, 5632 (2001).

[132] Bianconi, G. & Barabási, A. L. Competition and multiscaling in evolving networks. *Europhys. Lett.* **54**, 436–442 (2001).

[133] Krapivsky, P. L., Redner, S. & Leyvraz, F. Connectivity of growing random networks. *Phys. Rev. Lett.* **86**, 4629 (2000).

[134] Holme, P. & Kim, B. J. Growing scale-free networks with tunable clustering. *Phys. Rev. E* **65**, 026107 (2002).

[135] i Cancho, R. F. & Solé, R. The small world of human language. *Proc. R. Soc. Lond. B* **268**, 2261 (2001).

[136] i Cancho, R. F., Solé, R. & Köhler, R. Patterns in syntactic dependency networks. *Phys. Rev. E* **69**, 051915 (2004).

[137] Barabási, A. L., Albert, R. & Jeong, H. Scale-free characteristics of random networks: the topology of the world-wide web. *Physica A* **281**, 69–77 (2000).

[138] Redner, S. How popular is you paper? an empirical study of the citation distribution. *Eur. Phys. J.B.* **4**, 131–134 (1998).

[139] Tsallis, C. & de Albuquerque, M. P. Are citations of scientific papers a case of nonextensivity? *Eur. Phys. J.B.* **13**, 777–780 (2000).

[140] Evans, T. & Saramäki, J. Scale-free networks from self-organization. *Phys. Rev. E* **72**, 026138 (2005).

[141] Ravasz, E. & Barabási, A.-L. Hierarchical organization in complex networks. *Phys. Rev. E* **67**, 026112 (2003).

[142] Corso, G. Families and clustering in a natural numbers network. *Phys. Rev. E* **69**, 036106 (2004).

[143] Achter, J. D. Comment on "families and clustering in a natural numbers network". *Phys. Rev. E* **70**, 058103 (2004).

[144] Chandra, A. K. & Dasgupta, S. A small world network of prime numbers. *Physica A* **357**, 436–446 (2005).

[145] Frahm, K. M., Chepelianskii, A. D. & Shepelyansky, D. L. Pagerank of integers. *J. Phys. A* **45** (2012).

[146] Zhang, J. Y., Sun, W. G., Tong, L. Y. & Li, C. P. Topological properties of fibonacci networks. *Commun Theor Phys* **60** (2013).

[147] García-Pérez, G., Serrano, M. & Boguñá, M. Complex architecture of primes and natural numbers. *Phys. Rev. E* **90**, 022806 (2014).

[148] Ding-hua, S. & Hui-jie, Z. Natural number network and the prime number theorem. *Complex Systems and Complexity Science* **7**, 3813 (2010).

[149] Newman, M. E. J. Power laws, pareto distributions and zipf's law. *Contemporary Physics* **46**, 323–351 (2005).

[150] Goldstein, M. L., Morris, S. A. & Yen, G. G. Probelms with fitting to the power-law distribution. *Eur. Phys. J.B.* **41**, 255–258 (2004).

[151] Clauset, A., Shalizi, C. R. & Newman, M. E. J. Power-law distributions in empirical data. *SIAM Review* **51**, 661–703 (2009).

[152] Clauset, A., Young, M. & Gleditsch, K. S. On the frequency of severe terrorist events. *J. Conflict Resolution* **51**, 58–87 (2007).

[153] Burton, D. M. *Elementary number theory* (Tata McGraw-Hill Education, 2006).

[154] Apostol, T. M. *Introduction to analytic number theory* (Springer-Verlag, New York-Heidelberg, 1976).

[155] Johnson, S., Torres, J. J., Marro, J. & A., M. M. Entropic origin of dissortativity in complex networks. *Phys. Rev. Lett.* **104**, 108702(1–4) (2010).

Index